



DISTRIBUTION STATEMENT A
Approved for public release
Distribution Unlimited

AZIMUTH & RANGE OPTIMIZATION
OF THE VELOCITY AZIMUTH DISPLAY (VAD)
ALGORITHM IN THE WSR-88D

THESIS

David L. Craft, Captain, USAF

AFIT/GM/ENP/98M-01

19980408 120

DEPARTMENT OF THE AIR FORCE
AIR UNIVERSITY
AIR FORCE INSTITUTE OF TECHNOLOGY

DTIC QUALITY INSPECTED 4

Wright-Patterson Air Force Base, Ohio

AZIMUTH & RANGE OPTIMIZATION
OF THE VELOCITY AZIMUTH DISPLAY (VAD) ALGORITHM
IN THE WSR-88D

THESIS

David L. Craft, Captain, USAF

AFIT/GM/ENP/98M-01

The views expressed in this thesis are those of the author and do not reflect the official policy or position of the Department of Defense or the U.S. Government

AZIMUTH & RANGE OPTIMIZATION
OF THE VELOCITY AZIMUTH DISPLAY (VAD) ALGORITHM
IN THE WSR-88D

THESIS

Presented to the Faculty of the Graduate School of Engineering
Air Force Institute of Technology
Air University
In Partial Fulfillment of the Requirements
for the Degree of Master of Science
in Physical Meteorology

David L. Craft, Captain, USAF

March 1998

AZIMUTH & RANGE OPTIMIZATION
OF THE VELOCITY AZIMUTH DISPLAY (VAD) ALGORITHM
IN THE WSR-88D

David L. Craft, B.S.
Captain, USAF

Approved:

Cecilia A. Askue

CECILIA A. ASKUE, LT COL, USAF
Chairman, Advisory Committee

5 March 1998
date

Clifton E. Dunney

CLIFTON E. DUNGEY, MAJ, USAF
Member, Advisory Committee

5 Mar 98
date

Daniel E. Reynolds

DANIEL E. REYNOLDS, PROFESSOR
Member, Advisory Committee

5 March 1998
date

David E. Weeks

DAVID E. WEEKS, PROFESSOR
Member, Advisory Committee

5 March 1998
date

Acknowledgments

I would like to express my sincere appreciation to my faculty advisor, Lt Col Cecilia Askue, for her guidance and support throughout the course of this thesis effort. Her insight and experience were certainly appreciated. I would also like to thank my sponsor, Lt Col Andy White from the WSR-88D Operational Support Facility (OSF), and Dr. Tim O'Bannon from the OSF, for their support and technical guidance.

I am indebted to MSgt Pete Rahe, Superintendent of the AFIT weather lab who was a tremendous help in solving all the problems I encountered using the lab computers. Thank you to Lt Col Mike Walters for Fortran programming advice. And, thanks to Dr. Dan Reynolds for statistics advice.

Finally, thank you to my mother Judy and friend Spring. Without their love and support, this journey would have been a whole lot tougher.

David L. Craft

Table of Contents

	Page
List of Figures.....	v
List of Tables.....	vii
Abstract.....	ix
I. Introduction.....	1
Background.....	1
The Velocity Azimuth Display (VAD) Algorithm.....	3
Possible Causes of Inaccurate VAD Wind Profiles.....	8
Use of Rawinsondes.....	10
Use of Vertical Wind Profilers.....	12
Approach and Presentation.....	15
II. Literature Review.....	16
Intercomparison Research.....	16
VAD Optimization Research.....	18
III. Methodology.....	20
Scope.....	20
Stratification of the Data.....	21
Data Selection.....	22
Production of VAD Wind Profiles.....	24
Impact of Local Topography on the Denver WSR-88D.....	24
Azimuth Optimization.....	28
Range Optimization.....	29
Verification of VAD Wind Profiles.....	29
Determination of Alternative VWP Skill.....	31
IV. Results & Discussion.....	32
Azimuth Optimization Results.....	32
Range Optimization Results.....	33
Size of the Data Sets.....	33
Alternative Range Skill for Atmospheres which were Superrefractive at the Surface.....	35
Alternative Range Skill for Atmospheres which were Superrefractive Aloft.....	38

Alternative Range Skill for Atmospheres which were Not Superrefractive.....	41
Alternative Range Skill during Autumn.....	44
Alternative Range Skill during Winter.....	46
Alternative Range Skill during Spring.....	48
Alternative Range Skill during Summer.....	50
Alternative Range Skill Overall.....	52
 V. Summary & Conclusions.....	54
Summary.....	54
Conclusions.....	55
Recommendations for Further Research.....	57
 Appendix A: Microwave Propagation within the Troposphere.....	58
Refractivity.....	58
Propagation Classifications.....	60
Meteorological Causes of Anomalous Propagation.....	62
 Appendix B: Statistical Data.....	64
Number of Wind Estimates Produced by the VAD Algorithm.....	64
Statistics Calculated Using Profiler Verification.....	65
Autumn.....	65
Winter.....	74
Spring.....	83
Summer.....	92
Statistics Calculated Using Rawinsonde Verification.....	101
Autumn.....	101
Winter.....	110
Spring.....	119
Summer.....	128
Statistics Calculated Between Rawinsonde and Profiler Data.....	137
 References.....	140
 Vita.....	144

List of Figures

Figure	Page
1. Radial Velocity as a Function of Azimuth Angle for a Given Altitude.....	4
2. Velocity Azimuth Display Plot of the 2,000 ft AGL Wind over a WSR-88D.....	5
3. The VWP Product.....	6
4. Output from the Vertical Wind Profiler at Plateville, CO.....	14
5. The Front Range of Colorado, and the Location of Sources of Verification Data.....	21
6. Impact of Ground Contaminated Data on the Base Reflectivity Product of the Denver WSR-88D.....	26
7. Impact of Ground Contaminated Data on the Base Velocity Product of the Denver WSR-88D.....	27
8. Skill Scores for Alternative Ranges Obtained Using Profiler Data for Verification (Averaged over All Seasons for Atmospheres which were Superrefractive at the Surface).....	37
9. Skill Scores for Alternative Ranges Obtained Using Rawinsonde Data for Verification (Averaged over All Seasons for Atmospheres which were Superrefractive at the Surface).....	37
10. Skill Scores for Alternative Ranges Obtained Using Profiler Data for Verification (Averaged over All Seasons for Atmospheres which were Superrefractive Aloft).....	40
11. Skill Scores for Alternative Ranges Obtained Using Rawinsonde Data for Verification (Averaged over All Seasons for Atmospheres which were Superrefractive Aloft).....	40
12. Skill Scores for Alternative Ranges Obtained Using Profiler Data for Verification (Averaged over All Seasons for Atmospheres which were Not Superrefractive).....	43
13. Skill Scores for Alternative Ranges Obtained Using Rawinsonde Data for Verification (Averaged over All Seasons for Atmospheres which were Not Superrefractive).....	43
14. Skill Scores for Alternative Ranges Obtained Using Profiler Data as Verification (Averaged over All Atmospheric Refractivity States for the Autumn Season).....	45
15. Skill Scores for Alternative Ranges Obtained Using Rawinsonde Data as Verification (Averaged over All Atmospheric Refractivity States for the Autumn Season).....	45

16. Skill Scores for Alternative Ranges Obtained Using Profiler Data as Verification (Averaged over All Atmospheric Refractivity States for the Winter Season).....	47
17. Skill Scores for Alternative Ranges Obtained Using Rawinsonde Data as Verification (Averaged over All Atmospheric Refractivity States for the Winter Season).....	47
18. Skill Scores for Alternative Ranges Obtained Using Profiler Data as Verification (Averaged over All Atmospheric Refractivity States for the Spring Season).....	49
19. Skill Scores for Alternative Ranges Obtained Using Rawinsonde Data as Verification (Averaged over All Atmospheric Refractivity States for the Spring Season).....	49
20. Skill Scores for Alternative Ranges Obtained Using Profiler Data as Verification (Averaged over All Atmospheric Refractivity States for the Summer Season).....	51
21. Skill Scores for Alternative Ranges Obtained Using Rawinsonde Data as Verification (Averaged over All Atmospheric Refractivity States for the Summer Season).....	51
22. Skill Scores for Alternative Ranges Obtained Using Profiler Data as Verification (Averaged over All Atmospheric Refractivity States and All Seasons).....	53
23. Skill Scores for Alternative Ranges Obtained Using Rawinsonde Data as Verification (Averaged over All Atmospheric Refractivity States and All Seasons).....	53
A1. Standard and Anomalous Propagation Paths.....	61
A2. Temperature and Specific Humidity Distributions which Produce N-Gradients Responsible for Ducting.....	62

List of Tables

Table	Page
1. Stratification of Data Sets by Atmospheric Refractivity State and Season.....	22
2. The Number of Wind Estimates (N) Produced by the VAD Algorithm during this Study.....	34
3. Average Percent Improvement in Accuracy over the Default Range for Atmospheres which were Superrefractive at the surface.....	36
4. Average Percent Improvement in Accuracy over the Default Range for Atmospheres which were Superrefractive Aloft.....	39
5. Average Percent Improvement in Accuracy over the Default Range for Atmospheres which were Not Superrefractive.....	42
6. Average Percent Improvement in Accuracy over the Default Range during Autumn.....	44
7. Average Percent Improvement in Accuracy over the Default Range during Winter.....	46
8. Average Percent Improvement in Accuracy over the Default Range during Spring.....	48
9. Average Percent Improvement in Accuracy over the Default Range during Summer.....	50
10. Summary of Ranges which Yielded an Average Improvement over Default Range Accuracy for Each Atmospheric Refractivity State.....	55
11. Summary of Ranges which Yielded an Average Improvement over Default Range Accuracy for Each Season.....	56
B1. Total Number of Wind Barbs Displayed on the VWP during this Study by Range and Season.....	64
B2 - B10. Statistics Calculated Using Profiler Verification during Autumn.....	65 - 73
B11 - B19. Statistics Calculated Using Profiler Verification during Winter.....	74 - 82
B20 - B28. Statistics Calculated Using Profiler Verification during Spring.....	83 - 91
B29 - B37. Statistics Calculated Using Profiler Verification during Summer.....	92 - 100
B38 - B46. Statistics Calculated Using Rawinsonde Verification during Autumn.....	101 - 109

B47 - B55. Statistics Calculated Using Rawinsonde Verification during Winter.....	110 - 118
B56 - B64. Statistics Calculated Using Rawinsonde Verification during Spring.....	119 - 127
B65 - B73. Statistics Calculated Using Rawinsonde Verification during Summer.....	128 - 136
B74 - B76. Statistics Calculated between Rawinsonde and Profiler Data.....	137 - 139

Abstract

The Velocity Azimuth Display (VAD) algorithm occasionally produces inaccurate wind estimates for the VAD Wind Profile (VWP) product of the Weather Surveillance Radar - 1988 Doppler (WSR-88D) System. Weather forecasters have observed differences between the radar's wind profiles and wind profiles produced by rawinsondes and vertical wind profilers, when radiation and subsidence inversions in the atmosphere caused the radar beam to superrefract.

This thesis sought to improve the operational use of the VWP product for the WSR-88D near Denver, CO, by finding the optimal VAD algorithm Azimuth and Range parameter settings to overcome data contamination by hills located at the default range used by the algorithm. The WSR-88D Algorithm Testing and Display System (WATADS) processed 24 weeks of archived (level II) VAD wind data, which was verified by rawinsonde and vertical wind profiler data.

Azimuth optimization was unsuccessful. However, reducing the range not only provided an average improvement in the accuracy of winds obtained under superrefractive conditions, but also in the accuracy of those winds obtained when the atmosphere was not superrefractive. In the overall average, the range which produced the most improvement over default range (30 km) accuracy was 28 km. The 26-km range also performed well.

AZIMUTH & RANGE OPTIMIZATION OF THE VELOCITY AZIMUTH DISPLAY (VAD) ALGORITHM IN THE WSR-88D

Chapter 1. Introduction

Since the first deployments of the Weather Surveillance Radar - 1988 Doppler (WSR-88D) System, Air Force and National Weather Service (NWS) meteorologists have reported numerous disagreements between Velocity Azimuth Display (VAD) Wind Profiles (VWP) and rawinsonde derived wind profiles to the WSR-88D Operational Support Facility (OSF). Some reports show VWP winds stronger than winds on concurrent local upper air soundings, while others show VWP winds which are weaker. VWP wind directions have also been reported as much as 180 degrees different from winds derived at the same altitude on simultaneous upper air soundings (Davis et al., 1995; Lee and Ingram, 1995). Anomalous wind profiles can cause the WSR-88D to incorrectly dealias velocity data, and can cause duty forecasters to incorrectly assess the local weather regime. In one event, Altus Air Force Base (AFB) meteorologists issued a low-level wind shear advisory based on an anomalous VWP. Pilots reported no low-level wind shear was present (O'Bannon, 1994).

a. Background

In 1996, the U.S. Departments of Defense, Commerce, and Transportation completed installation of their jointly operated Doppler weather radar network. It consists of 142 operational WSR-88D systems within the contiguous United States, and 16 deployed

systems in Alaska, Hawaii, the Caribbean, and at U.S. military bases overseas¹. Except for small portions of western states where mountains block the lower-level scans, these radars provide nearly complete coverage of the contiguous U.S. at an altitude of 10,000 feet above site level (Klazura and Imy, 1993).

Each WSR-88D system “collects, processes, and displays high-resolution and high-accuracy reflectivity, mean radial velocity, and spectrum width data” (Crum and Alberty, 1993). Data collection occurs at the Radar Data Acquisition (RDA) tower. The data is then transferred to the Radar Product Generator (RPG) computers, which create numerous meteorological and hydrological products for display on the Principal User Processor (PUP) screens. Many of the algorithms within the RPG computers have adaptable parameters which may be adjusted in order to optimize algorithm performance for site-specific geographical and meteorological conditions.

WSR-88D systems continually archive the digital base data obtained at the RDA on 8mm tapes, before it is processed by the computer algorithms at the RPG. The archived base data, known as level II data, is collected by the National Climatic Data Center (NCDC). Researchers obtain level II data from the NCDC for all kinds of environmental research, including the development of enhanced meteorological algorithms for the WSR-88D, and to optimize the adaptable parameters for already existing meteorological algorithms. Thus, level II data was used in this research. Level II data comes complete with all of the necessary system status information (such as antenna scanning mode, date, time, and maintenance data) required to produce and interpret meteorological and hydrological products. One of the most attractive features of level II data is that it can be used on most

¹ From "WSR-88D RDA Locations." WWWeb, <http://www.ncdc.noaa.gov/pub/data/nexrad/stncoord.html> (28 Feb 98).

computer systems with a special computer software package known as the WSR-88D Algorithm Testing and Display System (WATADS) -- a WSR-88D is not required. This research utilized WATADS version 9.0 on UNIX based SPARC workstations.

b. The Velocity Azimuth Display (VAD) Algorithm

One of the most important applications of the radial velocity data collected by the radar lies within the Velocity Azimuth Display Algorithm. The algorithm creates a graphical plot of radial velocity versus azimuth angle (hence, the name VAD) for a maximum of 30 different horizontal levels above the radar. By specifying an altitude, radar operators may view one of the 30 plots when the radar is in clear air mode. The winds provided by these plots are used to update the radar's Environmental Winds Table, and to create the problematic vertical wind profile which is the focus of this research (the VAD Wind Profile, or VWP). The VWP is used by more Base Weather Stations and NWS offices than any of the WSR-88D's other algorithm derived products (Steadham and Lee, 1995).

To determine the wind direction and speed with height for the VAD plots and the VWP, the radar scans in a complete circle at constant elevation angles (Bluestein, 1992). The VAD algorithm obtains wind information for a particular height from the scattering of data points gathered by the elevation angle which directs the beam to intersect that height at a range of 30 km². The algorithm assumes that the radar beam is undergoing standard refraction, and that the horizontal winds at each height are uniform, i.e., no sharp gradients in the wind speed or direction. Under uniform horizontal flow, the graphical plot of radial velocity as a function of azimuth angle is sinusoidal. The algorithm uses this fact to determine the wind speed and direction even when velocity data is not available from each

² This distance is a default value for an adaptable parameter which may be changed in order to improve VAD algorithm performance. All seven of the algorithm's adaptable parameters will be discussed shortly.

azimuth of a circular scan. Once it receives at least 25 points³ of radial velocity information from a particular altitude, the algorithm uses a least squares methodology to fit a sine wave to the data. Figure 1 illustrates that the amplitude of the wave denotes the speed of the wind, while the phase of the wave indicates wind direction. As long as statistical error and symmetry thresholds (differences between inbound and outbound velocities) are not exceeded, that altitude's wind vector is output to the Environmental Winds Table and to the VWP product. Figure 2 depicts an example VAD plot with its fitted sine wave.

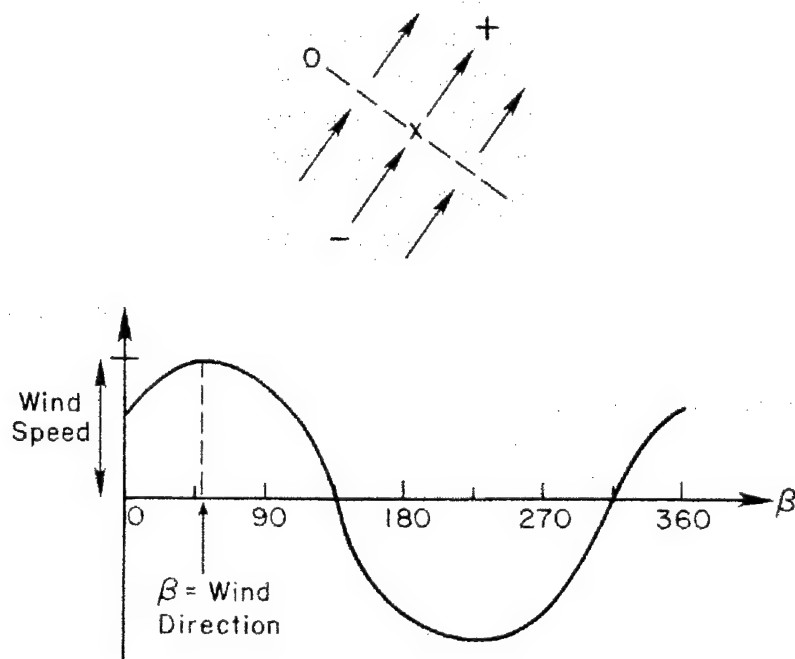


Fig. 1. Radial Velocity as a Function of Azimuth Angle for a Given Altitude. The vectors in the **top diagram** depict a SW wind from about 230°. A radar located at the **X** observes negative inbound radial velocities to the SW, and positive outbound velocities to the NE. The radial velocities are zero where the wind is perpendicular to the radar beam. The **bottom diagram** illustrates the sinusoidal variation of the measured radial velocity as the radar scans around a complete circle. The mathematical wind direction (β) is toward the NE at about 50°. (Bluestein, 1992)

³ This number is a default value for an adaptable parameter which may be changed in order to improve VAD algorithm performance. All seven of the algorithm's adaptable parameters will be discussed shortly.

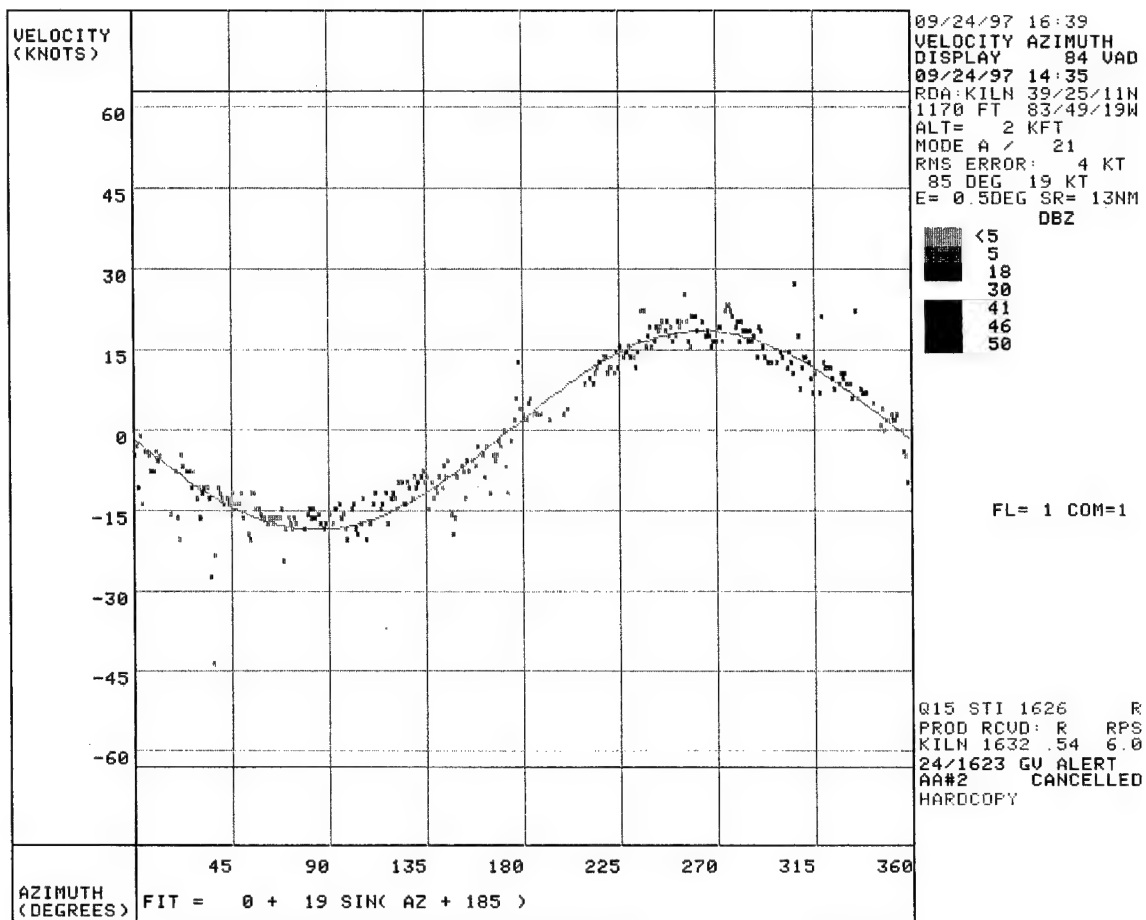


Fig. 2. Velocity Azimuth Display Plot of the 2,000 ft AGL Wind Over a WSR-88D

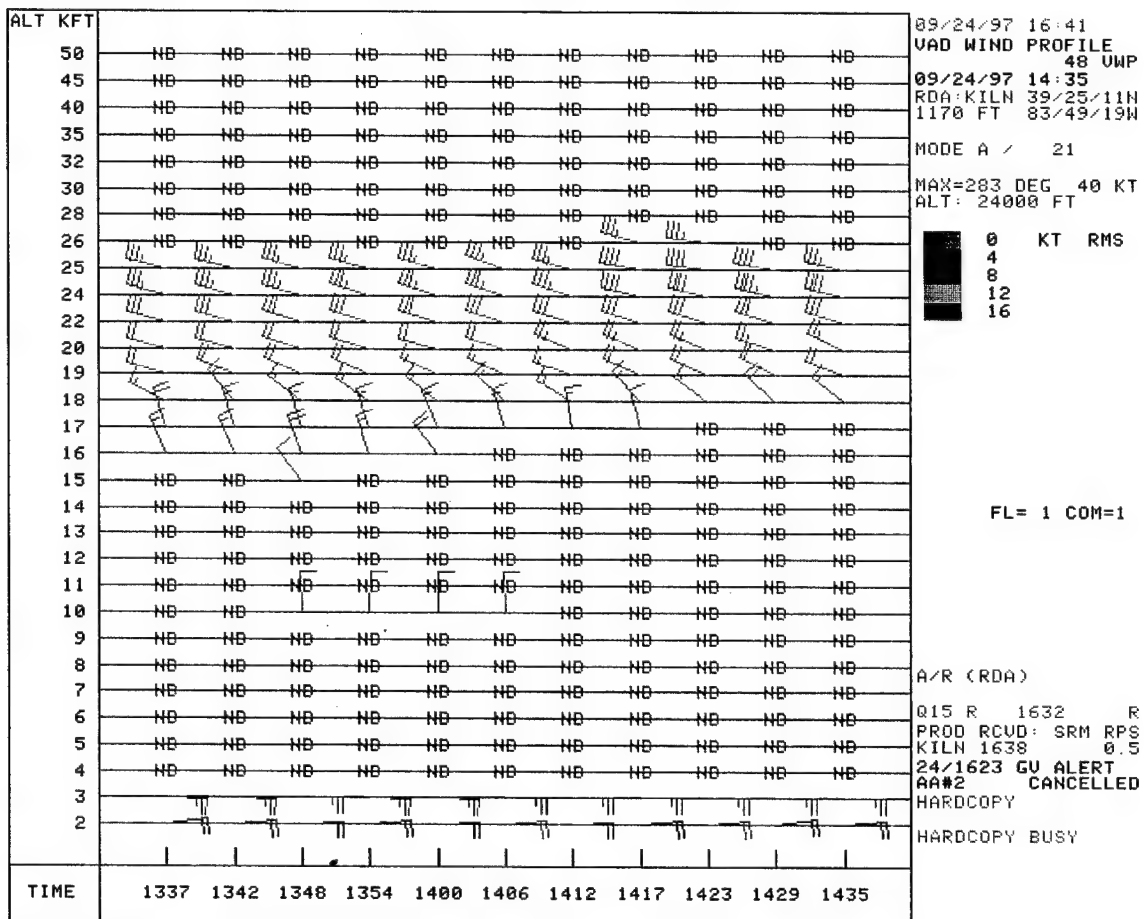


Fig. 3. The VWP Product. The 2,000 ft wind barb, displayed at 1435 UTC, was derived from the VAD plot in Figure 2.

The VWP product depicts a vertical profile of the mean horizontal wind vectors, calculated during the VAD analysis, as conventional wind barbs on a time versus height chart (see Figure 3). On the radar screen, the wind barbs are colored to reflect the quality of the fit (root-mean-square error) of the measured radial velocity values to the sine wave approximation. If statistical error or symmetry thresholds have been exceeded for a level, or if there is insufficient data to construct a sine wave, the letters "ND" are plotted instead of a wind barb. Wind barbs may be plotted for a maximum of 30 different altitudes, with at least 1,000 ft between levels, up to 50,000 ft (15.24 km). The current and ten previous profiles are displayed chronologically in a single diagram which is updated every 5 to 10 minutes. Such a plot helps forecasters "identify low- and high- level jets, thermal advection patterns, vertical wind shear, depths of frontal surfaces, and the development of isentropic lift situations" (Klazura and Imy, 1993).

The VAD algorithm has seven parameters which may be adjusted in order to obtain more accurate wind estimates. They are described below with default values in parenthesis (FMH-11, Part C, 1991).

1. **VAD Range (30 km):** The horizontal range used for the VAD analysis. Shortening the range forces the use of higher elevation angles. Although the resolution of the radar decreases at long ranges, the radar's back and side lobes may cause considerable ground contaminated return at short ranges.
2. **Beginning Azimuth (0°):** The beginning azimuth of any sector to be omitted from the VAD analysis. Contaminated sectors may be eliminated by using this in conjunction with the Ending Azimuth parameter.
3. **Ending Azimuth (0°):** The ending azimuth of any sector to be omitted from the VAD analysis.
4. **Threshold Velocity (5 m s⁻¹):** The maximum root mean square (RMS) velocity error allowed for a wind value to be used in the VAD analysis. Decreasing this threshold may

cause legitimate wind estimates to be omitted from the analysis. Increasing this threshold may cause spurious wind estimates to be included in the analysis.

5. **Threshold Symmetry (7 m s⁻¹):** The maximum allowed asymmetry for a valid least squares fit. Non-uniform flow, and sectors plagued by ground contamination, yield large asymmetry values and may result in a poorly fitted sine wave.
6. **Number of Fit Tests (2):** The number of times the fit test may be run. The test must be run twice to remove ground clutter biases.
7. **Minimum Number of Samples (25):** The minimum number of returns from scatterers which must be obtained before a Fourier least squares fit will be performed.

The last four of the above parameters influence the statistical curve fitting procedure used by the algorithm, and are largely independent of site-specific meteorological and geographical conditions. Changing these from their default values increases the chance that valid wind data will be ignored during the VAD analysis. This study did not attempt to optimize algorithm output for these four parameters. In contrast, the Range and Azimuth parameters have a physical influence on the selection of data used by the algorithm. Modifications made to them should depend largely on site-specific meteorological and geographical conditions. In particular, the OSF has suggested that reducing the Range parameter may improve algorithm performance for sites plagued by contaminated data in the lower elevation scans. Each of the Range and Azimuth parameters received careful consideration in this research.

c. Possible Causes of Inaccurate VAD Wind Profiles

The VAD algorithm may produce inaccurate wind estimates on the VWP product for many different reasons. Errors commonly result when the assumption of uniform flow is inapplicable. This occurs when frontal boundaries, thunderstorm outflows, and other nonlinearities in the wind field come within the range used by the algorithm to fit the sine wave for each altitude (Caya and Zawadzki, 1992). Major errors may also be caused by

airplanes, migrating birds, and other biological targets when they fly through the radar beam, or by vehicles on the ground when they pass through side lobes (O'Bannon, 1994; McLaughlin, 1993; Larkin, 1991). Minor errors may result if radar operators do not update the radar's Environmental Winds Table twice per day, with an estimate of the environmental wind profile, as recommended by the OSF. This update optimizes calculations involving wind data in all of the WSR-88D's meteorological and hydrological algorithms.

VWP winds are most likely to be in error when the assumption of standard radar beam propagation is violated (Davis et al., 1995; Lee et al., 1994). This occurs whenever vertical temperature and humidity distributions deviate from standard atmospheric conditions, causing the radar beam to refract more, or less, than expected by the algorithm. This phenomenon, known as anomalous propagation (AP), results in the radar miscalculating the height of the returned signal, and displaying wind estimates at the wrong altitude on the VWP.

This study focused on certain thermodynamic profiles which frequently occur and are especially problematic for VAD algorithm height computations. In particular, nocturnal inversions and subsidence inversions within the troposphere typically involve a decrease in moisture through a layer with an associated increase in temperature. Within these layers, the radar beam is refracted downward, or superrefracted, relative to standard atmospheric propagation. If superrefraction is strong enough, the radar beam will be trapped below a certain height or confined to a narrow atmospheric layer known as a duct. (For details on atmospheric refraction and radar beam propagation, refer to Appendix A). Since the VAD

algorithm assumes standard radar beam propagation, trapping by strongly superrefractive layers may lead to particularly gross errors on the VWP.

d. Use of Rawinsondes

Since the 1940s, rawinsondes have been the benchmark against which new upper-air observing technology is measured (Schwartz, 1989). They are the most widely employed tropospheric sounding systems worldwide (Douglas and Stensrud, 1996), and were used in this research to verify the winds displayed by the VWP.

Rawinsondes provide *in situ* measurements of temperature, relative humidity, and pressure aloft by means of a balloon-borne instrument package which is tracked by radar, or by a movable directional antenna. The hydrostatic equation is used to convert the pressure readings to equivalent altitudes which represent the height of the instrument package. Then, wind speed and direction are derived via trigonometric computations (AMS, 1989).

NWS rawinsondes rise at a nearly constant rate of 5 m s^{-1} , and take measurements in 6 second (or greater) intervals. Within the troposphere, measurements are averaged over time through layers 300 to 400 m thick and are assigned to the center of each layer. Depending on the strength of the flow aloft, rawinsondes may travel a significant horizontal distance in the 45 minutes typically required to reach the tropopause.

There are several uncertainties which should be considered when using wind profiles derived via rawinsondes. For instance, their Lagrangian sampling method leads to radar tracking uncertainties. These alone may cause RMS vector errors ranging from 1 m s^{-1} at the surface to 4 m s^{-1} at 12 km altitude (Lawrence et al., 1986). Another source of uncertainty are the time intervals used in the layer averaging of measurements by rawinsondes. If time intervals are too long, the rawinsonde data may not accurately resolve

important features of the vertical wind profile, like the peak of the low level jet. Jain et al. (1993) illustrated how this smoothing of data with time results in the damping of wind magnitude estimates in significant vertical shear. Golden et al. (1986) reported that such damping has led to an underestimate of the magnitude of the polar jet stream by as much as 20%. Despite these uncertainties, the National Weather Service (NWS) quotes the average functional precision of wind speed measurements by rawinsondes as 3.1 m s^{-1} below 30 kilometers (Lawrence et al., 1986).

Some differences in comparing rawinsonde data to VAD Wind Profile data should be expected because of the different scales on which the two systems sample wind motions. By measuring winds along the trajectory of the balloon, rawinsondes are impacted by microscale features as short as tens of meters. The VAD algorithm smoothes such small features by collecting data over a horizontal circle with a radius varying from 25 kilometers, at low altitudes, to 40 kilometers, at high altitudes. With a beamwidth of approximately 1° , the radar pulse length varies with altitude from 700 m to 1100m. The radar beam averaging which results may also cause discrepancies between the two types of measurements (Stensrud et al., 1990).

One disadvantage of using rawinsondes in this study was their temporal resolution. Rawinsondes only sample the atmosphere twice each day, around 0000 UTC and 1200 UTC. This low sampling rate could have prevented VAD algorithm optimization for meteorological conditions which occurred at other times of the day. Fortunately, the National Oceanic and Atmospheric Administration (NOAA) operates a network of vertical wind profilers. They provided hourly wind profiles of very high quality, and aided in the verification of the VAD Wind Profiles used in this research.

e. Use of Vertical Wind Profilers

The vertical wind profilers in the NOAA Profiler Network are highly sensitive Doppler radars which measure the horizontal wind speed and direction almost directly above their location. They operate on a frequency of 404.37 MHz (74 cm wavelength). Profilers detect fluctuations in the radio refractive index, on the order of half the radar wavelength, which result from the turbulent mixing of volumes of air with slightly different temperature and moisture contents. As turbulent eddies are advected by the mean flow, the profilers measure their translational velocities to obtain the mean wind vector.

In order to obtain the three dimensional mean wind vector, profilers electronically switch their beam between the three fixed positions. Two of the beam positions are orthogonal and point 73.7° above the horizon, while the third position is perfectly vertical. The orthogonal beams point toward the east and north, and are used to determine the respective u and v components of the radial wind velocity. The vertical beam measures the vertical component of the mean flow. This vertical component is subtracted from the u and v components of the radial wind to yield the horizontal components of the mean wind as follows:

$$u = v_e \sec 73.7^\circ - w \tan 73.7^\circ \quad (1a)$$

$$v = v_m \sec 73.7^\circ - w \tan 73.7^\circ \quad (1b)$$

where u , v , and w are the components of the mean flow at any altitude, while v_e and v_m are the components of the radial velocity measured in the east and north directions (van de Kamp, 1993). The wind speed is given by $(u^2 + v^2)^{1/2}$, and its direction is given by $\tan^{-1}(v/u)$. All three components of the wind field are assumed to be uniform over the distance

between the beams. They are also assumed not to vary significantly within a 6 minute sampling period.

Wind profilers sample the wind in two separate modes. The low mode measures the wind every 320 m between 0.5 km and 9.25 km. The high mode measures the wind every 900 m between 7.5 km and 16.25 km. Operating continuously, profilers alternate modes every minute, and switch beam positions every 2 minutes. Thus, a complete vertical wind profile is produced every 6 minutes. Centered every 250 m, winds in the profile are an average of measurements obtained over the spatial resolution of each mode (see van de Kamp for details, 1988). The final profile, displayed at the end of each hour, is a consensus average of the ten previous 6 minute profiles. Figure 4 shows an example of wind profiler output from Platteville, CO.

Profilers have many of the same limitations as the WSR-88D. The assumption of spatial and temporal homogeneity of the three-dimensional winds across the sample volume is likely to be violated during strong convection, or during strong lee waves and gravity waves (Nastrom and Vanzandt, 1996; Weber et al., 1992). And, sidelobe return may produce bad data. The hourly averaged profiler winds ought to smooth many of the spurious returns which may contaminate winds obtained during the 6 to 10 minute sampling period of the WSR-88D. However, birds have been shown to cause nonrandom errors as large as 15 m s^{-1} in profiler data during peak migration periods (Wilczak et al., 1995). Unlike the WSR-88D, profilers are also sensitive to coherent radio interference.

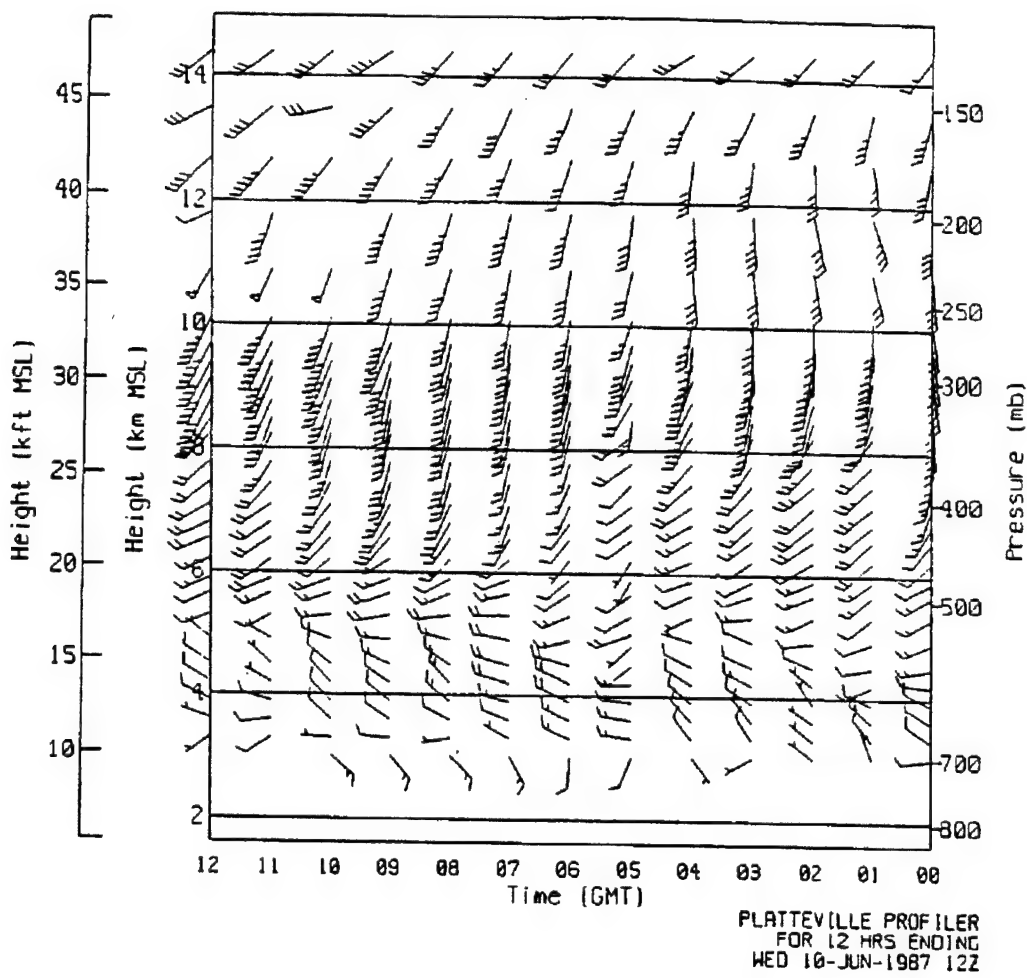


Fig. 4. Output from the Vertical Wind Profiler at Platteville, CO (van de Kamp, 1988)

Despite these limitations, the hourly winds obtained by wind profilers generally represent very accurate, high-quality data (Weber et al., 1990; Martner et al., 1993). This is mainly because profilers require their data to pass several quality control tests, including velocity aliasing checks and continuity checks, before it is displayed (Barth et al., 1994). A major advantage profilers have over the WSR-88D is their use of large elevation angles. Theoretical studies have shown that strong superrefraction, and ducting, should only be

expected within a horizontally stratified, superrefractive layer when the angle of incidence between the propagating electromagnetic wave and the layer is on the order of 1° to 2° (Battan, 1973). The WSR-88D commonly uses elevation angles below 2.5° , but profilers in the NOAA Profiler Network use elevation angles fixed well above this threshold at 73.7° and 90° . Because of its high accuracy, ability to overcome the effects of anomalous propagation, and relatively dense temporal resolution, profiler data was an invaluable tool in this research.

f. Approach and Presentation

This study sought to improve the operational use of the WSR-88D's VWP product by finding the optimal VAD algorithm Azimuth and Range parameter settings which minimize the effects of anomalous propagation through superrefractive layers. Both rawinsondes and profilers provided the truth against which the VAD data was measured. Ultimately, algorithm output obtained at alternative parameter settings was scored against output obtained at the default parameter settings to determine which ones worked best. Chapter 2 of this thesis will review the previous intercomparison research and optimization attempts from which this study stems. Chapters 3 and 4 will describe the methodology followed and the data used to arrive at the conclusions drawn in Chapter 5. Although the findings of this research are most applicable to the Denver radar (KFTG), for which the study was performed, they should provide insight to all WSR-88D operators attempting to overcome this problem.

a. Intercomparison Research

Previous intercomparison studies between operational wind profiling systems support the theory that superrefraction of the radar beam causes significant errors on the VWP. They also suggest that analysis of data sets by season aids in providing a physical explanation of intercomparison results. For reasons given in the previous section, research has shown that winds derived by the WSR-88D compare better to winds obtained by wind profilers than to winds obtained by rawinsondes.

During the Summer and Fall of 1994, and the Winter of 1995, OSF personnel compared 863 VWP - rawinsonde profile pairs from twelve different radar sites (mainly in the central United States). They noted that substantial VWP errors were more common in the Fall and Winter than in the Summer (Davis et al., 1995). Data analysis revealed that radar beam ducting due to atmospheric temperature inversions caused most of the VWP errors during Winter, but suggested something other than inversions was the culprit in the Fall, perhaps migrating birds. Continued OSF research compared 124 VWP - rawinsonde profile pairs obtained in Florida between June 1994 and November 1995 (Lee and Ingram, 1995). Substantial VWP errors were most common during Winter and Spring, with slightly fewer errors in the Fall, and the fewest errors during Summer. A wind rose analysis indicated radar signatures were seasonally dependent, leading the researchers to suggest migrating birds were the primary source of VWP errors in the Winter and Spring. However, they did not observe birds directly. They also conceded that it may not be possible to differentiate a bird signature from an inversion signature on wind rose plots

because birds migrate in the same direction as the seasonal wind. In one study, Jain et al. (1993) pointed out that most researchers, and the VAD algorithm, only consider the main lobe of the radar beam and do not account for side lobes. Side lobe energy often enters superrefractive layers at smaller angles, and is more likely to become trapped.⁴ If the returned signal from the main beam is weak because it is sampling clear air, ducting side lobes which sample regions of higher reflectivity (or intercept point targets, like birds) may significantly contribute to the power-weighted radial velocity estimates, resulting in VAD algorithm mistakes.

Nelson (1994) compared 2 months worth of Twin Lakes, OK, VAD wind data to nearby rawinsonde and NOAA Profiler Network data obtained during the fall of 1993. He found an average RMS vector difference between the rawinsonde and WSR-88D data of 12.40 kts, which indicated fairly good agreement. He found an average RMS vector difference between the profiler and WSR-88D data of 9.23 kts, which indicated even better agreement. However, he noted that the VAD algorithm performed poorly during cases of strong northerly flow in which there was a cold frontal inversion aloft. And, he suggested that anomalous propagation of the radar beam was the culprit. Nelson's study was different than this study in that Nelson visually interpreted wind speed and direction from the wind barbs on the VWP product. This study applied a more objective method by using the digital values of wind speed and direction provided by the WSR-88D Algorithm Testing and Display System (WATADS).

⁴ Theoretical studies have shown that ducting should be expected only when the angle of incidence between the propagating electromagnetic wave and the superrefractive layer is on the order of 1° to 2° (Battan, 1973). For details on atmospheric refraction, refer to Appendix A.

b. VAD Optimization Research

Published attempts to optimize the adaptable parameters of the VAD algorithm, and thereby reduce VWP errors, are scarce. There have only been two to date, and neither met with much success. The first took an empirical approach. Steve Allen,⁵ of the Houston/Galveston NWSO, incrementally increased the range adaptable parameter from the default value of 30 km and observed the impact on the VWP product. He found that setting the VAD range around 45 km successfully increased the number of displayed wind barbs, and decreased their RMS error. Unfortunately, he could not repeat his results under different weather scenarios.

The second study was more theoretical. Farris (1997) collected two weeks of Winter, Spring, and Summer data from the Vandenberg AFB WSR-88D at times when low level temperature inversions were present. He adjusted the VAD algorithm's adaptable parameters, and looked for the strongest statistical correlations between VWP winds, rawinsonde winds, and profiler winds. He discovered that only modification of the range adaptable parameter improved the correlations. Unfortunately, no single range value worked best in all cases. He determined the degree to which the range value optimized the VWP winds was seasonally dependent, and suggested that it was probably also station dependent.

The findings in each of the above studies were carefully considered during the research conducted for this thesis. Like Farris's study, this research was based on the theory that inversions are the primary cause of anomalous VWPs. Unlike Farris's study, this research found that wind component correlations did not provide much insight during the adaptable

⁵ From "Impacts of Optimum Slant Range on 88D VAD Wind Profiles." WWWeb, <http://www.osf.noaa.gov/app/vadhx/main.htm> (31 Jul 97).

parameter optimization process. In *Statistical Methods in the Atmospheric Sciences*, Wilks (1995) stressed that correlations do reflect linear association between wind component pairs, but they do not account for biases which may be present between the components. Each adaptable parameter setting of the VAD algorithm introduces a unique bias to the data collection process. For instance, a Range parameter setting of 24 km biases the algorithm toward the use of higher elevation angles than would be used at the 30-km (default) range setting. Since correlations overlook these biases, correlations may not be an entirely appropriate tool for the algorithm optimization process. Like the previously mentioned studies conducted by Nelson, and the OSF, this research relied on the RMS vector difference as the primary gauge of agreement between two wind profiles. As will be seen in the methodology section which follows, skill scores based on these RMS vector differences were calculated for each season of the year. They were used to indicate the percentage improvement in the accuracy of winds obtained using alternative adaptable parameter settings over the default accuracy of the algorithm.

Chapter 3. Methodology

As explained in the previous chapter, the success of any attempt to mitigate the problem of erroneous WSR-88D wind profiles via adaptable parameter optimization of the VAD algorithm will vary according to the location and season for which the attempt is made. These and other issues pertaining to the extent and methodology of this thesis will be clarified in this chapter. First, a discussion of scope will define the radar site chosen for the study and the sources verification data. Then, a justification will be provided for those algorithm adaptable parameter settings that were selected to produce the experimental data, followed by a description of the procedure used to verify the experimental data. Lastly, the statistical method for determining which adaptable parameter settings provided the most accurate winds will be discussed.

a. Scope

The VAD algorithm was optimized for the WSR-88D located in Farmington, Colorado, from September 1995 through September 1996. This radar was chosen because of its proximity to sources of verification data. Rawinsonde observations were taken at 00 UTC and 12 UTC each day by the National Weather Service Forecast Office (WSFO) at Stapleton Airport. Stapleton was located about 20 km to the west of the WSR-88D's antenna. Hourly vertical wind profiles were produced by the NOAA Profiler Network profiler in Platteville, which was about 50 km to the north of the radar antenna. Figure 5 depicts the location of Stapleton Airport and Platteville with respect to the topography of the region. Hourly station observations were also collected from the WSFO at Stapleton to determine the weather conditions for each day. This particular time period was chosen to obtain wind data representing all four seasons.

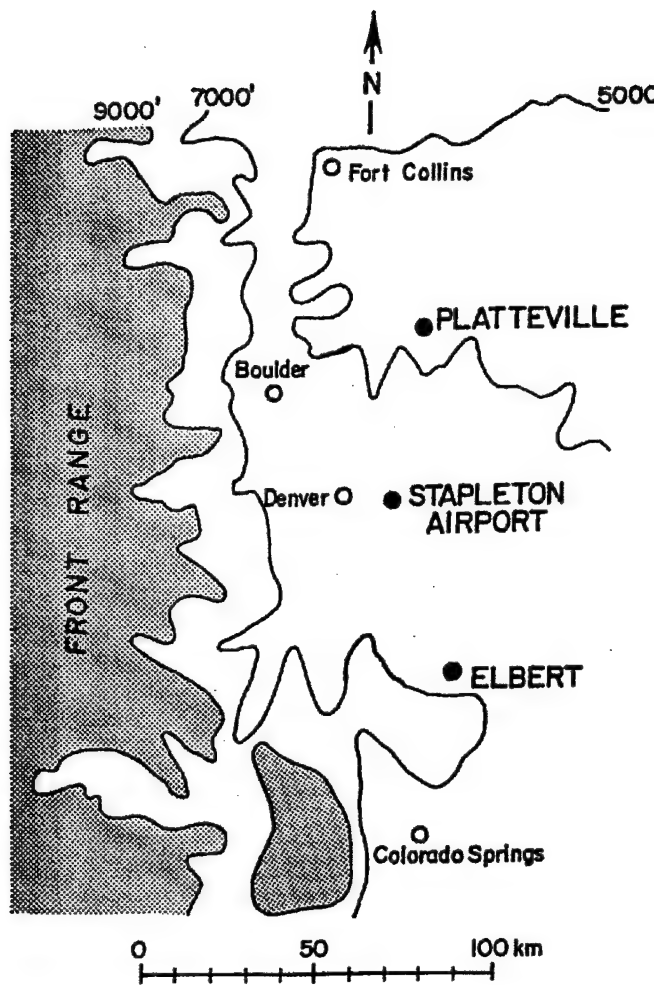


Fig. 5. The Front Range of Colorado, and the Location of the Sources of Verification Data (adapted from Martner et al., 1993). Profiler data was obtained from NOAA's 404 MHz wind profiler in Platteville. Rawinsonde data was obtained from the WSFO at Stapleton Airport. The WSR-88D's antenna was located about 20 km east of Stapleton at an elevation of 5,497 ft.

1) Stratification of the Data. The large amount of wind data had to be narrowed to focus on approximately 6 weeks in each season. Within each 6 week period, the data was stratified into three groups representing three different atmospheric refractivity conditions. The first group represented days in which the atmosphere was superrefractive at the surface.

The second group represented days in which the atmosphere was superrefractive in at least one horizontal layer aloft up to 700 mb. The third group represented days in which the atmosphere was not superrefractive below 700 mb. This enabled the researcher to determine the effectiveness of VAD algorithm optimization under different atmospheric refractivity states. Table 1 illustrates the division of the data by atmospheric refractivity condition and season.

Table 1. Stratification of Data Sets by Atmospheric Refractivity State and Season.

<i>Superrefractive at the Surface</i>				
	Autumn	Winter	Spring	Summer
Total Number of Days Selected to Represent this State of the Atmosphere and Season	14.5	14	15.5	14
Actual Number of Soundings with Surface Based Superrefractive Layers	18	7	9	8
<i>Superrefractive Aloft (up to 700 mb)</i>				
	Autumn	Winter	Spring	Summer
Total Number of Days Selected to Represent this State of the Atmosphere and Season	14	15.5	14.5	14.5
Actual Number of Soundings with Elevated Superrefractive Layers	5	7	12	9
<i>Not Superrefractive (below 700 mb)</i>				
	Autumn	Winter	Spring	Summer
Total Number of Days Selected to Represent this State of the Atmosphere and Season	14	14.5	15	15
Actual Number of Soundings which were Not Superrefractive	28	29	30	30

2) *Data Selection.* Choosing the data to study within each season and stratifying it according to the refractivity condition of the lower atmosphere was accomplished through careful analysis of the rawinsonde data. Recall from Chapter 1, and Appendix A, that

nocturnal inversions and subsidence inversions commonly produce the refractivity (N) gradients which force the radar's microwave energy to superrefract ($dN/dz < -54$ N-units km^{-1}). However, not all inversions create superrefraction significant enough to cause VAD algorithm errors. For this research, refractivity gradients stronger than -79 N-units km^{-1} were considered superrefractive.⁶ The refractivity was calculated at each level in the rawinsonde data (below 700 mb) using the approximation

$$N = \frac{77.6}{T} \left(p + 4810 \frac{e}{T} \right), \quad (2)$$

where p is pressure in hectopascals, T is temperature in Kelvin, and e is vapor pressure in hectopascals (Bean and Dutton, 1966). Pressure and temperature were taken directly from the rawinsonde data, but vapor pressure had to be calculated using

$$e = \frac{re_s}{100}, \quad (3)$$

where r is the percent relative humidity, and e_s is the saturation vapor pressure in hectopascals (Fleagle and Businger, 1980);

$$r = 100 \left(\frac{112 - 1.7T + T_d}{112 + 9T} \right)^8, \quad (4)$$

where T is temperature in degrees Kelvin, and T_d is the dew point temperature in degrees Kelvin (Babin, 1995); and

$$e_s = 6.112 \exp \left(\frac{17.67T}{T + 243.5} \right), \quad (5)$$

⁶ This was the value recommended by the Naval Ocean Systems Center in *Climatology of Marine Atmospheric Refractive Effects: A Compendium of the IREPS Historical Summaries*, (1982).

where T is in degrees Celsius (Bolton, 1980).⁷ The vertical refractivity gradient was then calculated using a standard, first order, forward differences scheme, and centered between rawinsonde reporting levels. The deepest and most strongly superrefractive layers were associated with surface based temperature inversions in the Fall. There were 11 surface ducts in the selected Fall, superrefractive at the surface, data set. The selected Winter and Spring, superrefractive at the surface, data sets contained two surface ducts each. There were no ducts discovered in any of the selected data sets representing a superrefractive atmosphere aloft. To be selected for a data set (superrefractive at the surface, superrefractive aloft, or not superrefractive), a day required a sounding which exhibited one of the specified refractivity states, or it had to occur adjacent to a day with a sounding which exhibited one of the specified refractivity states. NOAA Profiler Network and WSR-88D level II data were ordered for the same period as the selected rawinsonde data.

b. Production of VAD Wind Profiles

Recall from Chapter 1 that only the Azimuth and Range adaptable parameters physically influence the wind calculations of the WSR-88D's VAD algorithm. Since changes in the other four, statistically oriented, adaptable parameters increase the chance that valid wind data will be ignored by the algorithm, they were largely left alone during this research. Prior VAD optimization studies primarily focused on the Range parameter, as did this study. But, unique characteristics of the topography surrounding the Denver radar warranted a close look at the Beginning and Ending Azimuth parameters as well.

1) Impact of Local Topography on the Denver WSR-88D. Figure 5 illustrates that the terrain surrounding the Denver radar rises sharply, to the west and south, toward the front range of the Rocky Mountains. West of the radar, the most dramatic rise in elevation is well

⁷ Wexler's formula for saturation vapor pressure is correct to at least 0.3% for the range $-35^{\circ}\text{C} < T < +35^{\circ}\text{C}$.

outside of the default range used by the VAD algorithm during its analysis. But, Southwest of the radar, between Denver and Colorado Springs, lies an eastward protrusion of the foothills known as the Palmer Divide. Much of the divide is greater than 7,000 ft in elevation, which makes it easy to see in Figure 5 near Elbert. Some hills associated with the northern branch of the divide are located precisely within the 30 km default range used by the VAD algorithm. They reflect microwave energy emitted by the radar in the lowest elevation scans, and were consistently noticeable in low level reflectivity and velocity images during this research.

The impact of the rising terrain to the southwest of the radar is illustrated in Figure 6, a Base Reflectivity product, and Figure 7, a Base Velocity product. Both images were produced on a clear night using data from the radar's lowest elevation angle (0.5°). In Figure 6, the hills appear as two separate regions of anomalously high reflectivity values to the north and west of Parker. In Figure 7, they appear in the same locations as anomalously low velocity magnitudes. Topographic maps verified that these persistent anomalies were induced by local elevation maximums. The radar sits at an elevation of 5,497 ft, but the hills west of Parker reach elevations of nearly 7,000 feet. Although the hills north of Parker barely reach 6,350 ft, they were of primary importance to this study because they are located within the default range used by the VAD algorithm. The northern tip of this hilly region actually comes as close as 26 km (14 nm) to the radar. However, the hills consistently biased Base Velocity data displayed from 28 - 32 km (15 - 17.4 nm), and between 180° and 212° , during this study. The densest patch of contaminated data usually appeared from 200° to 212° . When the radar beam follows a standard atmospheric propagation path, the radar estimates the height of the main lobe to be as low as 6564 ft at a range of 28 km.

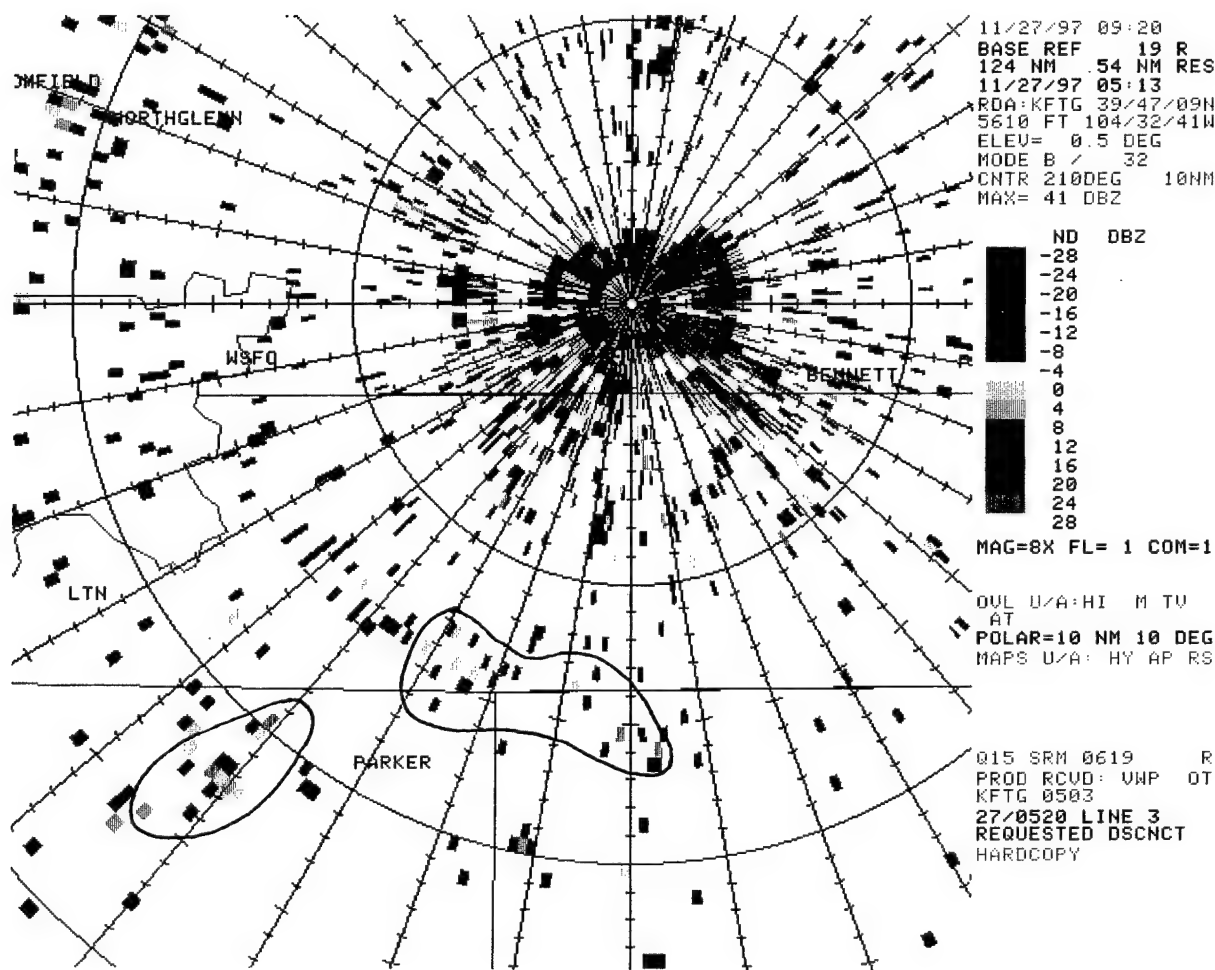


Fig. 6. Impact of Ground Contaminated Data on the *Base Reflectivity* Product of the Denver WSR-88D. Regions of anomalously large reflectivity values are circled. Range rings are positioned at intervals of 10 nm from the radar dish, with radials drawn every 10°. The default range used by the VAD algorithm is 16.2 nm (30 km).

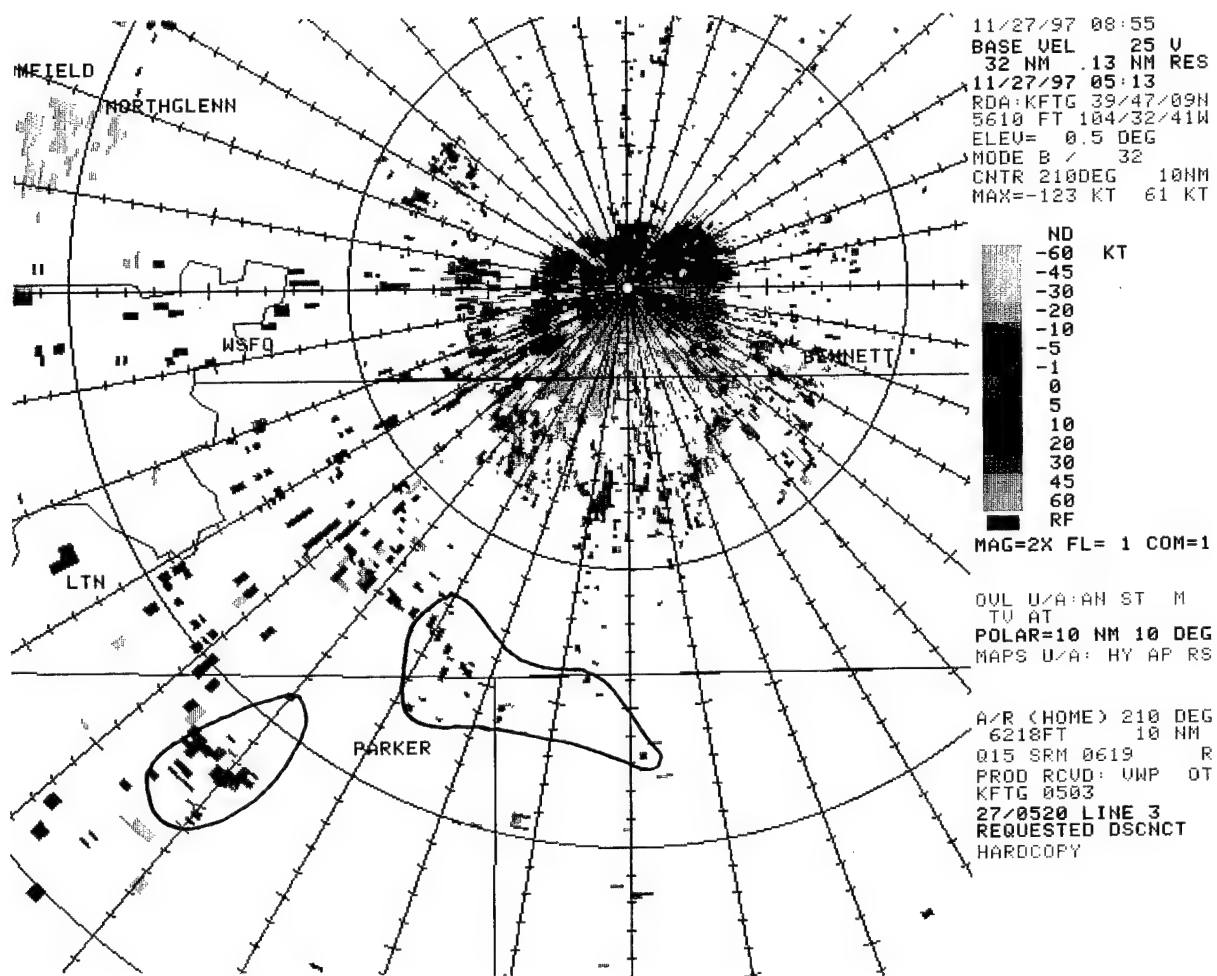


Fig. 7. Impact of Ground Contaminated Data on the *Base Velocity* Product of the Denver WSR-88D. Regions of anomalously small velocity magnitudes are circled. Range rings are positioned at intervals of 10 nm from the radar dish with radials drawn every 10°.

The default range used by the VAD algorithm is 16.2 nm (30 km).

This provides a clearance of only 214 ft as the beam passes over the hills at that range. If there are trees or buildings on the hills, or if the radar beam is superrefracting, the clearance is even less.

A region of ground contaminated return from the range used by the WSR-88D to perform the VAD analysis readily confuses the algorithm. If the anomalously low velocities manage to pass their RMS velocity error checks, they will artificially decrease the magnitude of the overall velocity estimate for that level. The ground contaminated return may assign enough near zero velocities, to a location incongruous with the rest of the data set, to cause asymmetry thresholds to be exceeded when the algorithm tries to fit a sine wave to the data. If this happens, no VAD plot will be produced for the level and the letters "ND" will be displayed on the VWP for that altitude. This confusion may be mitigated by prohibiting data obtained at contaminated azimuths from being considered during the VAD analysis (azimuth optimization), or by decreasing the range used by the algorithm to one which is not contaminated by bad data (range optimization).

2) *Azimuth Optimization.* This thesis attempted to mitigate the problems posed by the persistent, ground contaminated returns located within the default range used by the VAD algorithm by omitting them from the VAD analysis. WATADS produced one experimental data set with the Beginning Azimuth parameter set at 200° and the Ending Azimuth parameter at 212° . The Minimum Number of Samples parameter, which defines the minimum number of returns necessary for the algorithm to fit a sine wave to the data, was lowered from 25 to 24 to counteract the loss of good data due to the azimuthal scan restriction. All other adaptable parameter settings remained at their default values.

3) *Range Optimization.* This thesis also attempted to mitigate the problems posed by the persistent, ground contaminated returns located within the default range used by the VAD algorithm by decreasing the Range parameter. Decreasing the range forces the algorithm to use higher tilts when it produces the sine wave for a given altitude. The key to this strategy is to choose a range which requires the radar to radiate the target altitude using a tilt which directs the radar's energy above the source of contamination. Naturally, there is a trade-off. The higher the tilt used by the radar antenna, the greater the likelihood of back-lobe return contaminating the data. WATADS produced six more experimental data sets using ranges of 20, 22, 24, 26, 28, and 32 km. For these data sets, all of the algorithm's other adaptable parameters were left at their default values. WATADS also produced a default data set whose accuracy served as the benchmark against which the accuracy of each experimental data set was measured.

c. *Verification of VAD Wind Profiles*

Once VAD Wind Profiles were produced using the default and alternative adaptable parameter settings, they were verified using profiler and rawinsonde wind profiles. The profiler and rawinsonde winds were also compared to each other. A computer program compared the VAD-derived wind estimates to the profiler and rawinsonde derived wind estimates separately. It matched individual wind observations which were taken about the same time and near the same altitude. Individual wind estimates from two different devices were considered to match temporally if their times were within 6 minutes of each other. Spatial matches were slightly more complicated because of the different vertical resolution of each instrument. Since profiler winds are reported every 250 m, VAD heights were checked against profiler heights every 250 m from 2,024 - 7,524 m (msl). Rawinsonde

heights were checked against profiler heights over the same interval and range. If a VAD or rawinsonde height was within 150 m above or below a profiler height, the program identified a match. VAD heights were checked against rawinsonde heights every 300 m from 1,830 - 7,530 m (msl). Again, heights found within 150 m of each other were considered to match. The program listed all wind observation pairs for each season and atmospheric refractivity state by the altitudes where matches were made (every 250 m for profiler comparisons, every 300 m for rawinsonde comparisons). From this list, verification was accomplished by calculating the RMS Vector Difference (RMSVD).

The RMSVD (kts) is a single value which represents the accuracy of the winds obtained at a given level (adapted from Davis et al., 1995):

$$RMSVD = \sqrt{N^{-1} \sum_{i=1}^N \left[(U_T - U_w)_i^2 + (V_T - V_w)_i^2 \right]} \quad (6)$$

where U_T is the true zonal component of the wind (as measured by profiler or rawinsonde), U_w is the zonal component of the wind measured by the WSR-88D, V_T is the true meridional component of the wind (as measured by profiler or rawinsonde), V_w is the meridional component of the wind measured by the WSR-88D, N is the total number of matches found at the level, and i is the i^{th} match of the level. For perfect accuracy, RMSVD equals zero. The higher the RMSVD value, the lower the accuracy. Average RMSVDs were also calculated for each data set, but their role in the optimization process was limited because they are cumbersome to use. Since they are not relative, any comparisons made with average accuracies would have been difficult to interpret. To overcome this shortcoming, skill scores were calculated.

d. Determination of Alternative VWP Skill

The last step in the optimization process was to calculate skill scores for each level where the RMSVD was calculated, and to average them across each of the data sets.⁸ As a relative measure of alternative VWP accuracy, skill scores provided more insight to the optimization process than average RMSVD values could alone. Skill scores (%) were calculated using

$$SS_{alt} = \left(1 - \frac{RMSVD_{alt}}{RMSVD_{def}} \right) \times 100, \quad (7)$$

where SS_{alt} is the skill of VAD winds produced using alternative adaptable parameter settings, $RMSVD_{alt}$ is the accuracy of the same VAD winds, and $RMSVD_{def}$ is the accuracy of VAD winds obtained using the default adaptable parameter settings (Wilks, 1995). The SS_{alt} was interpreted as the percentage improvement in accuracy of the winds obtained at a given altitude, over the winds obtained at the same altitude using default adaptable parameter settings. $SS_{alt} = 0$ represented no improvement over the default accuracy of the VAD algorithm. $SS_{alt} = 20$ represented a 20% improvement over the default accuracy of the VAD algorithm. $SS_{alt} = -15$ represented a 15% impairment below the default accuracy of the VAD algorithm. As will be seen in the next chapter, the skill scores were averaged across all of the levels of each data set to determine which adaptable parameter settings were most skillful during each season, atmospheric refractivity condition, and overall.

⁸ The Pearson correlation coefficient (r), and the coefficient of determination (r^2) (Wilks, 1995) were also calculated between the wind components at each height where matches were made. A two tailed t-test was performed using (r) to assess the strength of the correlations. Unfortunately, the information they provided was not revealing. As mentioned in Chapter 2, correlations may not be appropriate for use during the VAD algorithm optimization process.

Chapter 4. Results & Discussion

Once calculated, skill scores for the VAD winds produced using alternative adaptable parameter settings were averaged across the various data sets to determine which settings provided the greatest improvement in accuracy for each season and atmospheric refractivity state. In this chapter, these averages will be presented and their implications discussed. Unfortunately, the attempt at azimuth optimization was unsuccessful. Its results will be discussed first. Since range optimization results were far more encouraging, the bulk of this chapter is devoted to them.

a. Azimuth Optimization Results

The 200 - 212° sector was omitted from the VAD analysis by setting the Beginning Azimuth parameter at 200° and the Ending Azimuth parameter at 212°. The Minimum Number of Samples parameter was also reduced to 24, but the rest of the adaptable parameters remained at their default values. After processing 8 weeks of level II data through WATADS, the azimuth optimization experiment was halted because the VAD algorithm had not produced a single wind barb on the VWP. The same 8 weeks of level II data processed through WATADS using the default adaptable parameter settings produced 88,689 wind barbs on the VWP. Examination of the digital VAD data produced by WATADS revealed that the number of samples obtained, when the 200-212° sector was omitted, was always smaller than the 24 required to fit a sine wave to the data. More data could have been produced if the Minimum Number of Samples parameter had been reduced further, but this was avoided out of concern for the representativeness of the sine wave which would have resulted. More data could also have been produced if a smaller sector was omitted, but this would have left much ground contaminated return within the

30-km range used by the algorithm. The 88,689 barb reduction in the number of wind estimates produced by the VAD algorithm due to an azimuthal scan restriction of just 12° seems extreme. It may have stemmed from a problem within WATADS, but this theory was not investigated during the study. Fortunately, the VAD data created at alternative ranges did not suffer from this dilemma.

b. Range Optimization Results

WATADS produced VAD Wind Profiles using the following ranges: 20, 22, 24, 26, 28, 30 (default), and 32 km. The winds were verified by both profiler and rawinsonde wind profiles. When averaging across data sets (e.g., over a year), there was general agreement between the two separate assessments of alternative range skill. When averaging within data sets (e.g., Autumn), the two skill assessments were often different. Proper interpretation of disagreements between the two different skill assessments requires an understanding of each data set used to obtain the skill scores. This section will begin with a brief discussion of the relative size of each verification data set, and will be followed by an analysis of the VAD data set size. Then, the average skill of alternative ranges under different refractivity conditions, during different seasons, and overall, will be assessed.

1) Size of the Data Sets. The number of matches made with VAD winds during the verification process is listed by level (every 250 m for profiler verification, every 300 m for rawinsonde verification) for each season and atmospheric refractivity state in Appendix B. The number of matching winds found between VAD and profiler data far exceeded the number of matches found between VAD and rawinsonde data because of the denser temporal resolution of the profiler data. As a result, the statistics calculated using profiler verification were more stable than those calculated using rawinsonde verification. The

number of matching winds found between profiler and rawinsonde data consistently exceeded the number of matches found between VAD and rawinsonde data because the greater sensitivity of profilers enabled them to produce more wind estimates. The RMSVD values calculated between the profiler and rawinsonde winds are listed in Appendix B for the sake of comparison.

Table 2. The Number of Wind Estimates (N) Produced by the VAD Algorithm during this Study

	Superrefractive at the Surface	Superrefractive Aloft	Not Superrefractive
<u>Azimuth</u>			
<u>Optimization:</u>			
200-212°	0	-	-
<u>Range</u>			
<u>Optimization:</u>			
20 km	93856	72556	83783
22 km	95146	81561	86294
24 km	94986	74999	86347
26 km	91368	71400	83388
28 km	86956	67051	79133
30 km	88689	68843	81744
32 km	85726	66209	78788
$n_{28}-n_{26}:$	-4412	-4349	-4255
$n_{30}-n_{26}:$	-2679	-2557	-1644
$n_{30}-n_{28}:$	1733	1792	2611

Unlike the number of wind barbs produced during the attempt at azimuth optimization, the VAD algorithm created a comparable number of wind estimates at each of the alternative range settings used during this study. Table 2 lists the number of wind barbs produced on the VWP for each Range parameter. The dramatic decrease in the number of wind estimates produced at ranges beyond 26 km appears to be evidence of the

influence of ground contaminated return on the algorithm. Recall from Chapter 3 that during VAD analysis, if the ground introduces a group of near zero velocities to a location which is inconsistent with the rest of the data set, RMS velocity error and symmetry thresholds are likely to be exceeded, and no wind estimate will be displayed on the VWP. If RMS and symmetry thresholds are not exceeded, the anomalously low velocities will likely bias the overall velocity estimate. Further analysis of the VAD Wind Profiles produced at different ranges verified that the vast majority of wind barbs lost between 26 and 28 km were from altitudes below 2,500 ft (agl). This decrease in the number of low level wind barbs produced at long ranges resulted in a sharp decrease in the number of matches found in the low levels between the ranges of 26 and 28 km during the verification process. The number of matches found at each level is listed in Appendix B for each season and refractivity state of the atmosphere. Not a single data set was exempted from a sharp reduction in the number of matches found below 2,300 m (msl) between the ranges of 26 and 28 km. Depending on the needs of the customer, the range dependence of the number of low level wind barbs produced by the VAD algorithm may be important to consider during the final optimization decision.

2) *Alternative Range Skill for Atmospheres which were Superrefractive at the Surface.* For each alternative range, the skill scores--calculated for atmospheres which were superrefractive at the surface--were averaged to obtain the average percent improvement over the default range accuracy by season. The results are tabulated in Table 3. At first glance, there appeared to be numerous disagreements between the average skill scores obtained via profiler verification and the average skill scores obtained via rawinsonde verification. However, for each season, they did agree that when the atmosphere was superrefractive at

the surface, improvement could be made over the default accuracy by decreasing the range used by the algorithm. When the skill scores were averaged over the entire year for the atmospheres which were superrefractive at the surface, the 26-km range was the most skillful for both sources of verification. According to profiler verification (Figure 8), the 26-km range provided 0.71 percent better average accuracy than the default range. According to rawinsonde verification (Figure 9), the 26-km range provided 2.72 percent better average accuracy than the default range. For both sources of verification, the 28-km range also proved more skillful than the default range setting.

Table 3. Average Percent Improvement in Accuracy over the Default Range for Atmospheres which were **Superrefractive at the Surface**

VAD Range:	20 km	22 km	24 km	26 km	28 km	32 km
Autumn						
<u>Comparison</u>						
VAD - Profiler	-8.1	-8.2	-7.1	-3.1	1.9	-0.7
VAD - Rawinsonde	-13.2	-10.2	-0.3	5.9	0.9	-1.1
Winter						
<u>Comparison</u>						
VAD - Profiler	-28.4	7.0	7.9	7.9	0.0	0.0
VAD - Rawinsonde	4.7	3.0	3.1	1.9	3.1	-7.7
Spring						
<u>Comparison</u>						
VAD - Profiler	2.9	1.9	1.4	1.3	0.8	-1.2
VAD - Rawinsonde	-5.9	-10.1	-2.6	0.8	-1.2	-1.5
Summer						
<u>Comparison</u>						
VAD - Profiler	2.7	2.6	1.2	0.2	0.5	-0.1
VAD - Rawinsonde	1.7	2.2	2.7	2.2	0.9	0.2

Note: The RMSVD and SS_{alt} values used to obtain these averages are listed in Appendix B.

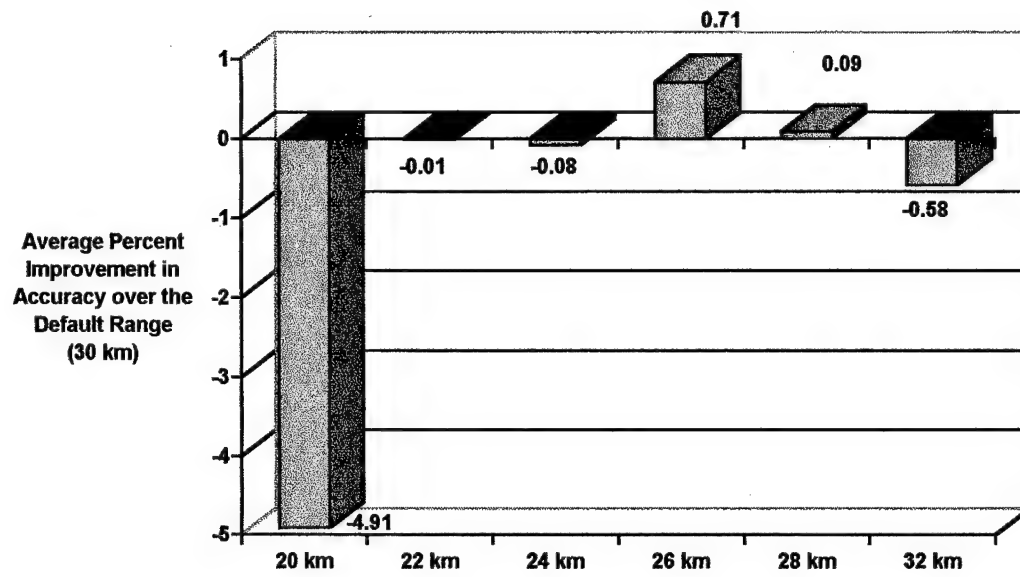


Fig. 8. Skill Scores for Alternative Ranges Obtained Using *Profiler* Data for Verification (Averaged over All Seasons for Atmospheres which Were **Superrefractive at the Surface**)

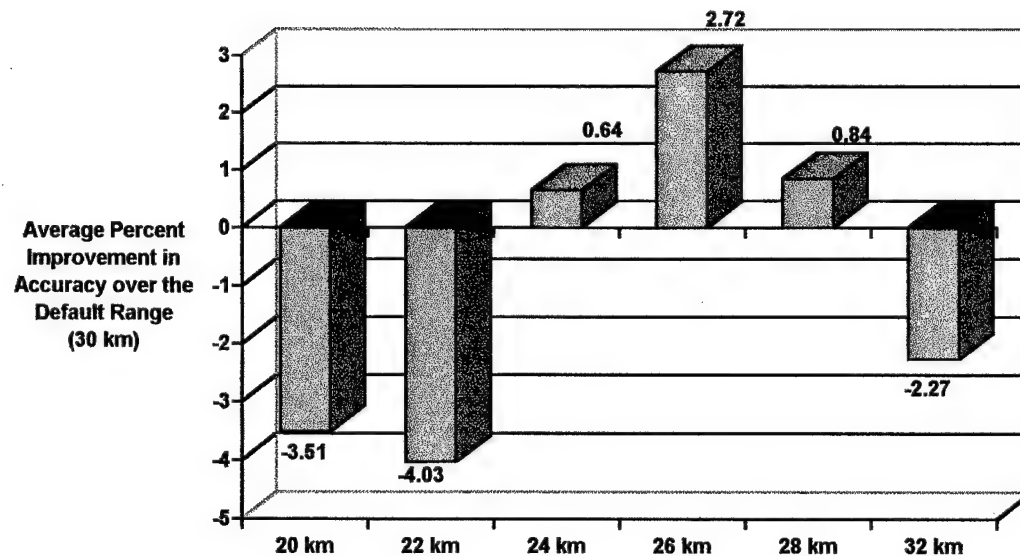


Fig. 9. Skill Scores for Alternative Ranges Obtained Using *Rawinsonde* Data for Verification (Averaged over All Seasons for Atmospheres which Were **Superrefractive at the Surface**)

3) *Alternative Range Skill for Atmospheres which were Superrefractive Aloft.* For each alternative range, the skill scores--calculated for atmospheres which were superrefractive aloft--were averaged to obtain the average percent improvement over the default range accuracy by season. The results are tabulated in Table 4. The skill scores produced using different means of verification did not appear to reach a consensus for this atmospheric refractivity condition, except during Spring and Summer where the 32-km range was clearly the least skillful of all ranges. When the skill scores were averaged over the entire year for the atmospheres which were superrefractive aloft, both verification sources agreed that the 28-km range provided improved average accuracy over the default range. According to profiler verification (Figure 10), 26 km was again the most skillful range, providing an average improvement in accuracy of 1.8 percent. The 28-km range was a close second, providing an average improvement of 1.74 percent. According to rawinsonde verification (Figure 11), 28 km was the only range more skillful than the default range, providing an average improvement in accuracy of 0.3 percent.

Table 4. Average Percent Improvement in Accuracy over the Default Range
for Atmospheres which were **Superrefractive Aloft**

VAD Range:	20 km	22 km	24 km	26 km	28 km	32 km
Autumn						
<u>Comparison</u>						
VAD - Profiler	-5.1	-5.1	-3.0	0.6	2.7	2.4
VAD - Rawinsonde	-15.6	-15.6	-20.2	-18.4	-0.5	-4.1
Winter						
<u>Comparison</u>						
VAD - Profiler	-0.1	-1.0	-1.6	4.7	2.0	0.9
VAD - Rawinsonde	-2.3	-1.7	-1.8	-0.7	-1.1	2.2
Spring						
<u>Comparison</u>						
VAD - Profiler	-0.5	-2.1	-2.3	-0.7	0.0	-3.2
VAD - Rawinsonde	7.3	2.5	1.3	2.2	0.0	-5.7
Summer						
<u>Comparison</u>						
VAD - Profiler	6.6	5.6	5.8	2.6	2.3	-1.2
VAD - Rawinsonde	2.3	-0.5	-0.4	0.4	2.1	-1.6

Note: The RMSVD and SS_{alt} values used to obtain these averages are listed in Appendix B.

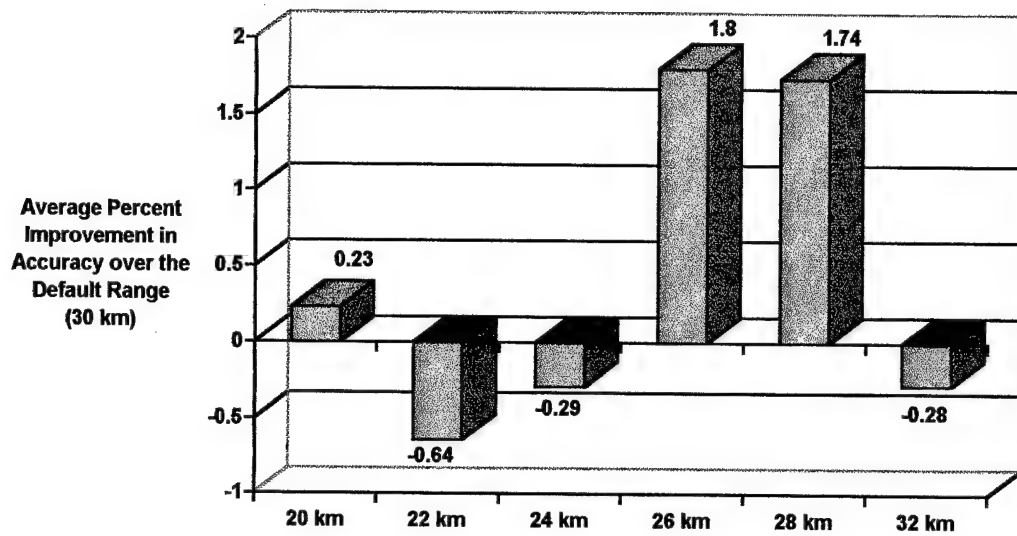


Fig. 10. Skill Scores for Alternative Ranges Obtained Using *Profiler* Data for Verification (Averaged over All Seasons for Atmospheres which Were **Superrefractive Aloft**)

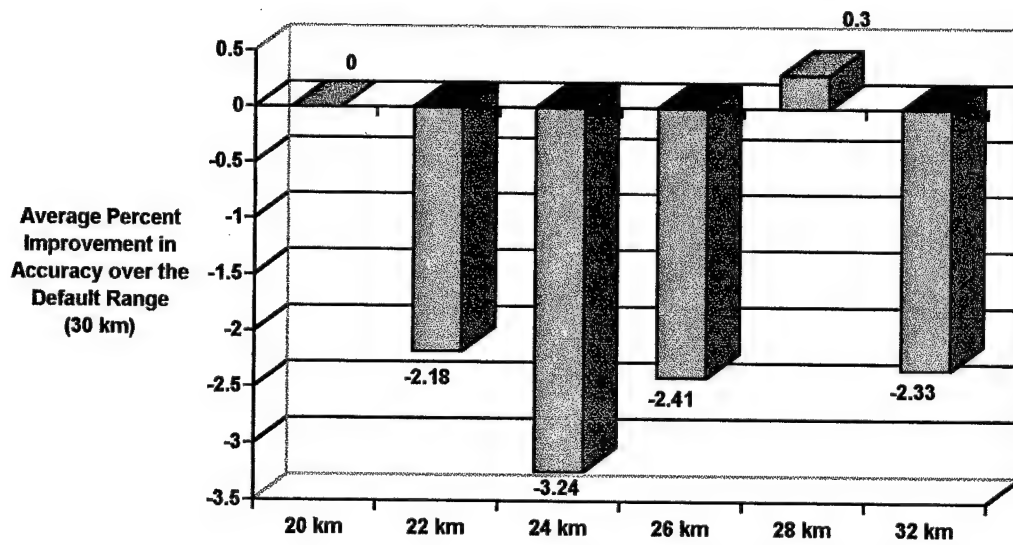


Fig. 11. Skill Scores for Alternative Ranges Obtained Using *Rawinsonde* Data for Verification (Averaged over All Seasons for Atmospheres which Were **Superrefractive Aloft**)

4) *Alternative Range Skill for Atmospheres which were Not Superrefractive.* For each alternative range, the skill scores--calculated for atmospheres which were not superrefractive--were averaged to obtain the average percent improvement over the default range accuracy by season. The results are tabulated in Table 5. Both verification sources agreed during Autumn that the least skillful range was 20 km. During winter they agreed that the most skillful range was 28 km. They did not concur during Summer or Spring. When the skill scores were averaged over the entire year for the atmospheres which were not superrefractive, both verification sources agreed that the 28-km range provided improved average accuracy over the default range, but they disagreed over the magnitude of improvement. According to profiler verification (Figure 12), 28 km only provided 0.06 percent average improvement. Rawinsonde verification (Figure 13) suggested the 28-km range yielded 1.38 percent better average accuracy. One interesting characteristic of the average skill scores in Figure 12 is that the ranges below 28 km are significantly less skillful than the 28- and 32-km ranges. This suggests that when the radar beam was not superrefracting, the accuracy of the wind data produced by the VAD algorithm was not seriously reduced by the hills to the southwest of the radar.

Table 5. Average Percent Improvement in Accuracy over the Default Range
for the Atmospheres which were **Not Superrefractive**

VAD Range:	20 km	22 km	24 km	26 km	28 km	32 km
Autumn						
<u>Comparison</u>						
VAD - Profiler	-8.6	-4.9	-5.2	-4.8	-0.2	1.5
VAD - Rawinsonde	-3.3	-3.0	-2.2	-0.8	1.9	-0.9
Winter						
<u>Comparison</u>						
VAD - Profiler	-3.7	-3.4	-3.4	-3.5	1.1	0.6
VAD - Rawinsonde	-3.2	-6.7	-3.4	-2.1	1.2	-1.6
Spring						
<u>Comparison</u>						
VAD - Profiler	-1.3	-1.1	-2.3	-1.8	-0.3	1.4
VAD - Rawinsonde	2.7	2.3	1.9	1.2	-0.1	-0.8
Summer						
<u>Comparison</u>						
VAD - Profiler	0.9	0.2	0.3	-0.5	-0.4	-0.2
VAD - Rawinsonde	1.3	-0.4	-0.7	4.2	2.6	0.6

Note: The RMSVD and SS_{alt} values used to obtain these averages are listed in Appendix B.

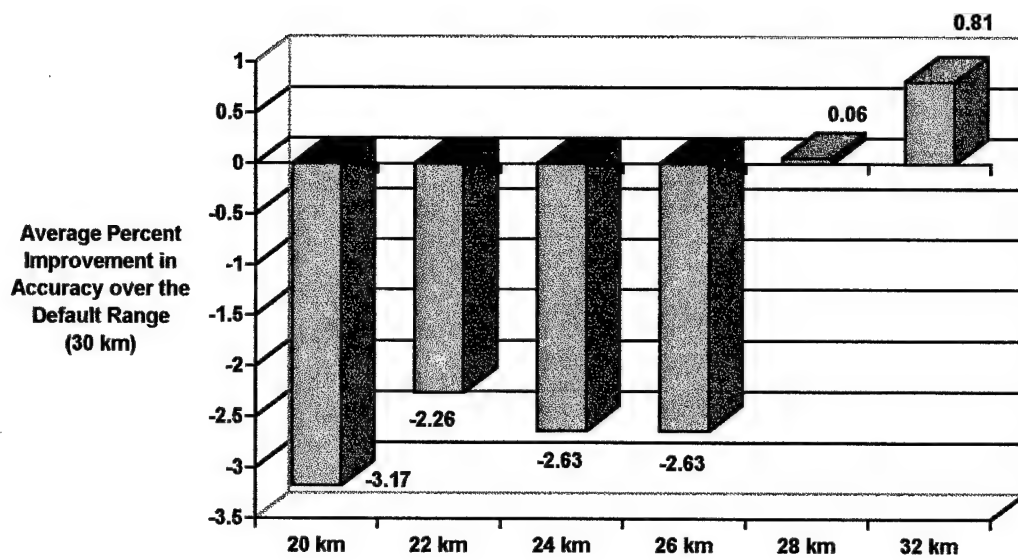


Fig. 12. Skill Scores for Alternative Ranges Obtained Using *Profiler* Data for Verification (Averaged over All Seasons for Atmospheres which were **Not Superrefractive**)

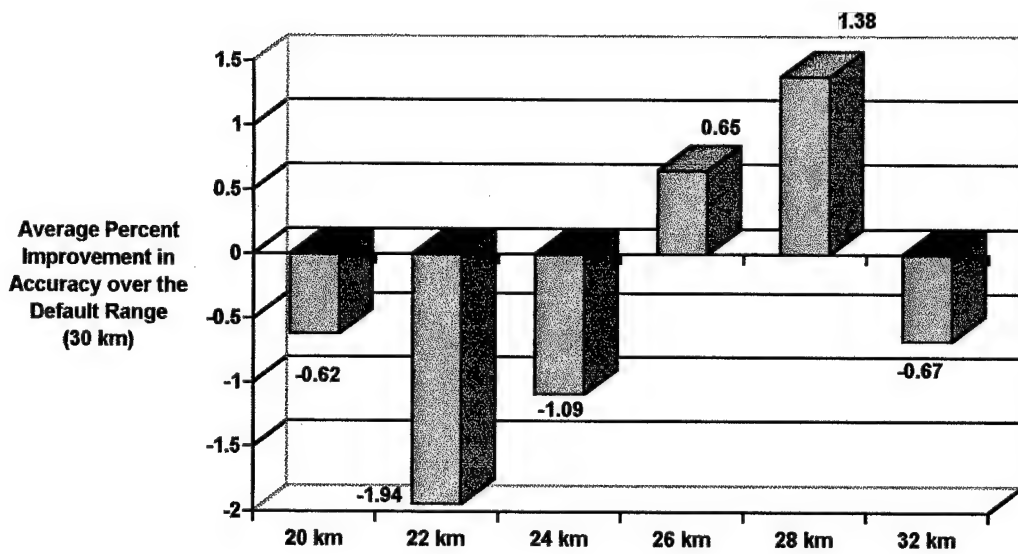


Fig. 13. Skill Scores for Alternative Ranges Obtained Using *Rawinsonde* Data as Verification (Averaged over All Seasons for Atmospheres which were **Not Superrefractive**)

5) *Alternative Range Skill during Autumn.* For each alternative range, the Autumn skill scores were averaged to obtain the average percent improvement in accuracy over the default range for each refractivity state of the atmosphere. The results are tabulated in Table 6. Both sources of verification agreed that during Autumn, the least skillful ranges were those below 26 km and the most skillful ranges were those above 24 km. This concurrence was evident again when the skill scores for each range were averaged over all atmospheric refractivity conditions for the Autumn season (Figures 14 and 15). Both sources of verification agreed that the least skillful ranges were those below 26 km, and that the 28-km range provided improved average accuracy over the default range used by the algorithm.

Table 6. Average Percent Improvement in Accuracy over the Default Range during Autumn

VAD Range:	20 km	22 km	24 km	26 km	28 km	32 km
Superrefractive at the Surface						
<u>Comparison</u>						
VAD - Profiler	-8.1	-8.2	-7.1	-3.1	1.9	-0.7
VAD - Rawinsonde	-13.2	-10.2	-0.3	5.9	0.9	-1.1
Superrefractive Aloft						
<u>Comparison</u>						
VAD - Profiler	-5.1	-5.1	-3.0	0.6	2.7	2.4
VAD - Rawinsonde	-15.6	-15.6	-20.2	-18.4	-0.5	-4.1
Not Superrefractive						
<u>Comparison</u>						
VAD - Profiler	-8.6	-4.9	-5.2	-4.8	-0.2	1.5
VAD - Rawinsonde	-3.3	-3.0	-2.2	-0.8	1.9	-0.9

Note: The RMSVD and SS_{alt} values used to obtain these averages are listed in Appendix B.

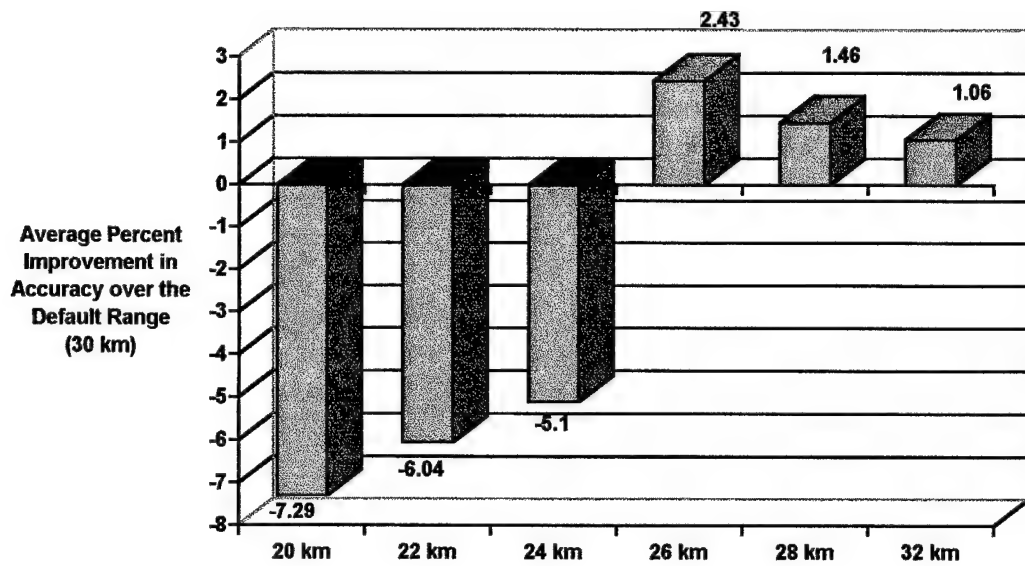


Fig. 14. Skill Scores for Alternative Ranges Obtained Using *Profiler* Data as Verification (Averaged over All Atmospheric Refractivity States for the **Autumn Season**)

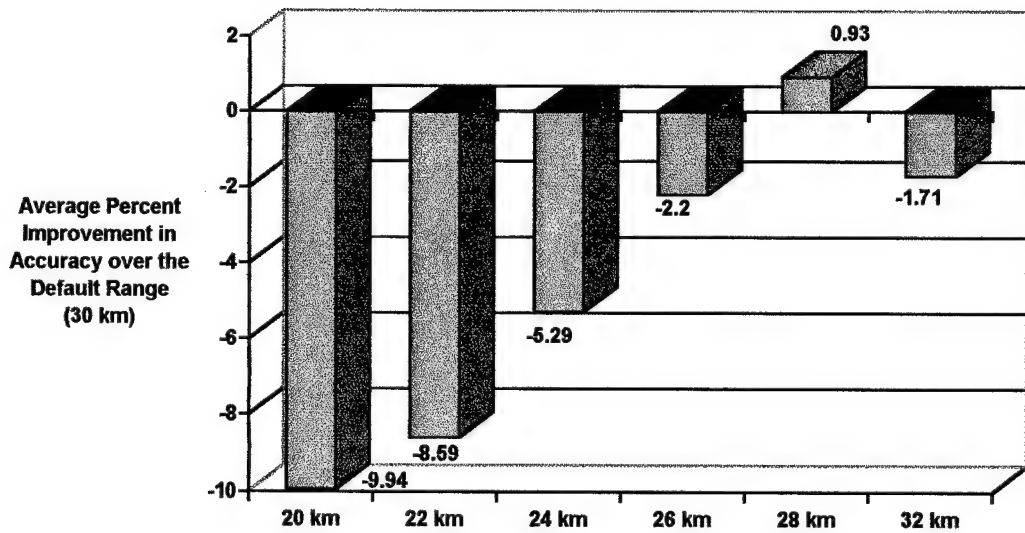


Fig. 15. Skill Scores for Alternative Ranges Obtained Using *Rawinsonde* Data as Verification (Averaged over All Atmospheric Refractivity States for the **Autumn Season**)

6) *Alternative Range Skill during Winter.* For each alternative range, the Winter skill scores were averaged to obtain the average percent improvement in accuracy over the default range for each refractivity state of the atmosphere. The results are tabulated in Table 7. There did not appear to be a strong concurrence in the average skill scores produced by the different sources of verification, except for atmospheres which were not superrefractive, where 28 km was unanimously the most skillful range. When the skill scores for each range were averaged over all atmospheric refractivity conditions for the Winter season (Figures 16 and 17), the results were very similar to those obtained in Autumn. Both sources of verification agreed that the ranges below 26 km were less skillful than the default range, and that the 28-km range provided improved average accuracy over the default range used by the algorithm.

Table 7. Average Percent Improvement in Accuracy over the Default Range during Winter

VAD Range:	20 km	22 km	24 km	26 km	28 km	32 km
Superrefractive at the Surface						
<u>Comparison</u>						
VAD - Profiler	-28.4	7.0	7.9	7.9	0.0	0.0
VAD - Rawinsonde	4.7	3.0	3.1	1.9	3.1	-7.7
Superrefractive Aloft						
<u>Comparison</u>						
VAD - Profiler	-0.1	-1.0	-1.6	4.7	2.0	0.9
VAD - Rawinsonde	-2.3	-1.7	-1.8	-0.7	-1.1	2.2
Not Superrefractive						
<u>Comparison</u>						
VAD - Profiler	-3.7	-3.4	-3.4	-3.5	1.1	0.6
VAD - Rawinsonde	-3.2	-6.7	-3.4	-2.1	1.2	-1.6

Note: The RMSVD and SS_{alt} values used to obtain these averages are listed in Appendix B.

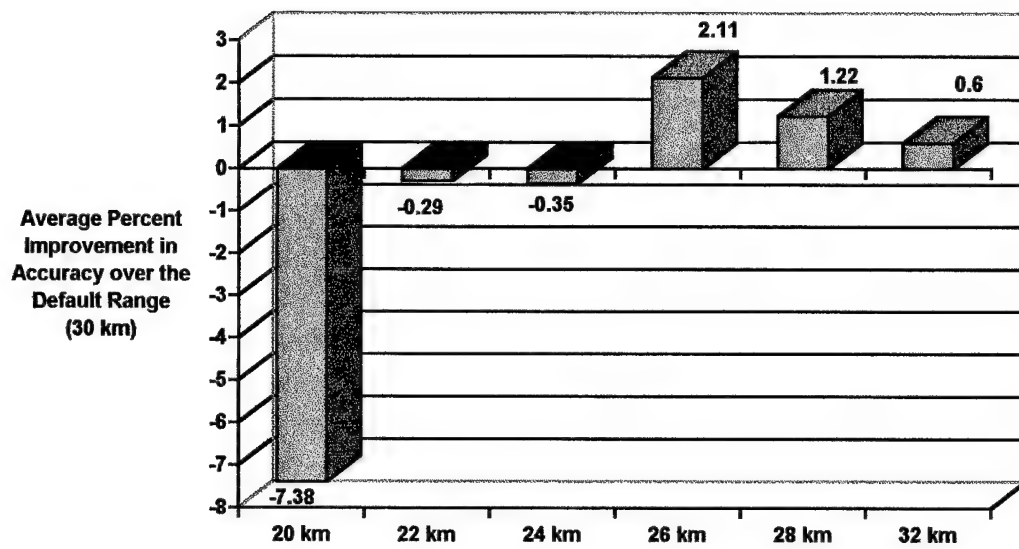


Fig. 16. Skill Scores for Alternative Ranges Obtained Using *Profiler* Data as Verification (Averaged over All Atmospheric Refractivity States for the **Winter Season**)

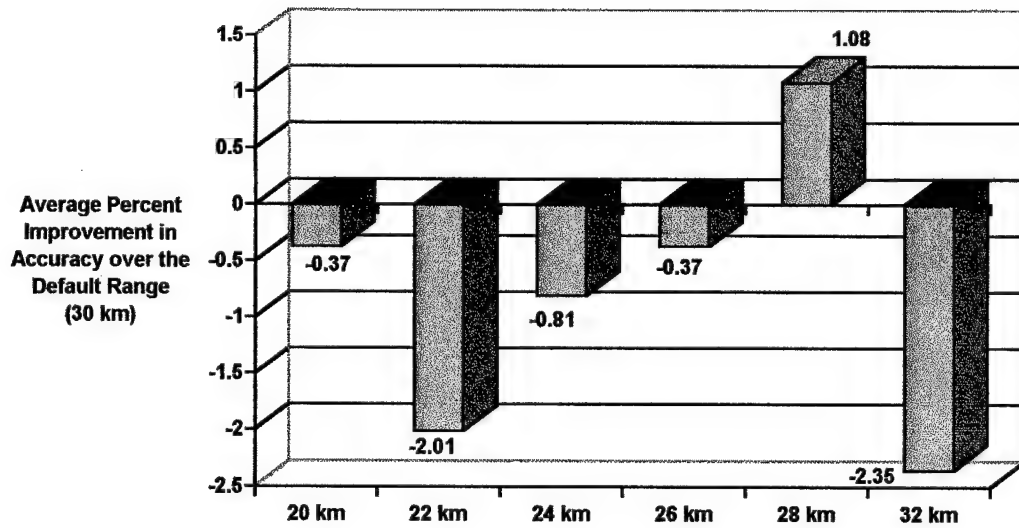


Fig. 17. Skill Scores for Alternative Ranges Obtained Using *Rawinsonde* Data as Verification (Averaged over All Atmospheric Refractivity States for the **Winter Season**)

7) *Alternative Range Skill during Spring.* For each alternative range, the Spring skill scores were averaged to obtain the average percent improvement in accuracy over the default range for each refractivity state of the atmosphere. The results are tabulated in Table 8. For this season, there was very little concordance between the skill scores resulting from the two sources of verification, except for atmospheres which were superrefractive aloft, where the 32-km range was at least 3.2 percent less skillful than the default range. When the skill scores for each range were averaged over all atmospheric refractivity conditions for the Spring season (Figures 18 and 19), the 20-km range provided the greatest average improved accuracy for both sources of verification.

Table 8. Average Percent Improvement in Accuracy over the Default Range during Spring

VAD Range:	20 km	22 km	24 km	26 km	28 km	32 km
Superrefractive at the Surface						
<u>Comparison</u>						
VAD - Profiler	2.9	1.9	1.4	1.3	0.8	-1.2
VAD - Rawinsonde	-5.9	-10.1	-2.6	0.8	-1.2	-1.5
Superrefractive Aloft						
<u>Comparison</u>						
VAD - Profiler	-0.5	-2.1	-2.3	-0.7	0.0	-3.2
VAD - Rawinsonde	7.3	2.5	1.3	2.2	0.0	-5.7
Not Superrefractive						
<u>Comparison</u>						
VAD - Profiler	-1.3	-1.1	-2.3	-1.8	-0.3	1.4
VAD - Rawinsonde	2.7	2.3	1.9	1.2	-0.1	-0.8

Note: The RMSVD and SS_{alt} values used to obtain these averages are listed in Appendix B.

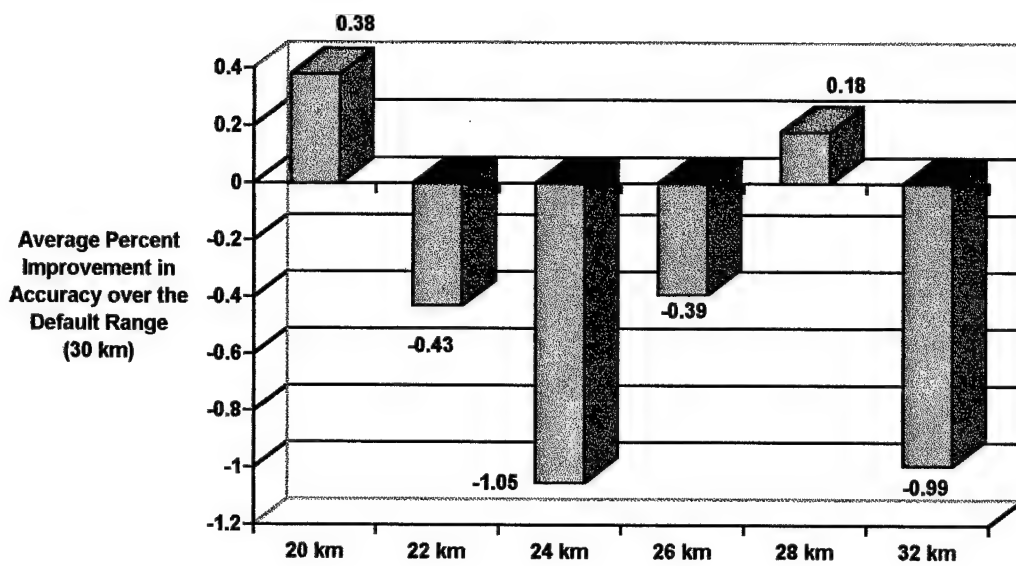


Fig. 18. Skill Scores for Alternative Ranges Obtained Using *Profiler* Data as Verification (Averaged over All Atmospheric Refractivity States for the **Spring Season**)

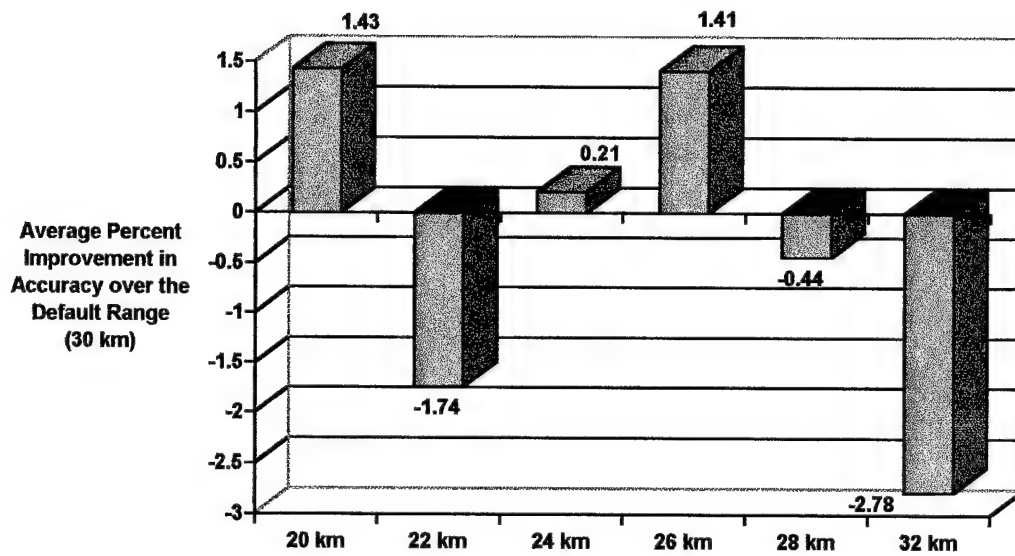


Fig. 19. Skill Scores for Alternative Ranges Obtained Using *Rawinsonde* Data as Verification (Averaged over All Atmospheric Refractivity States for the **Spring Season**)

8) *Alternative Range Skill during Summer*: For each alternative range, the Summer skill scores were averaged to obtain the average percent improvement in accuracy over the default range for each refractivity state of the atmosphere. The results are tabulated in Table 9. For this season, there was general concurrence between the two sources of verification that average accuracy was improved by decreasing the range. When the skill scores for each range were averaged over all atmospheric refractivity conditions for the Summer season (Figures 18 and 19), there was strong concordance that every alternative range shorter than the default range resulted in improved average accuracy, and that the 32-km range was less accurate than the default range. For profiler verification, the most skillful range was 20 km, producing 3.43 percent better average accuracy than the default range. For rawinsonde verification, the 26-km range was most skillful, providing 2.22 percent better average accuracy than the default range.

Table 9. Average Percent Improvement in Accuracy over the Default Range during Summer

VAD Range:	20 km	22 km	24 km	26 km	28 km	32 km
Superrefractive at the Surface						
<u>Comparison</u>						
VAD - Profiler	2.7	2.6	1.2	0.2	0.5	-0.1
VAD - Rawinsonde	1.7	2.2	2.7	2.2	0.9	0.2
Superrefractive Aloft						
<u>Comparison</u>						
VAD - Profiler	6.6	5.6	5.8	2.6	2.3	-1.2
VAD - Rawinsonde	2.3	-0.5	-0.4	0.4	2.1	-1.6
Not Superrefractive						
<u>Comparison</u>						
VAD - Profiler	0.9	0.2	0.3	-0.5	-0.4	-0.2
VAD - Rawinsonde	1.3	-0.4	-0.7	4.2	2.6	0.6

Note: The RMSVD and SS_{alt} values used to obtain these averages are listed in Appendix B.

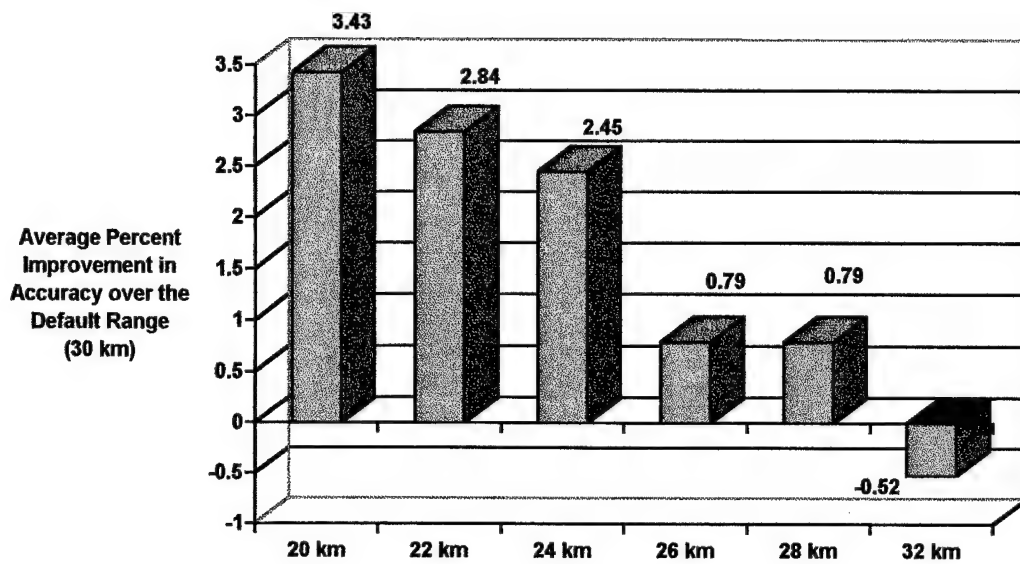


Fig. 20. Skill Scores for Alternative Ranges Obtained Using *Profiler* Data as Verification (Averaged over All Atmospheric Refractivity States for the **Summer Season**)

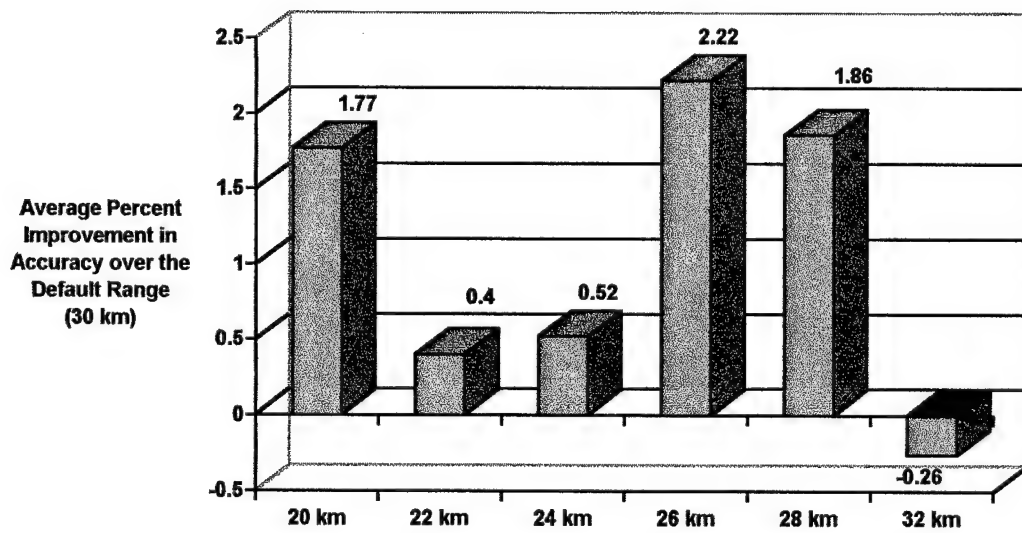


Fig. 21. Skill Scores for Alternative Ranges Obtained Using *Rawinsonde* Data as Verification (Averaged over All Atmospheric Refractivity States for the **Summer Season**)

9) *Alternative Range Skill Overall.* A sense of the overall alternative range skill was obtained by averaging the skill scores for each range over all of the seasons and atmospheric refractivity states. Figure 22 shows the results obtained using profiler verification, and Figure 23 shows the results obtained using rawinsonde verification. The most skillful range overall was 28 km, providing an average improvement in accuracy of at least 0.86 percent over the default range setting. The 26-km range faired well in the overall estimate of average skill using rawinsonde verification, providing an average improvement in accuracy of 0.4 percent over the default range. Using profiler verification, the 26-km range impaired average accuracy by 0.07 percent. Both sources of verification agreed that in the overall estimate of average skill, none of the other ranges provided any improvement in accuracy over the default range setting.⁹

⁹ At first glance, percentage improvements of 0.86 and 0.4 percent may seem fairly insignificant. Unfortunately, it is difficult to determine the statistical significance of these average skill scores without knowing their sampling distribution. Recall that these values represent a 24 week average. Individual skill scores varied widely over that period, with a number of percentage improvements being largely positive and a number of percentage improvements being largely negative.

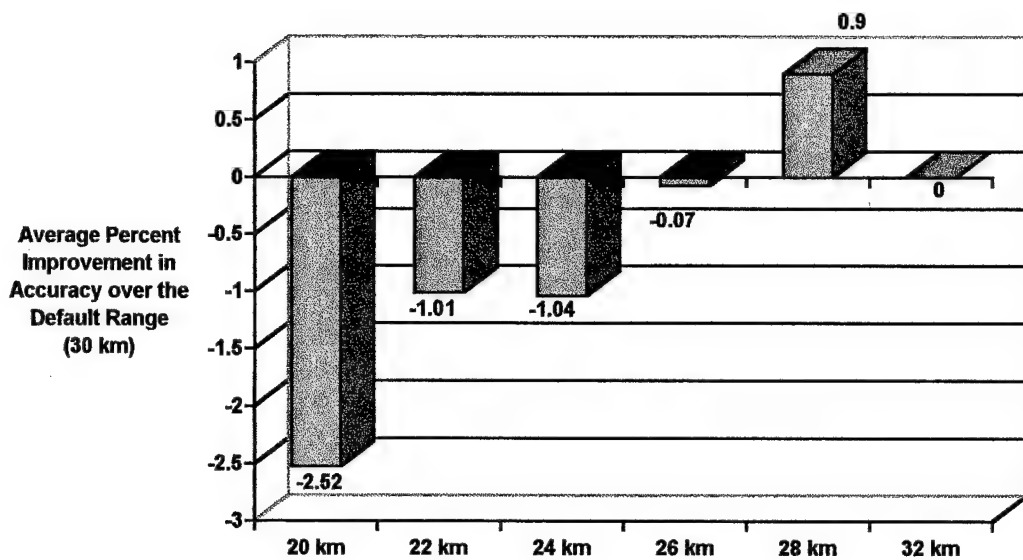


Fig. 22. Skill Scores for Alternative Ranges Obtained Using *Profiler* Data as Verification (Averaged over All Atmospheric Refractivity States and All Seasons)

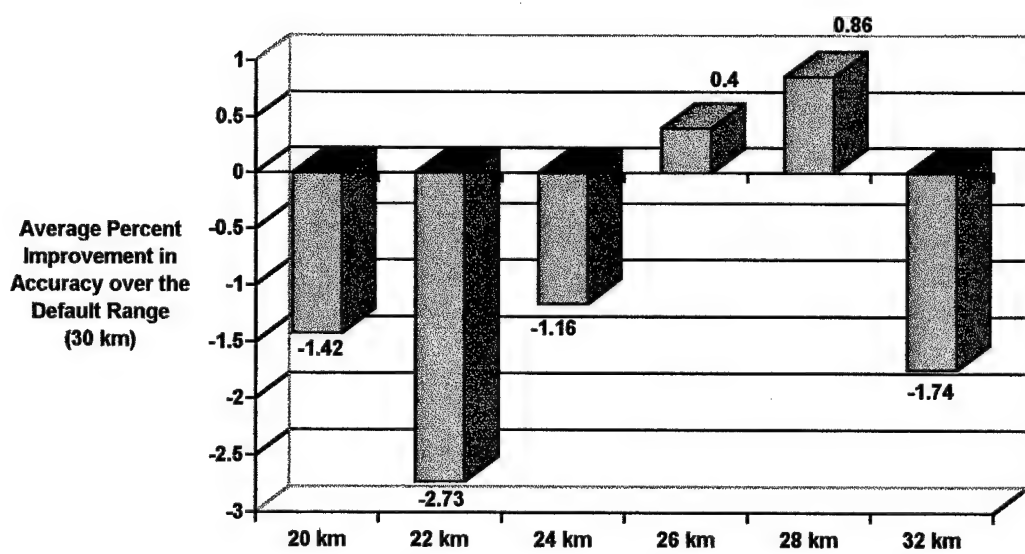


Fig. 23. Skill Scores for Alternative Ranges Obtained Using *Rawinsonde* Data as Verification (Averaged over All Atmospheric Refractivity States and All Seasons)

Chapter 5. Summary & Conclusions

a. Summary

This study sought to improve the operational use of the WSR-88D's VWP product by finding the optimal VAD algorithm Azimuth and Range parameter settings to minimize the reduction in accuracy which results from anomalous propagation through superrefractive layers. The radar chosen for the study, near Denver, suffered from ground contaminated return due to hills located within the default range used by the algorithm. Azimuth optimization was unsuccessful because the hilly sector was too large for the radar to omit from the VAD analysis and still obtain the minimum number of returns required to perform the analysis. On average, range optimization proved more fruitful. Because of the hills located at the 30 km default range used by the algorithm, reducing the range not only improved the accuracy of winds obtained under superrefractive conditions, but also those obtained when the atmosphere was not superrefractive.

b. Conclusions

1). For each refractivity state of the atmosphere, reducing the range resulted in an improvement over default range accuracy, on average. The range which resulted in the greatest average improvement varied for each refractivity state and source of verification data. All ranges which yielded improved accuracy over the default range are summarized for each refractivity condition in Table 10.

Table 10. Summary of Ranges which Yielded an Average* Improvement over Default Range (30 km) Accuracy for Each Atmospheric Refractivity State

Refractivity State of the Atmosphere	Range	Average % Improvement over Default Accuracy	Range	Average % Improvement over Default Accuracy
<i>(Profiler Verification)</i>				
Superrefractive at the Surface	26 km	0.71	26 km	2.72
	28 km	0.09	28 km	0.84
			24 km	0.64
Superrefractive Aloft	26 km	1.80	28 km	0.30
	28 km	1.74		
	20 km	0.23		
Not Superrefractive	32 km	0.81	28 km	1.38
	28 km	0.06	26 km	0.65

* Skill scores for each range were averaged over all four seasons for each refractivity state.

2). For each season, reducing the range resulted in an improvement over default range accuracy, on average. The range which resulted in the greatest average improvement varied for each season and source of verification data. All ranges which yielded improved accuracy over the default range are summarized by season in Table 11.

Table 11. Summary of Ranges which Yielded an Average* Improvement over Default Range (30 km) Accuracy for Each Season

Season	Range	Average % Improvement over Default Accuracy	Range	Average % Improvement over Default Accuracy
<i>(Profiler Verification)</i>				
Autumn	26 km	2.43	28 km	0.93
	28 km	1.46		
	32 km	1.06		
Winter	26 km	2.11	28 km	1.08
	28 km	1.22		
	32 km	0.60		
Spring	20 km	0.38	20 km	1.43
	28 km	0.18	26 km	1.41
			24 km	0.21
Summer	20 km	3.43	26 km	2.22
	22 km	2.84	28 km	1.86
	24 km	2.45	20 km	1.77
	26 km	0.79	24 km	0.52
	28 km	0.79	22 km	0.40

* Skill scores for each range were averaged over all three refractivity states for each season.

3). The most skillful range setting in the overall average was 28 km. It provided an average improvement in accuracy of at least 0.86 percent over the default range, according to both profiler and rawinsonde verification. The 26 km range setting also fared well in the

overall estimate of average skill using rawinsonde verification, but not as well using profiler verification. According to rawinsonde verification, the 26 km range provided an average improvement in accuracy of 0.4 percent over the default range. According to profiler verification, it impaired accuracy by 0.07 percent, on average. One advantage of operating the VAD algorithm with a 26 km range setting, as opposed to a 28 km range setting, was an increase in the number of wind estimates produced at low altitudes. Over the 24 weeks studied, the VAD algorithm provided 13,016 more wind estimates using the 26 km range than it did using the 28 km range. The vast majority of these winds was displayed below 2500 ft (agl) on the VWP.

c. Recommendations for Further Research

The degree to which the VAD algorithm may be optimized by changing its adaptable parameters appears to be dependent upon the topography and radio refractive climatology of the location studied. Stations near the coast or near hills are probably suffering the most from VWP inaccuracies, and could gain the most from a VAD optimization study.

The conclusions made from this research were based on a 24 week sample, and must be substantiated by further research for there to be any significant gain. For Denver in particular, it is important to verify that the winds produced by the VAD algorithm at 26 and 28 km are more accurate than those produced at the default range when the radar beam is undergoing standard refraction. Another study for the area should focus on obtaining much more data which represents standard atmospheric conditions. Implications from such a study would be important for all radars situated near hilly terrain.

Appendix A. Microwave Propagation within the Troposphere

a. Refractivity

The propagation of microwave energy within the troposphere is best understood in terms of the refractive index of the medium through which the energy travels. The index of refraction, n , is a unitless parameter defined as the ratio of the speed of light in a vacuum, c , to the speed of light through the medium, v :

$$n = \frac{c}{v}. \quad (A1)$$

The speed of light in a medium is always less than the speed of light in free space and is calculated from Maxwell's equations. For dry air, the index of refraction is given by

$$(n-1)10^6 = K_1 \frac{p}{T}, \quad (A2)$$

where p is air pressure in hectopascals, T is temperature in Kelvin, and K_1 is an empirically derived constant. For convenience, the left hand side of Equation (A2) is often set equal to N and termed "refractivity." Units of refractivity are known as "N-units," and are equal to $(n-1)10^6$. For dry air, the refractivity is independent of frequency, but when water vapor is added to the air, the refractivity becomes frequency dependent. At microwave frequencies, water molecules acquire electronic polarization and reorient themselves according to changes in the electric field. More complicated, the refractivity of water vapor,

$$N = (n-1)10^6 = \frac{K_3 e}{T^2} - \frac{K_2 e}{T}, \quad (A3)$$

incorporates two new empirically derived constants and is dependent upon the vapor pressure, e , measured in hectopascals. A survey conducted by Bean and Dutton (1966)

found K_1 , K_2 , and K_3 are approximately 77.6 K mb^{-1} , 5.6 K mb^{-1} , and $3.75 \times 10^5 \text{ K}^2 \text{ mb}^{-1}$ at microwave frequencies greater than 2 cm. The right hand sides of Equations (A2) and (A3) add to produce the refractivity for moist air

$$N = 77.6 \frac{p}{T} - 5.6 \frac{e}{T} + 3.75 \cdot 10^5 \frac{e}{T^2}, \quad (\text{A4})$$

where the last term is the contribution from the permanent dipole moment of the water vapor molecule. At all tropospheric temperatures, the contribution of the second term on the right hand side of Equation (A4) is small compared to the contribution from the other two terms. Neglecting the second term and the contribution from carbon dioxide, the refractivity of tropospheric air may be approximated to an accuracy of about 0.1 N-units by the simplified form

$$N = \frac{77.6}{T} \left(p + 4810 \frac{e}{T} \right). \quad (\text{A5})$$

Since the atmosphere is a nonhomogeneous medium, its refractivity varies on all spatial and temporal scales. The smallest scale refractivity fluctuations, on the order tens of centimeters, are tracked by the NOAA Profiler Network vertical wind profilers in order to estimate the translational velocity of the mean wind vector. Most applications concerning the direction of propagation of microwave energy, however, consider average variations only, so that small scale fluctuations are neglected. Also, horizontal variations of refractivity are usually small enough that only the vertical gradient of N is considered when describing the propagation of microwave energy through the near earth atmosphere.¹

¹ The assumption of horizontally uniform refractivity values is similar to the assumption of horizontally homogeneous flow made during the VAD analysis. This assumption is nullified when horizontal nonlinearities in the flow, and in the refractivity, are known to exist (e.g., across gust fronts, sea-breeze fronts, or extra-tropical frontal boundaries).

The vertical gradient of refractivity is easily ascertained through inspection of Equation (A5). Since T typically decreases slowly with height, while p and e decrease rapidly with height, N usually decreases with height. Equation (A1) indicates that an increase in the index of refraction corresponds to a decrease in the speed of light through the medium. Thus, microwave energy generally propagates faster at higher altitudes where refractivity values are smaller. In other words, the consequence of the downward directed refractivity gradient in the nonhomogeneous troposphere is the bending of the radar's beam downward from a straight line as it propagates.

b. Propagation Classifications

The VAD algorithm assumes the microwave energy transmitted by the WSR-88D rises linearly along its path through a 'standard' atmosphere² which consists of contiguous, horizontally stratified, layers of decreasing N . Within the first kilometer of the troposphere, these conditions correspond to a vertical gradient of refractivity between $-25 \text{ N-units km}^{-1}$ (dry atmosphere) and $-54 \text{ N-units km}^{-1}$ (saturated atmosphere). Such a refractivity gradient causes the path of the radar beam to be bent in the shape of an arc, relative to the surface of the earth, with an approximate radius of $4/3$ times the earth's radius. Making the assumption of standard refraction enables the radar to estimate the altitude of scatterers returning energy from any point along the beam's path.

When atmospheric temperature and humidity distributions depart from standard in any layer, anomalous propagation of the radar beam results. $dN/dz > -25 \text{ N-units km}^{-1}$ results in the microwave energy bending less than normal, a condition known as subrefraction. $dN/dz < -54 \text{ N-units km}^{-1}$ results in the microwave energy bending more than normal, a

² Within the troposphere, the standard atmosphere is closely approximated by a linear decrease in temperature of $6.5 \text{ }^{\circ}\text{C km}^{-1}$ and an exponential decrease in pressure from a value of 1013.25 hpa at sea level.

condition known as superrefraction. If superrefraction within a layer is strong enough, $dN/dz < -157$ N-units km⁻¹, and if the microwave energy penetrates the layer with a small enough angle of incidence, the radar beam will be confined within the layer or below a certain height. This circumstance is known as trapping, and the layer of confinement is called a duct (Battan, 1973). Trapped radar beams notoriously intercept meteorological and non-meteorological targets, including objects on the ground, to extended ranges. Ducting layers may also change the shape of the radar beam considerably, resulting in distorted observations. Theoretical studies have shown that trapping should only be expected when the angle of incidence between the radar beam and the superrefractive layer is on the order of 1° to 2° (Battan, 1973; Doviak et al., 1993). Figure A1 illustrates the different classifications of microwave propagation within the troposphere.

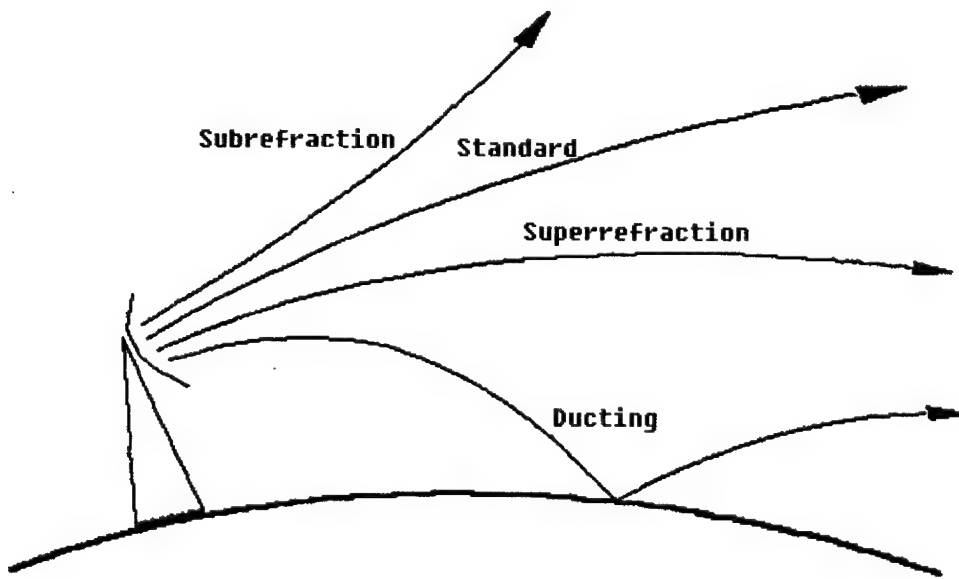


Fig. A1. Standard and Anomalous Propagation Paths (Doggett, 1997)

c. Meteorological Causes of Anomalous Propagation

Once the vertical distributions of temperature and vapor pressure as a function of pressure are known, Equation A5 may be used to calculate the vertical refractivity distribution. As noted previously, refractivity gradients smaller than $-157 \text{ N-units km}^{-1}$ lead to the most significant anomalous propagation. They result from a rapid decrease in vapor pressure or a rapid increase in temperature with increasing height. The most common environment for the simultaneous development of such gradients is within a temperature inversion. By enhancing stability, inversions inhibit turbulent mixing and will induce strong vertical gradients of humidity, providing there is a significant source of moisture at the surface.

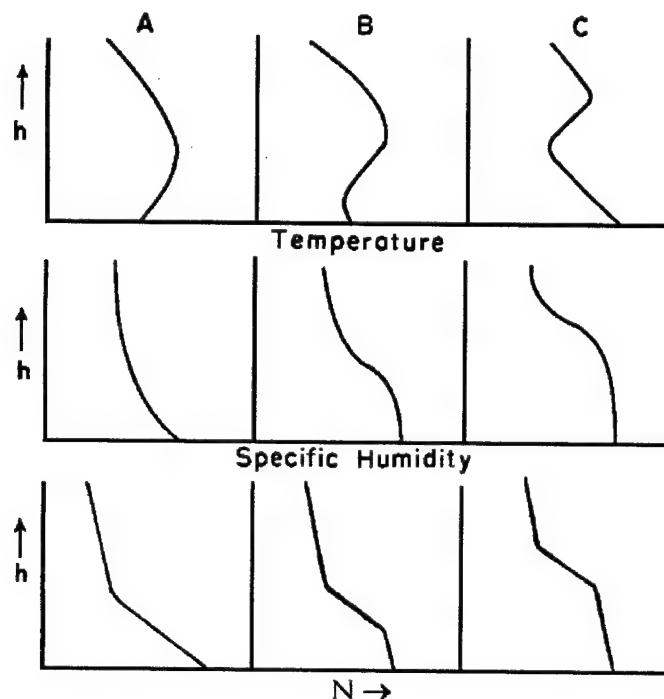


Fig. A2. Temperature and Specific Humidity Distributions Which Induce N Gradients Responsible for Ducting (adapted from Battan, 1973). Columns A and B represent surface ducts, while C represents an elevated duct.

Figure A2 illustrates three different distributions of temperature and specific humidity which produce refractivity gradients strong enough to cause the radar beam to duct. Column A represents one of the most common duct-producing situations over the high plains of Colorado. Radiational cooling on a clear night will typically trigger this kind of surface based temperature inversion. If the ground is moist enough to cause a sharp decrease in moisture with height, then a surface based duct will likely develop. Such profiles may also be triggered by the cool, moist, outflow diverging from underneath a thunderstorm. However, ducts induced by thunderstorms are usually quite localized and last for less than an hour. The profiles in column A are also common in maritime environments when warm, dry air advects over cooler bodies of water.

The profiles in columns B and C also develop in eastern Colorado. The N distribution in column B represents a low level duct triggered by high pressure near the surface. Subsidence within the high results in adiabatic compression and the formation of a temperature inversion close to the ground. Given a strong moisture gradient in the lowest levels, the duct which develops may extend all the way to the ground. The elevated duct within the refractivity distribution of column C results from mid- and upper-level ridges. Subsidence within the ridge may cause an elevated temperature inversion, but a deep moist layer is usually also required to trigger the duct. For this reason, the duct in example B is probably more common in Colorado than the kind in example C. Example B ducts may also occur in maritime environments when turbulent winds advect warm, dry air over cooler water (Battan, 1973).

Appendix B. Statistical Data

This appendix bears the statistical data created for this research. First, the number of wind estimates produced by the VAD algorithm during the study is listed by season. This is followed by lists of the number of matching wind observations, RMSVD values, and SS_{alt} values. Lastly, the RMSVD values calculated during the profiler and rawinsonde comparison are listed. Values which could not be tabulated because of too few matches at a level are represented by "*****."

a. Number of Wind Estimates Produced by the VAD Algorithm

Table B1. Total Number of Wind Barbs Displayed on the VWP during this Study by Range and Season

	Autumn	Winter	Spring	Summer
<u>Range</u>				
20 km	43992	40934	71256	94013
22 km	52230	42587	73615	94569
24 km	45726	42459	73494	94653
26 km	43547	41220	69844	91545
Mean of shortest 4 ranges	46373.8	41800	72052.3	93695
28 km	40143	38310	66020	88667
30 km	42093	39098	67822	90263
32 km	40123	37639	65088	87873
Mean of longest 3 ranges	40786.3	38349	66310	88934.3
Total	307854	282247	487139	641583

Note: This study only examined 6 weeks of data per season.

b. *Statistics Calculated Using Profiler Verification*

1) *Autumn.*

Table B2. The Number of Matches Made between *Profiler* and VAD Data at Each Level during **Autumn** for the Atmosphere which was **Superrefractive at the Surface**

Range:	20 km	22 km	24 km	26 km	28 km	30 km	32 km
Height (m)							
2024	70	70	70	70	30	30	30
2274	72	72	72	72	32	32	32
2524	36	62	62	62	62	62	62
2774	33	31	31	31	31	62	61
3024	61	61	61	31	30	30	30
3274	60	60	59	59	59	59	30
3524	55	55	55	55	56	57	57
3774	56	56	56	56	57	58	58
4024	51	51	51	50	50	50	53
4274	47	47	47	47	47	47	47
4524	41	37	37	37	37	37	37
4774	33	33	33	33	33	33	33
5024	33	33	33	33	33	33	33
5274	29	29	29	29	34	34	34
5524	30	30	30	30	30	33	33
5774	29	29	29	29	29	29	30
6024	23	25	25	25	25	25	25
6274	15	15	20	20	20	20	20
6524	15	15	20	20	20	20	20
6774	14	14	14	18	18	18	18
7024	11	11	11	12	12	12	12
7274	9	9	9	9	11	11	11
7524	8	8	8	8	8	8	8

Table B3. RMSVD Calculated between *Profiler* and VAD Data at Each Level during **Autumn** for the Atmosphere which was **Superrefractive at the Surface**

Range:	20 km	22 km	24 km	26 km	28 km	30 km	32 km
<u>Height (m)</u>							
2024	9.953	9.953	9.953	9.953	6.252	6.252	6.252
2274	9.374	9.374	9.374	9.374	5.541	5.541	5.541
2524	6.62	9.42	9.42	9.42	9.42	9.42	9.42
2774	5.92	5.069	5.069	5.069	5.069	9.137	9.467
3024	12.34	12.34	12.34	7.521	6.786	6.786	6.786
3274	13.62	13.62	15.1	15.03	15.03	15.03	13.65
3524	13.74	13.39	13.39	13.39	15.9	15.73	15.73
3774	12.46	12.39	12.39	12.39	15.56	15.55	15.55
4024	12.59	12.59	12.59	12.74	12.74	12.74	15.85
4274	12.96	12.96	12.96	12.96	12.96	12.87	12.87
4524	12.41	13.07	13.07	13.07	13.07	13.07	13.07
4774	12.05	12.05	12.05	12.69	12.69	12.69	12.69
5024	13.18	13.18	13.18	13.59	13.59	13.59	13.59
5274	16.43	16.43	16.43	16.43	15.28	15.28	15.28
5524	17.04	17.04	17.04	17.04	17.04	16.69	16.69
5774	15.81	15.81	15.81	15.81	15.81	15.81	15.25
6024	16.39	15.6	15.6	15.6	15.6	15.6	15.6
6274	17.36	17.36	14.76	14.76	14.76	14.76	14.76
6524	17.92	17.92	15.41	15.41	15.41	15.41	15.41
6774	20.87	20.87	20.87	18.29	18.29	18.29	18.29
7024	18.06	18.06	18.06	15.72	15.72	15.72	15.72
7274	15.35	15.35	15.35	15.35	14.61	14.61	14.61
7524	14.93	12.65	12.65	12.65	12.65	13	13
Average:	13.80	13.76	13.60	13.23	13.03	13.20	13.26
Standard Deviation:	3.63	3.48	3.31	3.20	3.80	3.47	3.46

Table B4. Skill Score Calculated Using *Profiler* Verification at Each Level during **Autumn** for the Atmosphere which was **Superrefractive at the Surface**

Range:	20 km	22 km	24 km	26 km	28 km	32 km
<u>Height</u> (m)						
2024	-59.2	-59.2	-59.2	-59.2	0.0	0.0
2274	-69.2	-69.2	-69.2	-69.2	0.0	0.0
2524	29.7	0.0	0.0	0.0	0.0	0.0
2774	35.2	44.5	44.5	44.5	44.5	-3.6
3024	-81.8	-81.8	-81.8	-10.8	0.0	0.0
3274	9.4	9.4	-0.5	0.0	0.0	9.2
3524	12.7	14.9	14.9	14.9	-1.1	0.0
3774	19.9	20.3	20.3	20.3	-0.1	0.0
4024	1.2	1.2	1.2	0.0	0.0	-24.4
4274	-0.7	-0.7	-0.7	-0.7	-0.7	0.0
4524	5.0	0.0	0.0	0.0	0.0	0.0
4774	5.0	5.0	5.0	0.0	0.0	0.0
5024	3.0	3.0	3.0	0.0	0.0	0.0
5274	-7.5	-7.5	-7.5	-7.5	0.0	0.0
5524	-2.1	-2.1	-2.1	-2.1	-2.1	0.0
5774	0.0	0.0	0.0	0.0	0.0	3.5
6024	-5.1	0.0	0.0	0.0	0.0	0.0
6274	-17.6	-17.6	0.0	0.0	0.0	0.0
6524	-16.3	-16.3	0.0	0.0	0.0	0.0
6774	-14.1	-14.1	-14.1	0.0	0.0	0.0
7024	-14.9	-14.9	-14.9	0.0	0.0	0.0
7274	-5.1	-5.1	-5.1	-5.1	0.0	0.0
7524	-14.8	2.7	2.7	2.7	2.7	0.0
Average:	-8.1	-8.2	-7.1	-3.1	1.9	-0.7

Table B5. The Number of Matches Made between *Profiler* and VAD Data at Each level during **Autumn** for the Atmosphere which was **Superrefractive Aloft**

Range:	20 km	22 km	24 km	26 km	28 km	30 km	32 km
Height (m)							
2024	176	176	176	176	36	36	36
2274	177	177	177	177	36	36	36
2524	41	41	99	99	99	99	99
2774	41	41	41	41	41	69	60
3024	89	89	89	41	32	32	32
3274	68	68	55	53	53	53	30
3524	47	47	44	44	47	45	45
3774	47	47	44	44	46	44	44
4024	39	39	39	37	37	37	37
4274	33	33	33	33	33	32	32
4524	37	37	28	28	28	28	28
4774	36	36	36	27	27	27	27
5024	36	36	36	27	27	27	27
5274	27	27	27	27	21	21	21
5524	29	29	29	29	29	23	23
5774	35	35	35	35	35	35	25
6024	28	28	29	29	29	29	29
6274	28	28	24	24	24	24	24
6524	28	28	24	24	24	24	24
6774	28	28	28	28	28	28	28
7024	32	32	32	30	30	30	30
7274	30	30	30	30	28	28	28
7524	37	37	37	37	37	33	33

Table B6. RMSVD Calculated between *Profiler* and VAD Data at Each Level during **Autumn** for the Atmosphere which was **Superrefractive Aloft**

Range:	20 km	22 km	24 km	26 km	28 km	30 km	32 km
<u>Height (m)</u>							
2024	12.43	12.43	12.43	12.43	10.49	10.49	10.49
2274	14.22	14.22	14.22	14.22	12.51	12.51	12.51
2524	10.9	10.9	17.87	17.87	17.87	17.87	17.87
2774	10.48	10.48	12.79	12.79	12.79	15.9	14.99
3024	16.87	16.87	16.87	11.89	8.65	8.65	8.65
3274	16	16	15.57	15.62	15.62	15.62	7.214
3524	12.89	12.89	11.07	11.07	11.95	12.49	12.49
3774	14.41	14.41	12.2	12.2	13.36	14	14
4024	10.72	10.72	10.72	11.25	11.25	11.25	10.91
4274	7.989	7.989	7.989	7.989	7.989	10.09	10.09
4524	10.75	10.75	6.288	6.288	6.288	6.288	6.288
4774	12.28	12.28	12.28	10.4	10.4	10.4	10.4
5024	12.11	12.11	12.11	10.68	10.68	10.68	10.68
5274	11.37	11.37	11.37	11.37	12.06	12.06	12.06
5524	14.35	14.35	14.35	14.35	14.35	15.38	15.38
5774	14.64	14.64	14.64	14.64	14.64	14.64	15.84
6024	15.64	15.64	15.15	15.15	15.15	15.15	15.15
6274	14.97	14.97	15.25	15.25	15.25	15.25	15.25
6524	16.28	16.28	17.03	17.03	17.03	17.03	17.03
6774	17.04	17.04	17.04	16.63	16.63	16.63	16.63
7024	18.65	18.65	18.65	19.17	19.17	19.17	19.17
7274	18.88	18.88	18.88	18.88	19.15	19.15	19.15
7524	21.64	21.64	21.61	21.61	21.61	22.78	22.78
Average:	14.15	14.15	14.19	13.86	13.69	14.06	13.70
Standard Deviation :	3.24	3.24	3.60	3.69	3.85	3.86	4.11

Table B7. Skill Score Calculated Using *Profiler* Verification at Each Level during **Autumn** for the Atmosphere which was **Superrefractive Aloft**

Range:	20 km	22 km	24 km	26 km	28 km	32 km
<u>Height (m)</u>						
2024	-18.5	-18.5	-18.5	-18.5	0.0	0.0
2274	-13.7	-13.7	-13.7	-13.7	0.0	0.0
2524	39.0	39.0	0.0	0.0	0.0	0.0
2774	34.1	34.1	19.6	19.6	19.6	5.7
3024	-95.0	-95.0	-95.0	-37.5	0.0	0.0
3274	-2.4	-2.4	0.3	0.0	0.0	53.8
3524	-3.2	-3.2	11.4	11.4	4.3	0.0
3774	-2.9	-2.9	12.9	12.9	4.6	0.0
4024	4.7	4.7	4.7	0.0	0.0	3.0
4274	20.8	20.8	20.8	20.8	20.8	0.0
4524	-71.0	-71.0	0.0	0.0	0.0	0.0
4774	-18.1	-18.1	-18.1	0.0	0.0	0.0
5024	-13.4	-13.4	-13.4	0.0	0.0	0.0
5274	5.7	5.7	5.7	5.7	0.0	0.0
5524	6.7	6.7	6.7	6.7	6.7	0.0
5774	0.0	0.0	0.0	0.0	0.0	-8.2
6024	-3.2	-3.2	0.0	0.0	0.0	0.0
6274	1.8	1.8	0.0	0.0	0.0	0.0
6524	4.4	4.4	0.0	0.0	0.0	0.0
6774	-2.5	-2.5	-2.5	0.0	0.0	0.0
7024	2.7	2.7	2.7	0.0	0.0	0.0
7274	1.4	1.4	1.4	1.4	0.0	0.0
7524	5.0	5.0	5.1	5.1	5.1	0.0
Average:	-5.1	-5.1	-3.0	0.6	2.7	2.4

Table B8. The Number of Matches Made between *Profiler* and VAD Data at Each level during **Autumn** for the Atmosphere which was **Not Superrefractive**

Range: <u>Height (m)</u>	20 km	22 km	24 km	26 km	28 km	30 km	32 km
2024	338	338	338	338	139	139	139
2274	334	334	334	334	137	137	137
2524	143	280	280	280	280	280	280
2774	134	124	124	124	124	277	246
3024	257	257	257	119	82	82	82
3274	194	194	200	197	197	197	82
3524	187	181	181	181	188	187	187
3774	187	181	181	181	188	187	187
4024	166	166	166	165	165	165	173
4274	143	143	143	143	143	144	144
4524	143	136	136	136	136	136	136
4774	123	123	123	124	124	124	124
5024	126	126	126	127	127	127	127
5274	121	121	121	121	123	123	123
5524	112	112	112	112	112	117	117
5774	102	102	102	102	102	102	110
6024	97	95	95	95	95	95	95
6274	90	90	89	89	89	89	89
6524	90	90	89	89	89	89	89
6774	80	80	80	80	80	80	80
7024	73	73	73	68	68	68	68
7274	66	66	66	66	69	69	69
7524	61	56	56	56	56	61	61

Table B9. RMSVD Calculated between *Profiler* and VAD Data at Each Level during Autumn for the Atmosphere which was Not Superrefractive

Range:	20 km	22 km	24 km	26 km	28 km	30 km	32 km
Height (m)							
2024	11.15	11.15	11.15	11.15	13.07	13.07	13.07
2274	13.56	13.56	13.56	13.56	15.39	15.39	15.39
2524	16.59	11.01	11.01	11.01	11.01	11.01	11.01
2774	18.02	16.75	16.75	16.75	16.75	16	13.2
3024	17.53	17.53	17.53	18.23	7.533	7.533	7.533
3274	12.69	12.69	13.9	14.23	14.23	14.23	10.16
3524	12.77	11.94	11.94	11.94	13.29	13.45	13.45
3774	13.76	12.66	12.66	12.66	14.15	14.04	14.04
4024	11.73	11.73	11.73	11.65	11.65	11.65	13.23
4274	13.8	13.8	13.8	13.8	13.8	13.85	13.85
4524	19.6	17.84	17.84	17.84	17.84	17.84	17.84
4774	15.75	15.75	15.75	14.99	14.99	14.99	14.99
5024	15.3	15.3	15.3	14.45	14.45	14.45	14.45
5274	16.03	16.03	16.03	16.03	15.66	15.66	15.66
5524	16.23	16.23	16.23	16.23	16.23	16.1	16.1
5774	17.15	17.15	17.15	17.15	17.15	17.15	16.85
6024	18.59	18.61	18.61	18.61	18.61	18.61	18.61
6274	17.56	17.56	17.39	17.39	17.39	17.39	17.39
6524	17.47	17.47	17.33	17.33	17.33	17.33	17.33
6774	16.52	16.52	16.52	16.03	16.03	16.03	16.03
7024	16.47	16.47	16.47	15.52	15.52	15.52	15.52
7274	17.29	17.29	17.29	17.29	15.9	15.9	15.9
7524	16.86	16.18	16.18	16.18	16.18	16.35	16.35
Average:	15.76	15.27	15.31	15.22	14.96	14.94	14.69
Standard Deviation :	2.27	2.39	2.33	2.35	2.51	2.48	2.61

Table B10. Skill Score Calculated Using *Profiler* Verification at Each Level during **Autumn** for the Atmosphere which was **Not Superrefractive**

Range:	20 km	22 km	24 km	26 km	28 km	32 km
<u>Height (m)</u>						
2024	14.7	14.7	14.7	14.7	0.0	0.0
2274	11.9	11.9	11.9	11.9	0.0	0.0
2524	-50.7	0.0	0.0	0.0	0.0	0.0
2774	-12.6	-4.7	-4.7	-4.7	-4.7	17.5
3024	-132.7	-132.7	-132.7	-142.0	0.0	0.0
3274	10.8	10.8	2.3	0.0	0.0	28.6
3524	5.1	11.2	11.2	11.2	1.2	0.0
3774	2.0	9.8	9.8	9.8	-0.8	0.0
4024	-0.7	-0.7	-0.7	0.0	0.0	-13.6
4274	0.4	0.4	0.4	0.4	0.4	0.0
4524	-9.9	0.0	0.0	0.0	0.0	0.0
4774	-5.1	-5.1	-5.1	0.0	0.0	0.0
5024	-5.9	-5.9	-5.9	0.0	0.0	0.0
5274	-2.4	-2.4	-2.4	-2.4	0.0	0.0
5524	-0.8	-0.8	-0.8	-0.8	-0.8	0.0
5774	0.0	0.0	0.0	0.0	0.0	1.7
6024	0.1	0.0	0.0	0.0	0.0	0.0
6274	-1.0	-1.0	0.0	0.0	0.0	0.0
6524	-0.8	-0.8	0.0	0.0	0.0	0.0
6774	-3.1	-3.1	-3.1	0.0	0.0	0.0
7024	-6.1	-6.1	-6.1	0.0	0.0	0.0
7274	-8.7	-8.7	-8.7	-8.7	0.0	0.0
7524	-3.1	1.0	1.0	1.0	1.0	0.0
Average:	-8.6	-4.9	-5.2	-4.8	-0.2	1.5

2) *Winter.*

Table B11. The Number of Matches Made between *Profiler* and VAD Data at Each level during **Winter** for the Atmosphere which was **Superrefractive at the Surface**

Range:	20 km	22 km	24 km	26 km	28 km	30 km	32 km
Height (m)							
2024	10	10	10	10	2	2	2
2274	10	10	10	10	2	2	2
2524	4	4	4	4	4	4	4
2774	4	3	3	3	3	3	0
3024	8	8	8	4	0	0	0
3274	4	4	2	2	2	2	0
3524	3	3	3	3	2	2	2
3774	3	3	3	3	2	2	2
4024	0	0	0	0	0	0	1
4274	0	0	0	0	0	0	0
4524	3	0	0	0	0	0	0
4774	3	3	3	0	0	0	0
5024	3	3	3	0	0	0	0
5274	3	3	3	3	0	0	0
5524	0	0	0	0	0	0	0
5774	0	0	0	0	0	0	0
6024	0	0	0	0	0	0	0
6274	1	1	1	1	1	1	1
6524	1	1	1	1	1	1	1
6774	3	3	3	3	3	3	3
7024	2	2	2	2	2	2	2
7274	0	0	0	0	0	0	0
7524	1	1	1	1	1	1	1

Table B12. RMSVD Calculated between *Profiler* and VAD Data at Each Level during Winter for the Atmosphere which was **Superrefractive at the Surface**

Range:	20 km	22 km	24 km	26 km	28 km	30 km	32 km
<u>Height (m)</u>							
2024	11.85	11.85	11.85	11.85	23.21	23.21	23.21
2274	11.6	11.6	11.6	11.6	26.44	26.44	26.44
2524	27.39	5.22	5.22	5.22	5.22	5.22	5.22
2774	27.56	27.67	27.67	27.67	27.67	27.67	*****
3024	22.01	22.01	22.01	29.32	*****	*****	*****
3274	11.89	11.89	10.71	10.71	10.71	10.71	*****
3524	12.37	12.37	12.37	12.37	11.66	11.66	11.66
3774	13.87	13.87	13.87	13.87	13.33	13.33	13.33
4024	*****	*****	*****	*****	*****	*****	19.18
4274	*****	*****	*****	*****	*****	*****	*****
4524	21.81	*****	*****	*****	*****	*****	*****
4774	10.12	10.12	10.12	*****	*****	*****	*****
5024	12.05	12.05	12.05	*****	*****	*****	*****
5274	10.25	10.25	10.25	10.25	*****	*****	*****
5524	*****	*****	*****	*****	*****	*****	*****
5774	*****	*****	*****	*****	*****	*****	*****
6024	*****	*****	*****	*****	*****	*****	*****
6274	50.51	50.51	50.51	50.51	50.51	50.51	50.51
6524	62.23	62.23	62.23	62.23	62.23	62.23	62.23
6774	101.9	101.9	101.9	101.9	101.9	101.9	101.9
7024	58.47	58.47	58.47	58.47	58.47	58.47	58.47
7274	*****	*****	*****	*****	*****	*****	*****
7524	73.97	73.97	73.97	73.97	73.97	73.97	73.97
Average:	31.76	31.00	30.93	34.28	38.78	38.78	40.56
Standard Deviation :	27.54	29.11	29.17	30.05	30.32	30.32	30.91

Table B13. Skill Score Calculated Using *Profiler* Verification at Each Level during Winter for the Atmosphere which was **Superrefractive at the Surface**

Range:	20 km	22 km	24 km	26 km	28 km	32 km
<u>Height (m)</u>						
2024	48.9	48.9	48.9	48.9	0.0	0.0
2274	56.1	56.1	56.1	56.1	0.0	0.0
2524	-424.7	0.0	0.0	0.0	0.0	0.0
2774	0.4	0.0	0.0	0.0	0.0	*****
3024	*****	*****	*****	*****	*****	*****
3274	-11.0	-11.0	0.0	0.0	0.0	*****
3524	-6.1	-6.1	-6.1	-6.1	0.0	0.0
3774	-4.1	-4.1	-4.1	-4.1	0.0	0.0
4024	*****	*****	*****	*****	*****	*****
4274	*****	*****	*****	*****	*****	*****
4524	*****	*****	*****	*****	*****	*****
4774	*****	*****	*****	*****	*****	*****
5024	*****	*****	*****	*****	*****	*****
5274	*****	*****	*****	*****	*****	*****
5524	*****	*****	*****	*****	*****	*****
5774	*****	*****	*****	*****	*****	*****
6024	*****	*****	*****	*****	*****	*****
6274	0.0	0.0	0.0	0.0	0.0	0.0
6524	0.0	0.0	0.0	0.0	0.0	0.0
6774	0.0	0.0	0.0	0.0	0.0	0.0
7024	0.0	0.0	0.0	0.0	0.0	0.0
7274	*****	*****	*****	*****	*****	*****
7524	0.0	0.0	0.0	0.0	0.0	0.0
Average:	-28.4	7.0	7.9	7.9	0.0	0.0

Table B14. The Number of Matches Made between *Profiler* and VAD Data at Each level during **Winter** for the Atmosphere which was **Superrefractive Aloft**

Range:	20 km	22 km	24 km	26 km	28 km	30 km	32 km
Height (m)							
2024	171	171	171	172	25	25	25
2274	171	171	171	172	25	25	25
2524	28	184	184	184	184	184	184
2774	29	28	28	28	28	107	99
3024	110	110	110	29	21	21	21
3274	89	89	88	89	89	89	26
3524	72	71	71	71	79	82	82
3774	70	69	69	69	79	82	82
4024	69	69	69	66	66	66	69
4274	60	60	60	60	60	57	57
4524	59	62	62	62	62	62	62
4774	59	59	59	62	62	62	62
5024	59	59	59	62	62	62	62
5274	64	64	64	64	65	65	65
5524	64	64	64	64	64	65	65
5774	69	69	69	69	69	69	67
6024	71	72	72	72	72	72	72
6274	67	67	69	69	69	69	69
6524	67	67	69	69	69	69	69
6774	71	71	71	68	68	68	68
7024	68	68	68	65	65	65	65
7274	71	71	71	70	62	63	62
7524	71	63	63	63	63	55	55

Table B15. RMSVD Calculated between *Profiler* and VAD Data at Each Level during
Winter for the Atmosphere which was **Superrefractive Aloft**

Range:	20 km	22 km	24 km	26 km	28 km	30 km	32 km
Height (m)							
2024	11.4	11.4	11.4	11.38	12.24	12.24	12.24
2274	13.48	13.48	13.48	13.47	12.69	12.69	12.69
2524	11.51	17.04	17.04	17.04	17.04	17.04	17.04
2774	10.84	9.942	9.942	9.942	9.942	17.56	17.9
3024	18.63	18.63	18.63	6.776	7.995	7.995	7.995
3274	17.1	17.1	20.9	21.02	21.02	21.02	10.61
3524	17.24	16.49	16.49	16.48	21.1	20.87	20.87
3774	19.13	18.25	18.25	18.25	22.6	22.09	22.09
4024	16.99	16.99	16.99	17.74	17.74	17.74	23.45
4274	16.65	16.65	16.65	16.65	16.65	16.89	16.89
4524	17.64	16.95	16.95	16.95	16.95	16.95	16.95
4774	17.11	17.11	17.11	16.73	16.73	16.73	16.73
5024	18.49	18.49	18.49	18.05	18.05	18.05	18.05
5274	20.14	20.14	20.14	20.14	19.91	19.91	19.91
5524	21.02	21.02	21.02	21.02	21.02	20.81	20.81
5774	26.11	26.11	26.11	26.11	26.11	26.11	24.79
6024	27.36	27.11	27.11	27.11	27.11	27.11	27.11
6274	26.31	26.31	25.8	25.8	25.8	25.8	25.8
6524	27.52	27.52	27.06	27.06	27.06	27.06	27.06
6774	26.37	26.37	26.37	26.55	26.55	26.55	26.55
7024	26.89	26.89	26.89	27.46	27.46	27.46	27.46
7274	27.05	27.05	27.05	27.01	28.69	28.7	28.69
7524	26.68	28.52	28.52	28.52	28.52	30.03	30.03
Average:	20.07	20.24	20.36	19.88	20.39	20.76	20.51
Standard Deviation:	5.64	5.59	5.50	6.22	6.15	5.84	6.16

Table B16. Skill Score Calculated Using *Profiler* Verification at Each Level during **Winter** for the Atmosphere which was **Superrefractive Aloft**

Range: <u>Height (m)</u>	20 km	22 km	24 km	26 km	28 km	32 km
2024	6.9	6.9	6.9	7.0	0.0	0.0
2274	-6.2	-6.2	-6.2	-6.1	0.0	0.0
2524	32.5	0.0	0.0	0.0	0.0	0.0
2774	38.3	43.4	43.4	43.4	43.4	-1.9
3024	-133.0	-133.0	-133.0	15.2	0.0	0.0
3274	18.6	18.6	0.6	0.0	0.0	49.5
3524	17.4	21.0	21.0	21.0	-1.1	0.0
3774	13.4	17.4	17.4	17.4	-2.3	0.0
4024	4.2	4.2	4.2	0.0	0.0	-32.2
4274	1.4	1.4	1.4	1.4	1.4	0.0
4524	-4.1	0.0	0.0	0.0	0.0	0.0
4774	-2.3	-2.3	-2.3	0.0	0.0	0.0
5024	-2.4	-2.4	-2.4	0.0	0.0	0.0
5274	-1.2	-1.2	-1.2	-1.2	0.0	0.0
5524	-1.0	-1.0	-1.0	-1.0	-1.0	0.0
5774	0.0	0.0	0.0	0.0	0.0	5.1
6024	-0.9	0.0	0.0	0.0	0.0	0.0
6274	-2.0	-2.0	0.0	0.0	0.0	0.0
6524	-1.7	-1.7	0.0	0.0	0.0	0.0
6774	0.7	0.7	0.7	0.0	0.0	0.0
7024	2.1	2.1	2.1	0.0	0.0	0.0
7274	5.7	5.7	5.7	5.9	0.0	0.0
7524	11.2	5.0	5.0	5.0	5.0	0.0
Average:	-0.1	-1.0	-1.6	4.7	2.0	0.9

Table B17. The Number of Matches Made between *Profiler* and VAD Data at Each level during Winter for the Atmosphere which was **Not Superrefractive**

Range: <u>Height (m)</u>	20 km	22 km	24 km	26 km	28 km	30 km	32 km
2024	104	104	104	104	80	79	80
2274	104	104	104	104	80	79	80
2524	80	61	61	61	61	61	61
2774	81	78	78	78	78	83	51
3024	82	82	82	77	46	46	46
3274	57	57	58	55	55	55	49
3524	56	51	51	51	56	50	50
3774	56	51	51	51	56	50	50
4024	39	39	39	37	37	37	40
4274	39	39	39	39	39	34	34
4524	34	25	25	25	25	25	25
4774	26	26	26	22	22	22	22
5024	26	26	26	22	22	22	22
5274	21	21	21	21	18	18	18
5524	20	20	20	20	20	15	15
5774	19	19	19	19	19	18	16
6024	19	19	19	19	19	19	19
6274	18	18	16	16	16	16	16
6524	18	18	16	16	16	16	16
6774	18	18	18	15	15	15	15
7024	20	20	20	14	14	14	14
7274	18	18	18	18	14	14	14
7524	14	13	13	13	13	12	12

Table B18. RMSVD Calculated between *Profiler* and VAD Data at Each Level during **Winter** for the Atmosphere which was **Not Superrefractive**

Range:	20 km	22 km	24 km	26 km	28 km	30 km	32 km
Height (m)							
2024	9.345	9.345	9.345	9.345	6.173	6.194	6.173
2274	10.24	10.24	10.24	10.24	6.197	6.191	6.197
2524	5.416	7.201	7.201	7.201	7.201	7.201	7.201
2774	5.597	6.912	6.912	6.912	6.912	7.393	6.498
3024	8.323	8.323	8.323	8.4	6.199	6.199	6.199
3274	11.73	11.73	10.58	10.83	10.83	10.83	9.789
3524	11.7	9.454	9.454	9.454	11.6	11.79	11.79
3774	14.93	12.42	12.42	12.42	14.61	14.98	14.98
4024	13.25	13.25	13.25	14.79	14.79	14.8	17.19
4274	16.68	16.68	16.68	16.68	16.68	18.58	18.58
4524	19.66	14.06	14.06	14.06	14.06	14.06	14.06
4774	16.39	16.39	16.39	14.23	14.23	14.23	14.23
5024	16.95	16.95	16.95	14.15	14.15	14.15	14.15
5274	11.81	11.81	11.81	11.81	12.91	12.91	12.91
5524	14.32	14.32	14.32	14.32	14.32	14.91	14.91
5774	15.99	15.99	15.99	15.99	15.99	15.95	14.78
6024	15.05	18.19	18.19	18.19	18.19	18.19	18.19
6274	18.02	18.02	19.04	19.04	19.04	19.04	19.04
6524	19.8	19.8	20.92	20.92	20.92	20.92	20.92
6774	18.49	18.49	18.49	20.13	20.13	20.13	20.13
7024	17.18	17.18	17.18	20.46	20.46	20.46	20.46
7274	16.24	16.24	16.24	16.24	17.02	17.02	17.02
7524	15.54	16.91	16.91	16.91	16.91	17.03	17
Average:	14.03	13.91	13.95	14.03	13.89	14.05	14.02
Standard Deviation:	4.13	3.90	4.07	4.25	4.75	4.79	4.91

Table B19. Skill Score Calculated Using *Profiler* Verification at Each Level during **Winter** for the Atmosphere which was **Not Superrefractive**

Range: <u>Height (m)</u>	20 km	22 km	24 km	26 km	28 km	32 km
2024	-50.9	-50.9	-50.9	-50.9	0.3	0.3
2274	-65.4	-65.4	-65.4	-65.4	-0.1	-0.1
2524	24.8	0.0	0.0	0.0	0.0	0.0
2774	24.3	6.5	6.5	6.5	6.5	12.1
3024	-34.3	-34.3	-34.3	-35.5	0.0	0.0
3274	-8.3	-8.3	2.3	0.0	0.0	9.6
3524	0.8	19.8	19.8	19.8	1.6	0.0
3774	0.3	17.1	17.1	17.1	2.5	0.0
4024	10.5	10.5	10.5	0.1	0.1	-16.1
4274	10.2	10.2	10.2	10.2	10.2	0.0
4524	-39.8	0.0	0.0	0.0	0.0	0.0
4774	-15.2	-15.2	-15.2	0.0	0.0	0.0
5024	-19.8	-19.8	-19.8	0.0	0.0	0.0
5274	8.5	8.5	8.5	8.5	0.0	0.0
5524	4.0	4.0	4.0	4.0	4.0	0.0
5774	-0.3	-0.3	-0.3	-0.3	-0.3	7.3
6024	17.3	0.0	0.0	0.0	0.0	0.0
6274	5.4	5.4	0.0	0.0	0.0	0.0
6524	5.4	5.4	0.0	0.0	0.0	0.0
6774	8.1	8.1	8.1	0.0	0.0	0.0
7024	16.0	16.0	16.0	0.0	0.0	0.0
7274	4.6	4.6	4.6	4.6	0.0	0.0
7524	8.7	0.7	0.7	0.7	0.7	0.2
Average:	-3.7	-3.4	-3.4	-3.5	1.1	0.6

3) *Spring*

Table B20. The Number of Matches Made between *Profiler* and VAD Data at Each level during **Spring** for the Atmosphere which was **Superrefractive at the Surface**

Range:	20 km	22 km	24 km	26 km	28 km	30 km	32 km
Height (m)							
2024	531	531	531	531	364	364	364
2274	533	533	533	533	365	365	365
2524	361	485	485	485	485	485	485
2774	348	333	333	333	333	471	451
3024	441	441	441	313	272	272	272
3274	374	374	381	341	341	341	215
3524	348	308	308	308	328	295	295
3774	350	310	310	310	330	298	298
4024	287	287	287	244	244	244	266
4274	225	225	225	225	225	184	184
4524	248	195	195	195	195	195	195
4774	215	215	215	177	177	177	177
5024	213	213	213	175	175	175	175
5274	191	191	191	191	178	178	178
5524	202	202	202	202	202	181	181
5774	201	201	201	201	201	201	173
6024	191	187	187	187	187	187	187
6274	184	184	181	181	181	181	181
6524	184	184	181	181	181	181	181
6774	186	186	186	158	158	158	158
7024	159	159	159	159	159	159	159
7274	165	165	165	165	155	155	155
7524	148	163	163	163	163	135	135

Table B21. RMSVD Calculated between *Profiler* and VAD Data at Each Level during Spring for the Atmosphere which was **Superrefractive at the Surface**

Range:	20 km	22 km	24 km	26 km	28 km	30 km	32 km
<u>Height (m)</u>							
2024	11.13	11.13	11.13	11.13	10.8	10.8	10.8
2274	10.41	10.41	10.41	10.41	10.67	10.67	10.67
2524	10.07	10.53	10.53	10.53	10.53	10.53	10.53
2774	11.1	11.33	11.33	11.33	11.33	10.99	11.61
3024	11.5	11.5	11.5	11.36	11.97	11.97	11.97
3274	11.94	11.94	12.42	13.07	13.07	13.07	12.48
3524	12.13	12.78	12.78	12.78	13.51	14.57	14.57
3774	13.05	13.55	13.55	13.55	14.37	15.45	15.45
4024	14.64	14.64	14.64	14.96	14.96	14.96	16.7
4274	13.96	13.96	13.96	13.96	13.96	14.79	14.79
4524	12.79	13.53	13.53	13.53	13.53	13.53	13.53
4774	12.14	12.14	12.14	13.27	13.27	13.27	13.27
5024	13.37	13.37	13.37	14.03	14.03	14.03	14.03
5274	12.21	12.21	12.21	12.21	12.56	12.56	12.56
5524	11.21	11.21	11.21	11.21	11.21	12.11	12.11
5774	10.67	10.67	10.67	10.67	10.67	10.67	12.27
6024	9.708	10.26	10.26	10.26	10.26	10.26	10.26
6274	9.869	9.869	10.36	10.36	10.36	10.36	10.36
6524	9.95	9.95	10.04	10.04	10.04	10.04	10.04
6774	10.51	10.51	10.51	9.219	9.219	9.219	9.219
7024	11.97	11.97	11.97	11.8	11.8	11.8	11.8
7274	11.81	11.81	11.81	11.81	11.12	11.12	11.12
7524	11.78	11.73	11.73	11.73	11.73	11.06	11.06
Average:	11.65	11.78	11.83	11.88	11.96	12.08	12.23
Standard Deviation:	1.32	1.34	1.31	1.52	1.60	1.80	1.91

Table B22. Skill Score Calculated Using *Profiler* Verification at Each Level during Spring for the Atmosphere which was **Superrefractive at the Surface**

Range: <u>Height (m)</u>	20 km	22 km	24 km	26 km	28 km	32 km
2024	-3.1	-3.1	-3.1	-3.1	0.0	0.0
2274	2.4	2.4	2.4	2.4	0.0	0.0
2524	4.4	0.0	0.0	0.0	0.0	0.0
2774	-1.0	-3.1	-3.1	-3.1	-3.1	-5.6
3024	3.9	3.9	3.9	5.1	0.0	0.0
3274	8.6	8.6	5.0	0.0	0.0	4.5
3524	16.7	12.3	12.3	12.3	7.3	0.0
3774	15.5	12.3	12.3	12.3	7.0	0.0
4024	2.1	2.1	2.1	0.0	0.0	-11.6
4274	5.6	5.6	5.6	5.6	5.6	0.0
4524	5.5	0.0	0.0	0.0	0.0	0.0
4774	8.5	8.5	8.5	0.0	0.0	0.0
5024	4.7	4.7	4.7	0.0	0.0	0.0
5274	2.8	2.8	2.8	2.8	0.0	0.0
5524	7.4	7.4	7.4	7.4	7.4	0.0
5774	0.0	0.0	0.0	0.0	0.0	-15.0
6024	5.4	0.0	0.0	0.0	0.0	0.0
6274	4.7	4.7	0.0	0.0	0.0	0.0
6524	0.9	0.9	0.0	0.0	0.0	0.0
6774	-14.0	-14.0	-14.0	0.0	0.0	0.0
7024	-1.4	-1.4	-1.4	0.0	0.0	0.0
7274	-6.2	-6.2	-6.2	-6.2	0.0	0.0
7524	-6.5	-6.1	-6.1	-6.1	-6.1	0.0
Average:	2.9	1.9	1.4	1.3	0.8	-1.2

Table B23. The Number of Matches Made between *Profiler* and VAD Data at Each level
during **Spring** for the Atmosphere which was **Superrefractive Aloft**

Range: <u>Height (m)</u>	20 km	22 km	24 km	26 km	28 km	30 km	32 km
2024	143	143	143	143	51	51	51
2274	145	145	145	145	51	51	51
2524	60	125	125	125	125	125	125
2774	60	57	57	57	57	57	115
3024	143	143	143	58	38	38	38
3274	124	124	115	114	114	114	41
3524	116	110	110	110	104	104	103
3774	117	111	111	111	105	105	104
4024	84	84	84	84	84	84	86
4274	60	60	60	60	60	60	61
4524	51	46	46	46	46	46	46
4774	52	52	52	50	50	50	50
5024	57	57	57	55	55	55	55
5274	46	46	46	46	48	48	48
5524	35	35	35	35	35	35	35
5774	28	28	28	28	28	28	34
6024	22	21	21	21	21	21	22
6274	26	26	28	28	28	28	28
6524	26	26	28	28	28	28	28
6774	28	28	28	30	30	30	30
7024	20	20	20	24	24	24	25
7274	23	23	23	23	28	28	28
7524	18	24	24	24	24	24	23

Table B24. RMSVD Calculated between *Profiler* and VAD Data at Each Level during Spring for the Atmosphere which was Superrefractive Aloft

Range:	20 km	22 km	24 km	26 km	28 km	30 km	32 km
Height (m)							
2024	9.141	9.141	9.141	9.141	7.806	7.806	7.806
2274	10.84	10.84	10.84	10.84	7.442	7.442	7.442
2524	7.726	12.29	12.29	12.29	12.29	12.29	12.29
2774	8.48	8.522	8.522	8.522	8.522	8.522	13.83
3024	15.89	15.89	15.89	10.63	13.57	13.57	13.57
3274	14.68	14.68	17.07	17.43	17.43	17.43	11.99
3524	15.2	15.83	15.83	15.83	19.34	19.34	19.81
3774	17.74	18.45	18.45	18.45	21.4	21.4	21.94
4024	17.57	17.57	17.57	17.78	17.78	17.78	23.07
4274	17.85	17.85	17.85	17.85	17.85	17.85	17.7
4524	18.99	19.21	19.21	19.21	19.21	19.21	19.21
4774	19.72	19.72	19.72	20.47	20.47	20.47	20.47
5024	23.4	23.4	23.4	24.11	24.11	24.11	24.11
5274	24.82	24.82	24.82	24.82	24.9	24.9	24.9
5524	24.73	24.73	24.73	24.73	24.73	24.73	25.25
5774	27.17	27.17	27.17	27.17	27.17	27.17	25.3
6024	23.01	24.23	24.23	24.23	24.23	24.23	23.69
6274	24.16	24.16	23.19	23.19	23.19	23.19	23.19
6524	26.41	26.41	25.31	25.31	25.31	25.31	25.31
6774	24.22	24.22	24.22	23.75	23.75	23.75	23.75
7024	24.72	24.72	24.72	23.3	23.3	23.3	25.92
7274	29.37	29.37	29.37	29.37	27.51	27.51	27.51
7524	27.5	24.04	24.04	24.04	24.04	24.04	24.95
Average:	19.71	19.88	19.89	19.67	19.80	19.80	20.13
Standard Deviation:	6.50	6.02	5.87	6.08	6.13	6.13	6.06

Table B25. Skill Score Calculated Using *Profiler* Verification at Each Level during Spring for the Atmosphere which was Superrefractive Aloft

Range: Height (m)	20 km	22 km	24 km	26 km	28 km	32 km
2024	-17.1	-17.1	-17.1	-17.1	0.0	0.0
2274	-45.7	-45.7	-45.7	-45.7	0.0	0.0
2524	37.1	0.0	0.0	0.0	0.0	0.0
2774	0.5	0.0	0.0	0.0	0.0	-62.3
3024	-17.1	-17.1	-17.1	21.7	0.0	0.0
3274	15.8	15.8	2.1	0.0	0.0	31.2
3524	21.4	18.1	18.1	18.1	0.0	-2.4
3774	17.1	13.8	13.8	13.8	0.0	-2.5
4024	1.2	1.2	1.2	0.0	0.0	-29.8
4274	0.0	0.0	0.0	0.0	0.0	0.8
4524	1.1	0.0	0.0	0.0	0.0	0.0
4774	3.7	3.7	3.7	0.0	0.0	0.0
5024	2.9	2.9	2.9	0.0	0.0	0.0
5274	0.3	0.3	0.3	0.3	0.0	0.0
5524	0.0	0.0	0.0	0.0	0.0	-2.1
5774	0.0	0.0	0.0	0.0	0.0	6.9
6024	5.0	0.0	0.0	0.0	0.0	2.2
6274	-4.2	-4.2	0.0	0.0	0.0	0.0
6524	-4.3	-4.3	0.0	0.0	0.0	0.0
6774	-2.0	-2.0	-2.0	0.0	0.0	0.0
7024	-6.1	-6.1	-6.1	0.0	0.0	-11.2
7274	-6.8	-6.8	-6.8	-6.8	0.0	0.0
7524	-14.4	0.0	0.0	0.0	0.0	-3.8
Average:	-0.5	-2.1	-2.3	-0.7	0.0	-3.2

Table B26. The Number of Matches Made between *Profiler* and VAD Data at Each level during **Spring** for the Atmosphere which was **Not Superrefractive**

Range: <u>Height (m)</u>	20 km	22 km	24 km	26 km	28 km	30 km	32 km
2024	318	318	318	318	118	118	118
2274	322	322	322	322	118	118	118
2524	142	344	344	344	344	342	344
2774	143	134	134	134	134	304	269
3024	272	272	272	132	102	102	102
3274	221	221	237	226	226	225	97
3524	207	202	202	202	206	210	210
3774	207	202	202	202	205	209	209
4024	195	195	195	201	201	201	212
4274	175	175	175	175	175	176	176
4524	182	167	167	167	167	167	167
4774	158	158	158	160	160	159	160
5024	159	159	159	161	161	160	161
5274	148	148	148	148	157	157	157
5524	149	149	149	149	149	149	150
5774	158	158	158	158	158	158	146
6024	158	163	163	163	163	163	163
6274	156	156	148	148	148	148	148
6524	156	156	148	148	148	148	148
6774	151	151	151	144	144	144	144
7024	151	151	151	137	137	137	137
7274	130	130	130	130	125	125	125
7524	144	131	131	131	131	128	128

Table B27. RMSVD Calculated between *Profiler* and VAD Data at Each Level during Spring for the Atmosphere which was Not Superrefractive

Range: Height (m)	20 km	22 km	24 km	26 km	28 km	30 km	32 km
2024	14.51	14.51	14.51	14.51	14.45	14.45	14.45
2274	15.77	15.77	15.77	15.77	16.45	16.45	16.45
2524	16.07	18.33	18.33	18.33	18.33	18.38	18.33
2774	17.49	19.92	19.92	19.92	19.92	21.27	19.08
3024	19	19	19	18.11	9.627	9.635	9.627
3274	12.77	12.77	16.4	16.86	16.86	16.69	9.392
3524	15.29	14.36	14.36	14.36	17.66	17.91	17.9
3774	16.75	15.92	15.92	15.92	19.37	19.49	19.5
4024	17.2	17.2	17.2	17.04	17.04	17.04	20.55
4274	15.68	15.68	15.68	15.68	15.68	15.29	15.29
4524	20.69	16.38	16.38	16.38	16.38	16.38	16.38
4774	15.88	15.88	15.88	15.19	15.19	15.23	15.19
5024	18.36	18.36	18.36	17.56	17.56	17.61	17.56
5274	16.91	16.91	16.91	16.91	16.56	16.56	16.56
5524	15.87	15.87	15.87	15.87	15.87	16.19	16.14
5774	15.87	15.87	15.87	15.87	15.87	15.87	16.28
6024	15.47	15.27	15.27	15.27	15.27	15.27	15.27
6274	17.72	17.72	18.39	18.39	18.39	18.39	18.39
6524	19.7	19.7	20.33	20.33	20.33	20.34	20.33
6774	18.79	18.79	18.79	19.32	19.32	19.32	19.32
7024	19.95	19.95	19.95	20.29	20.29	20.29	20.29
7274	20.86	20.86	20.86	20.86	24.62	24.62	24.62
7524	24.1	26.09	26.09	26.09	26.09	22.95	22.95
Average:	17.42	17.44	17.65	17.60	17.70	17.64	17.38
Standard Deviation:	2.50	2.79	2.65	2.67	3.35	3.12	3.54

Table B28. Skill Score Calculated Using *Profiler* Verification at Each Level during Spring for the Atmosphere which was Not Superrefractive

Range: Height (m)	20 km	22 km	24 km	26 km	28 km	32 km
2024	-0.4	-0.4	-0.4	-0.4	0.0	0.0
2274	4.1	4.1	4.1	4.1	0.0	0.0
2524	12.6	0.3	0.3	0.3	0.3	0.3
2774	17.8	6.3	6.3	6.3	6.3	10.3
3024	-97.2	-97.2	-97.2	-88.0	0.1	0.1
3274	23.5	23.5	1.7	-1.0	-1.0	43.7
3524	14.6	19.8	19.8	19.8	1.4	0.1
3774	14.1	18.3	18.3	18.3	0.6	-0.1
4024	-0.9	-0.9	-0.9	0.0	0.0	-20.6
4274	-2.6	-2.6	-2.6	-2.6	-2.6	0.0
4524	-26.3	0.0	0.0	0.0	0.0	0.0
4774	-4.3	-4.3	-4.3	0.3	0.3	0.3
5024	-4.3	-4.3	-4.3	0.3	0.3	0.3
5274	-2.1	-2.1	-2.1	-2.1	0.0	0.0
5524	2.0	2.0	2.0	2.0	2.0	0.3
5774	0.0	0.0	0.0	0.0	0.0	-2.6
6024	-1.3	0.0	0.0	0.0	0.0	0.0
6274	3.6	3.6	0.0	0.0	0.0	0.0
6524	3.1	3.1	0.0	0.0	0.0	0.0
6774	2.7	2.7	2.7	0.0	0.0	0.0
7024	1.7	1.7	1.7	0.0	0.0	0.0
7274	15.3	15.3	15.3	15.3	0.0	0.0
7524	-5.0	-13.7	-13.7	-13.7	-13.7	0.0
Average:	-1.3	-1.1	-2.3	-1.8	-0.3	1.4

4) *Summer*

Table B29. The Number of Matches Made between *Profiler* and VAD Data at Each level during **Summer** for the Atmosphere which was **Superrefractive at the Surface**

Range:	20 km	22 km	24 km	26 km	28 km	30 km	32 km
Height (m)							
2024	293	293	293	293	196	196	196
2274	296	296	296	296	199	199	199
2524	198	278	278	278	278	278	278
2774	186	180	180	180	180	258	238
3024	226	226	226	147	129	129	129
3274	209	209	209	197	197	197	121
3524	197	185	185	185	187	184	184
3774	193	183	183	183	185	180	180
4024	165	165	165	151	151	151	159
4274	124	124	124	124	124	115	115
4524	137	97	97	97	97	97	97
4774	99	99	100	88	88	88	88
5024	99	99	100	88	88	88	88
5274	87	87	88	88	89	89	89
5524	92	92	93	93	93	98	98
5774	106	106	107	107	107	107	109
6024	105	104	105	105	105	105	105
6274	97	97	101	101	101	101	101
6524	97	97	101	101	101	101	101
6774	98	98	98	108	108	108	108
7024	88	88	88	94	94	94	94
7274	89	89	89	89	84	84	84
7524	77	80	80	80	80	82	82

Table B30. RMSVD Calculated between *Profiler* and VAD Data at Each Level during **Summer** for the Atmosphere which was **Superrefractive at the Surface**

Range: <u>Height (m)</u>	20 km	22 km	24 km	26 km	28 km	30 km	32 km
2024	12.71	12.71	12.71	12.71	11.53	11.53	11.53
2274	11.14	11.14	11.14	11.14	10.47	10.47	10.47
2524	12.21	10.39	10.39	10.39	10.39	10.39	10.39
2774	12.31	12.78	12.78	12.78	12.78	12.03	11.5
3024	11.76	11.76	11.76	12.11	13.25	13.25	13.25
3274	12.51	12.51	12.36	12.21	12.21	12.21	12.3
3524	12.22	12.27	12.27	12.27	12.2	12.54	12.54
3774	12.58	12.83	12.83	12.83	12.71	12.96	12.96
4024	13.34	13.34	13.34	14.02	14.02	14.02	13.94
4274	15.18	15.18	15.18	15.18	15.18	16.45	16.45
4524	14.63	15.48	15.48	15.48	15.48	15.48	15.48
4774	14.7	14.7	14.92	15.48	15.48	15.48	15.48
5024	15.77	15.77	16.02	16.41	16.41	16.41	16.41
5274	14.62	14.62	15.02	15.02	16.62	16.62	16.62
5524	13.82	13.82	14.28	14.28	14.28	16.66	16.66
5774	13.61	13.61	14.03	14.03	14.03	14.03	14.96
6024	12.18	12.97	13.34	13.34	13.34	13.34	13.34
6274	11.89	11.89	13.19	13.19	13.19	13.19	13.19
6524	12.11	12.11	13.38	13.38	13.38	13.38	13.38
6774	11.91	11.91	11.91	12.54	12.54	12.54	12.54
7024	10.99	10.99	10.99	11.68	11.68	11.68	11.68
7274	12.89	12.89	12.89	12.89	12.1	12.1	12.1
7524	10.63	10.89	10.89	10.89	10.89	10.02	10.02
Average:	12.86	12.89	13.09	13.23	13.22	13.34	13.36
Standard Deviation:	1.38	1.50	1.56	1.57	1.77	2.03	2.07

Table B31. Skill Score Calculated Using *Profiler* Verification at Each Level during Summer for the Atmosphere which was **Superrefractive at the Surface**

Range: <u>Height (m)</u>	20 km	22 km	24 km	26 km	28 km	32 km
2024	-10.2	-10.2	-10.2	-10.2	0.0	0.0
2274	-6.4	-6.4	-6.4	-6.4	0.0	0.0
2524	-17.5	0.0	0.0	0.0	0.0	0.0
2774	-2.3	-6.2	-6.2	-6.2	-6.2	4.4
3024	11.2	11.2	11.2	8.6	0.0	0.0
3274	-2.5	-2.5	-1.2	0.0	0.0	-0.7
3524	2.6	2.2	2.2	2.2	2.7	0.0
3774	2.9	1.0	1.0	1.0	1.9	0.0
4024	4.9	4.9	4.9	0.0	0.0	0.6
4274	7.7	7.7	7.7	7.7	7.7	0.0
4524	5.5	0.0	0.0	0.0	0.0	0.0
4774	5.0	5.0	3.6	0.0	0.0	0.0
5024	3.9	3.9	2.4	0.0	0.0	0.0
5274	12.0	12.0	9.6	9.6	0.0	0.0
5524	17.0	17.0	14.3	14.3	14.3	0.0
5774	3.0	3.0	0.0	0.0	0.0	-6.6
6024	8.7	2.8	0.0	0.0	0.0	0.0
6274	9.9	9.9	0.0	0.0	0.0	0.0
6524	9.5	9.5	0.0	0.0	0.0	0.0
6774	5.0	5.0	5.0	0.0	0.0	0.0
7024	5.9	5.9	5.9	0.0	0.0	0.0
7274	-6.5	-6.5	-6.5	-6.5	0.0	0.0
7524	-6.1	-8.7	-8.7	-8.7	-8.7	0.0
Average:	2.7	2.6	1.2	0.2	0.5	-0.1

Table B32. The Number of Matches Made between *Profiler* and VAD Data at Each level during **Summer** for the Atmosphere which was **Superrefractive Aloft**

Range: <u>Height (m)</u>	20 km	22 km	24 km	26 km	28 km	30 km	32 km
2024	216	216	216	216	189	189	189
2274	211	211	211	211	184	184	184
2524	181	196	196	196	196	196	196
2774	164	155	155	155	155	175	168
3024	160	160	160	140	115	115	115
3274	134	134	134	115	115	115	95
3524	135	108	108	108	108	90	90
3774	132	104	104	104	104	88	88
4024	94	94	94	70	70	70	71
4274	84	84	84	84	84	60	60
4524	115	62	62	62	62	62	62
4774	90	90	90	59	59	59	59
5024	90	90	90	59	59	59	59
5274	71	71	71	71	60	60	60
5524	65	65	65	65	65	61	61
5774	71	71	71	71	71	71	65
6024	78	81	81	81	81	81	81
6274	87	87	75	75	75	75	75
6524	87	87	75	75	75	75	75
6774	81	81	81	84	84	84	84
7024	83	83	83	88	88	88	88
7274	90	90	90	90	87	87	87
7524	81	92	92	92	92	85	85

Table B33. RMSVD Calculated between *Profiler* and VAD Data at Each Level during **Summer** for the Atmosphere which was **Superrefractive Aloft**

Range: <u>Height (m)</u>	20 km	22 km	24 km	26 km	28 km	30 km	32 km
2024	14.44	14.44	14.44	14.44	12.02	12.02	12.02
2274	12.1	12.1	12.1	12.1	11.43	11.43	11.43
2524	11.77	11.45	11.45	11.45	11.45	11.45	11.45
2774	10.56	11.49	11.49	11.49	11.49	11.13	11.86
3024	12.08	12.08	12.08	12.38	13.89	13.89	13.89
3274	11.76	11.76	11.93	13.27	13.27	13.27	13.46
3524	12.53	11.45	11.45	11.45	11.65	13.49	13.49
3774	13.24	11.78	11.78	11.78	12.02	14.11	14.11
4024	13.5	13.5	13.5	13.99	13.99	13.99	14.3
4274	14.5	14.5	14.5	14.5	14.5	16.77	16.77
4524	12.31	16	16	16	16	16	16
4774	13.43	13.43	13.43	16.74	16.74	16.74	16.74
5024	13.54	13.54	13.54	17	17	17	17
5274	14.69	14.69	14.69	14.69	16.92	16.92	16.92
5524	9.852	9.852	9.852	9.852	9.852	12.91	12.91
5774	10.87	10.87	10.87	10.87	10.87	10.87	12.78
6024	12.41	12.38	12.38	12.38	12.38	12.38	12.38
6274	11.41	11.41	11.45	11.45	11.45	11.45	11.45
6524	11.52	11.52	10.94	10.94	10.94	10.94	10.94
6774	9.728	9.728	9.728	9.864	9.864	9.864	9.864
7024	9.628	9.628	9.628	11.55	11.55	11.55	11.55
7274	11.51	11.51	11.51	11.51	12.13	12.13	12.13
7524	11.34	12.79	12.79	12.79	12.79	11.7	11.7
Average:	12.12	12.26	12.24	12.72	12.79	13.13	13.27
Standard Deviation:	1.48	1.65	1.66	2.03	2.16	2.20	2.13

Table B34. Skill Score Calculated Using *Profiler* Verification at Each Level during **Summer** for the Atmosphere which was **Superrefractive Aloft**

Range: <u>Height (m)</u>	20 km	22 km	24 km	26 km	28 km	32 km
2024	-20.1	-20.1	-20.1	-20.1	0.0	0.0
2274	-5.9	-5.9	-5.9	-5.9	0.0	0.0
2524	-2.8	0.0	0.0	0.0	0.0	0.0
2774	5.1	-3.2	-3.2	-3.2	-3.2	-6.6
3024	13.0	13.0	13.0	10.9	0.0	0.0
3274	11.4	11.4	10.1	0.0	0.0	-1.4
3524	7.1	15.1	15.1	15.1	13.6	0.0
3774	6.2	16.5	16.5	16.5	14.8	0.0
4024	3.5	3.5	3.5	0.0	0.0	-2.2
4274	13.5	13.5	13.5	13.5	13.5	0.0
4524	23.1	0.0	0.0	0.0	0.0	0.0
4774	19.8	19.8	19.8	0.0	0.0	0.0
5024	20.4	20.4	20.4	0.0	0.0	0.0
5274	13.2	13.2	13.2	13.2	0.0	0.0
5524	23.7	23.7	23.7	23.7	23.7	0.0
5774	0.0	0.0	0.0	0.0	0.0	-17.6
6024	-0.2	0.0	0.0	0.0	0.0	0.0
6274	0.3	0.3	0.0	0.0	0.0	0.0
6524	-5.3	-5.3	0.0	0.0	0.0	0.0
6774	1.4	1.4	1.4	0.0	0.0	0.0
7024	16.6	16.6	16.6	0.0	0.0	0.0
7274	5.1	5.1	5.1	5.1	0.0	0.0
7524	3.1	-9.3	-9.3	-9.3	-9.3	0.0
Average:	6.6	5.6	5.8	2.6	2.3	-1.2

Table B35. The Number of Matches Made between *Profiler* and VAD Data at Each level during **Summer** for the Atmosphere which was **Not Superrefractive**

Range: Height (m)	20 km	22 km	24 km	26 km	28 km	30 km	32 km
2024	493	493	493	493	322	322	322
2274	489	489	489	489	318	318	318
2524	324	470	470	470	470	470	470
2774	312	302	302	302	302	455	443
3024	426	426	426	270	253	253	253
3274	393	393	399	382	382	382	226
3524	372	354	354	354	354	342	342
3774	373	355	355	355	355	343	343
4024	305	305	305	284	284	284	289
4274	245	245	245	245	245	257	257
4524	264	223	223	223	223	223	223
4774	206	206	206	190	190	190	190
5024	205	205	205	190	190	190	190
5274	190	190	190	190	189	189	189
5524	191	191	191	191	191	185	185
5774	183	183	183	183	183	183	167
6024	167	165	165	165	165	165	165
6274	155	155	159	159	159	159	159
6524	154	154	158	158	158	158	158
6774	145	145	145	144	144	143	144
7024	131	131	131	136	136	136	136
7274	115	115	115	115	121	121	121
7524	99	104	104	104	104	110	110

Table B36. RMSVD Calculated between *Profiler* and VAD Data at Each Level during **Summer** for the Atmosphere which was **Not Superrefractive**

Range:	20 km	22 km	24 km	26 km	28 km	30 km	32 km
<u>Height (m)</u>							
2024	13.87	13.87	13.87	13.87	12.81	12.81	12.81
2274	12.73	12.73	12.73	12.73	12.23	12.23	12.23
2524	13.06	12.31	12.31	12.31	12.31	12.31	12.31
2774	12.57	13.46	13.46	13.46	13.46	12.76	12.98
3024	12.05	12.05	12.05	11.7	13.58	13.58	13.58
3274	11.88	11.88	12.14	12.63	12.63	12.63	12.53
3524	11.8	12.91	12.91	12.91	13.06	13.58	13.58
3774	12.86	13.76	13.76	13.76	13.96	14.25	14.25
4024	13.56	13.56	13.56	14.89	14.89	14.89	14.98
4274	15.43	15.43	15.43	15.43	15.43	15.72	15.72
4524	15.83	16.15	16.15	16.15	16.15	16.15	16.15
4774	15.62	15.62	15.62	15.78	15.78	15.78	15.78
5024	16.57	16.57	16.57	16.44	16.44	16.44	16.44
5274	15.73	15.73	15.73	15.73	15.67	15.67	15.67
5524	14.99	14.99	14.99	14.99	14.99	15	15
5774	13.97	13.97	13.97	13.97	13.97	13.97	14.28
6024	13.67	13.33	13.33	13.33	13.33	13.33	13.33
6274	12.82	12.82	12.61	12.61	12.61	12.61	12.61
6524	12.82	12.82	12.58	12.58	12.58	12.58	12.58
6774	13.35	13.35	13.35	13.71	13.71	13.47	13.71
7024	12.1	12.1	12.1	12.67	12.67	12.67	12.67
7274	14.34	14.34	14.34	14.34	13.79	13.79	13.79
7524	16.27	16.4	16.4	16.4	16.4	14.83	14.83
Average:	13.82	13.92	13.91	14.02	14.02	13.96	13.99
Standard Deviation:	1.50	1.47	1.47	1.44	1.40	1.34	1.34

Table B37. Skill Score Calculated Using *Profiler* Verification at Each Level during **Summer** for the Atmosphere which was **Not Superrefractive**

Range: <u>Height (m)</u>	20 km	22 km	24 km	26 km	28 km	32 km
2024	-8.3	-8.3	-8.3	-8.3	0.0	0.0
2274	-4.1	-4.1	-4.1	-4.1	0.0	0.0
2524	-6.1	0.0	0.0	0.0	0.0	0.0
2774	1.5	-5.5	-5.5	-5.5	-5.5	-1.7
3024	11.3	11.3	11.3	13.8	0.0	0.0
3274	5.9	5.9	3.9	0.0	0.0	0.8
3524	13.1	4.9	4.9	4.9	3.8	0.0
3774	9.8	3.4	3.4	3.4	2.0	0.0
4024	8.9	8.9	8.9	0.0	0.0	-0.6
4274	1.8	1.8	1.8	1.8	1.8	0.0
4524	2.0	0.0	0.0	0.0	0.0	0.0
4774	1.0	1.0	1.0	0.0	0.0	0.0
5024	-0.8	-0.8	-0.8	0.0	0.0	0.0
5274	-0.4	-0.4	-0.4	-0.4	0.0	0.0
5524	0.1	0.1	0.1	0.1	0.1	0.0
5774	0.0	0.0	0.0	0.0	0.0	-2.2
6024	-2.6	0.0	0.0	0.0	0.0	0.0
6274	-1.7	-1.7	0.0	0.0	0.0	0.0
6524	-1.9	-1.9	0.0	0.0	0.0	0.0
6774	0.9	0.9	0.9	-1.8	-1.8	-1.8
7024	4.5	4.5	4.5	0.0	0.0	0.0
7274	-4.0	-4.0	-4.0	-4.0	0.0	0.0
7524	-9.7	-10.6	-10.6	-10.6	-10.6	0.0
Average:	0.9	0.2	0.3	-0.5	-0.4	-0.2

c. Statistics Calculated Using rawinsonde Verification

1) Autumn

Table B38. The Number of Matches Made between *rawinsonde* and VAD Data at Each level during **Autumn** for the Atmosphere which was **Superrefractive at the Surface**

Range: <u>Height (m)</u>	20 km	22 km	24 km	26 km	28 km	30 km	32 km
1830	8	8	7	7	7	7	7
2130	26	26	25	25	5	5	5
2430	6	22	21	21	21	21	21
2730	6	6	5	5	5	19	19
3030	16	16	15	4	5	5	5
3330	6	6	5	4	4	4	2
3630	15	16	15	15	16	16	16
3930	4	4	3	4	4	4	4
4230	17	17	16	16	16	16	16
4530	4	4	4	4	4	4	4
4830	13	13	12	10	10	10	10
5130	4	4	3	3	3	3	3
5430	7	7	7	7	7	6	6
5730	8	8	7	7	7	7	6
6030	9	8	7	7	7	7	7
6330	1	1	1	1	1	1	1
6630	4	4	4	4	4	4	4
6930	0	0	0	0	0	0	0
7230	3	3	2	2	3	3	3
7530	7	5	4	4	4	5	5

Table B39. RMSVD Calculated between *rawinsonde* and VAD Data at Each Level during **Autumn** for the Atmosphere which was **Superrefractive at the Surface**

Range:	20 km	22 km	24 km	26 km	28 km	30 km	32 km
<u>Height (m)</u>							
1830	14.45	14.45	15.33	15.33	15.33	15.33	15.33
2130	14.95	14.95	15.15	15.15	23.29	23.29	23.29
2430	21.2	15.86	15.83	15.83	15.83	15.83	15.83
2730	16.17	16.14	17.37	17.37	17.37	15.22	17.62
3030	14.78	14.78	13.78	10.8	13.61	13.61	13.61
3330	26.42	26.42	25.23	15.57	15.57	15.57	10.34
3630	19.34	18.76	17.63	17.63	17.56	19.25	19.25
3930	19.19	19.19	9.958	7.009	7.009	7.009	10.28
4230	19.69	19.69	18.95	18.95	18.95	19.87	19.87
4530	21.58	22.2	22.2	22.2	22.2	22.2	22.2
4830	20.18	20.18	18.97	20.59	20.59	20.59	20.59
5130	20.77	20.77	16.3	16.3	16.3	16.3	16.3
5430	13.32	13.32	13.32	13.32	13.32	14.1	14.1
5730	21.25	21.25	19.24	19.24	19.24	19.24	17.68
6030	22.26	23.75	21.89	21.89	21.89	21.89	21.89
6330	8.343	8.343	8.343	8.343	8.343	8.343	8.343
6630	15.03	15.03	15.03	15.08	15.08	15.08	15.08
6930	*****	*****	*****	*****	*****	*****	*****
7230	7.084	7.084	6.901	6.901	11.5	11.5	11.5
7530	14.47	10.51	11.57	11.57	11.57	13.13	13.13
Average:	17.39	16.98	15.95	15.21	16.03	16.18	16.12
Standard Deviation:	4.86	5.11	4.73	4.62	4.50	4.49	4.35

Table B40. Skill Score Calculated Using *rawinsonde* Verification at Each Level during **Autumn** for the Atmosphere which was **Superrefractive at the Surface**

Range:	20 km	22 km	24 km	26 km	28 km	32 km
Height (m)						
1830	5.7	5.7	0.0	0.0	0.0	0.0
2130	35.8	35.8	35.0	35.0	0.0	0.0
2430	-33.9	-0.2	0.0	0.0	0.0	0.0
2730	-6.2	-6.0	-14.1	-14.1	-14.1	-15.8
3030	-8.6	-8.6	-1.2	20.6	0.0	0.0
3330	-69.7	-69.7	-62.0	0.0	0.0	33.6
3630	-0.5	2.5	8.4	8.4	8.8	0.0
3930	-173.8	-173.8	-42.1	0.0	0.0	-46.7
4230	0.9	0.9	4.6	4.6	4.6	0.0
4530	2.8	0.0	0.0	0.0	0.0	0.0
4830	2.0	2.0	7.9	0.0	0.0	0.0
5130	-27.4	-27.4	0.0	0.0	0.0	0.0
5430	5.5	5.5	5.5	5.5	5.5	0.0
5730	-10.4	-10.4	0.0	0.0	0.0	8.1
6030	-1.7	-8.5	0.0	0.0	0.0	0.0
6330	0.0	0.0	0.0	0.0	0.0	0.0
6630	0.3	0.3	0.3	0.0	0.0	0.0
6930	*****	*****	*****	*****	*****	*****
7230	38.4	38.4	40.0	40.0	0.0	0.0
7530	-10.2	20.0	11.9	11.9	11.9	0.0
Average:	-13.2	-10.2	-0.3	5.9	0.9	-1.1

Table B41. The Number of Matches Made between *rawinsonde* and VAD Data at Each level during **Autumn** for the Atmosphere which was **Superrefractive Aloft**

Range: <u>Height (m)</u>	20 km	22 km	24 km	26 km	28 km	30 km	32 km
1830	0	0	0	0	0	0	0
2130	11	11	11	11	2	2	2
2430	2	2	5	5	5	5	5
2730	2	2	2	2	2	3	3
3030	3	3	3	2	0	0	0
3330	0	0	0	0	0	0	0
3630	0	0	0	0	0	0	0
3930	0	0	0	0	0	0	0
4230	2	2	2	2	2	2	2
4530	0	0	0	0	0	0	0
4830	0	0	0	2	2	2	2
5130	0	0	0	0	0	0	0
5430	1	1	1	1	1	2	2
5730	1	1	1	1	1	1	1
6030	1	1	1	1	1	1	1
6330	0	0	0	0	0	0	0
6630	0	0	0	0	0	0	0
6930	2	2	2	2	2	2	2
7230	2	2	2	2	2	2	2
7530	2	2	2	2	2	3	3

Table B42. RMSVD Calculated between *rawinsonde* and VAD Data at Each Level during **Autumn** for the Atmosphere which was **Superrefractive Aloft**

Range:	20 km	22 km	24 km	26 km	28 km	30 km	32 km
<u>Height (m)</u>							
1830	*****	*****	*****	*****	*****	*****	*****
2130	18.13	18.13	18.13	18.13	6.109	6.109	6.109
2430	2.049	2.049	14.13	14.13	14.13	14.13	14.13
2730	3.098	3.098	3.813	3.813	3.813	6.403	9.324
3030	8.213	8.213	8.213	3.873	*****	*****	*****
3330	*****	*****	*****	*****	*****	*****	*****
3630	*****	*****	*****	*****	*****	*****	*****
3930	*****	*****	*****	*****	*****	*****	*****
4230	14.63	14.63	14.63	14.63	14.63	19.64	19.64
4530	*****	*****	*****	*****	*****	*****	*****
4830	*****	*****	*****	13.23	13.23	13.23	13.23
5130	*****	*****	*****	*****	*****	*****	*****
5430	16.47	16.47	16.47	16.47	16.47	10.31	10.31
5730	5.246	5.246	5.246	5.246	5.246	5.246	5.246
6030	24.3	24.3	16.17	16.17	16.17	16.17	16.17
6330	*****	*****	*****	*****	*****	*****	*****
6630	*****	*****	*****	*****	*****	*****	*****
6930	11.18	11.18	11.18	11.18	11.18	11.18	11.18
7230	15.41	15.41	15.41	15.41	15.41	15.41	15.41
7530	28.73	28.73	28.73	28.73	28.73	25.67	25.67
Average:	13.41	13.41	13.83	13.42	13.19	13.05	13.31
Standard Deviation:	8.51	8.51	6.85	6.97	6.89	6.19	5.94

Table B43. Skill Score Calculated Using *rawinsonde* Verification at Each Level during Autumn for the Atmosphere which was Superrefractive Aloft

Range:	20 km	22 km	24 km	26 km	28 km	32 km
Height (m)						
1830	*****	*****	*****	*****	*****	*****
2130	-196.8	-196.8	-196.8	-196.8	0.0	0.0
2430	85.5	85.5	0.0	0.0	0.0	0.0
2730	51.6	51.6	40.4	40.4	40.4	-45.6
3030	*****	*****	*****	*****	*****	*****
3330	*****	*****	*****	*****	*****	*****
3630	*****	*****	*****	*****	*****	*****
3930	*****	*****	*****	*****	*****	*****
4230	25.5	25.5	25.5	25.5	25.5	0.0
4530	*****	*****	*****	*****	*****	*****
4830	*****	*****	*****	0.0	0.0	0.0
5130	*****	*****	*****	*****	*****	*****
5430	-59.7	-59.7	-59.7	-59.7	-59.7	0.0
5730	0.0	0.0	0.0	0.0	0.0	0.0
6030	-50.3	-50.3	0.0	0.0	0.0	0.0
6330	*****	*****	*****	*****	*****	*****
6630	*****	*****	*****	*****	*****	*****
6930	0.0	0.0	0.0	0.0	0.0	0.0
7230	0.0	0.0	0.0	0.0	0.0	0.0
7530	-11.9	-11.9	-11.9	-11.9	-11.9	0.0
Average:	-15.6	-15.6	-20.2	-18.4	-0.5	-4.1

Table B44. The Number of Matches Made between *rawinsonde* and VAD Data at Each level during **Autumn** for the Atmosphere which was **Not Superrefractive**

Range: <u>Height (m)</u>	20 km	22 km	24 km	26 km	28 km	30 km	32 km
1830	10	10	10	10	10	10	10
2130	28	28	28	28	10	10	10
2430	15	21	21	21	21	21	21
2730	11	10	10	10	10	20	19
3030	19	19	19	10	8	8	8
3330	7	7	7	7	7	7	2
3630	14	13	13	13	13	13	13
3930	3	3	3	3	3	3	3
4230	11	11	11	11	11	11	11
4530	5	5	5	5	5	5	5
4830	6	6	6	6	6	6	6
5130	4	4	4	4	5	5	5
5430	1	1	1	1	1	1	1
5730	7	7	7	7	7	7	7
6030	7	7	7	7	7	7	7
6330	0	0	0	0	0	0	0
6630	0	0	0	0	0	0	0
6930	3	3	3	3	3	3	3
7230	4	4	4	4	3	3	3
7530	6	4	4	4	4	2	2

Table B45. RMSVD Calculated between *rawinsonde* and VAD Data at Each Level during **Autumn** for the Atmosphere which was **Not Superrefractive**

Range: Height (m)	20 km	22 km	24 km	26 km	28 km	30 km	32 km
1830	9.865	9.865	9.865	9.865	9.865	9.865	9.865
2130	11.11	11.11	11.11	11.11	13.43	13.43	13.43
2430	11.54	12.19	11.36	11.36	11.36	11.36	11.36
2730	11.33	10.8	10.8	10.8	10.8	12.25	12.59
3030	14.19	14.19	14.19	13.25	10.8	10.8	10.8
3330	18	18	16.94	16.92	16.92	16.92	12.63
3630	16.35	16.34	16.34	16.34	15.93	16.05	16.05
3930	12.2	12.2	12.2	12.64	12.64	12.64	18.71
4230	18.77	18.77	18.77	18.77	18.77	17.88	17.88
4530	21.09	19.03	19.03	19.03	19.03	19.03	19.03
4830	15.97	15.97	15.97	15.17	15.17	15.17	15.17
5130	21.06	21.06	21.06	21.06	19.87	19.87	19.87
5430	10.32	10.32	10.32	10.32	10.32	10.32	10.32
5730	20.66	20.66	20.66	20.66	20.66	20.66	18.65
6030	20.61	20.87	20.87	20.87	20.87	20.87	20.87
6330	*****	*****	*****	*****	*****	*****	*****
6630	*****	*****	*****	*****	*****	*****	*****
6930	25.77	25.77	25.77	22.44	22.44	22.44	22.44
7230	20.65	20.65	20.65	20.65	15.32	15.32	15.32
7530	25.01	25.8	25.8	25.8	25.8	34.97	34.97
Average:	16.92	16.87	16.76	16.50	16.11	16.66	16.66
Standard Deviation:	5.10	5.11	5.15	4.88	4.73	6.03	5.98

Table B46. Skill Score Calculated Using *rawinsonde* Verification at Each Level during **Autumn** for the Atmosphere which was **Not Superrefractive**

Range: <u>Height (m)</u>	20 km	22 km	24 km	26 km	28 km	32 km
1830	0.0	0.0	0.0	0.0	0.0	0.0
2130	17.3	17.3	17.3	17.3	0.0	0.0
2430	-1.6	-7.3	0.0	0.0	0.0	0.0
2730	7.5	11.8	11.8	11.8	11.8	-2.8
3030	-31.4	-31.4	-31.4	-22.7	0.0	0.0
3330	-6.4	-6.4	-0.1	0.0	0.0	25.4
3630	-1.9	-1.8	-1.8	-1.8	0.7	0.0
3930	3.5	3.5	3.5	0.0	0.0	-48.0
4230	-5.0	-5.0	-5.0	-5.0	-5.0	0.0
4530	-10.8	0.0	0.0	0.0	0.0	0.0
4830	-5.3	-5.3	-5.3	0.0	0.0	0.0
5130	-6.0	-6.0	-6.0	-6.0	0.0	0.0
5430	0.0	0.0	0.0	0.0	0.0	0.0
5730	0.0	0.0	0.0	0.0	0.0	9.7
6030	1.2	0.0	0.0	0.0	0.0	0.0
6330	*****	*****	*****	*****	*****	*****
6630	*****	*****	*****	*****	*****	*****
6930	-14.8	-14.8	-14.8	0.0	0.0	0.0
7230	-34.8	-34.8	-34.8	-34.8	0.0	0.0
7530	28.5	26.2	26.2	26.2	26.2	0.0
Average:	-3.3	-3.0	-2.2	-0.8	1.9	-0.9

2) *Winter*Table B47. The Number of Matches Made between *rawinsonde* and VAD Data at Each level during **Winter** for the Atmosphere which was **Superrefractive at the Surface**

Range: <u>Height (m)</u>	20 km	22 km	24 km	26 km	28 km	30 km	32 km
1830	5	5	5	5	5	5	5
2130	16	15	15	16	6	6	6
2430	6	3	3	4	4	4	4
2730	6	6	6	6	6	9	5
3030	6	6	6	6	6	6	6
3330	3	3	3	3	3	3	2
3630	7	7	7	7	7	7	7
3930	0	0	0	0	0	0	0
4230	8	8	8	8	8	8	8
4530	0	0	0	0	0	0	0
4830	6	6	6	6	6	6	6
5130	5	5	5	5	3	3	3
5430	2	2	2	2	2	2	2
5730	2	2	2	2	2	2	2
6030	4	4	4	4	4	4	4
6330	0	0	0	0	0	0	0
6630	0	0	0	0	0	0	0
6930	2	2	2	2	2	2	2
7230	2	2	2	2	2	2	2
7530	3	4	4	4	4	4	4

Table B48. RMSVD Calculated between *rawinsonde* and VAD Data at Each Level during Winter for the Atmosphere which was Superrefractive at the Surface

Range: <u>Height (m)</u>	20 km	22 km	24 km	26 km	28 km	30 km	32 km
1830	8.157	8.157	8.157	8.157	8.157	8.157	8.157
2130	9.019	9.748	9.748	9.468	7.359	7.359	7.359
2430	7.297	11.52	11.52	11.61	11.61	11.61	11.61
2730	9.124	8.235	8.235	8.235	8.235	11.17	15.2
3030	6.839	6.839	6.839	6.839	9.147	9.147	9.147
3330	11.59	11.59	11.44	11.42	11.42	11.42	8.809
3630	9.14	9.734	9.734	9.734	9.767	10.22	10.22
3930	*****	*****	*****	*****	*****	*****	*****
4230	15.94	15.94	15.94	15.94	15.94	17.45	17.45
4530	*****	*****	*****	*****	*****	*****	*****
4830	20.47	20.47	20.47	26.41	26.41	26.41	26.41
5130	20.79	20.79	20.79	20.79	11.47	11.47	11.47
5430	22.89	22.89	22.89	22.89	22.89	22.89	22.89
5730	4.085	4.085	4.085	4.085	4.085	4.085	8.585
6030	16.22	15.01	15.01	15.01	15.01	15.01	15.01
6330	*****	*****	*****	*****	*****	*****	*****
6630	*****	*****	*****	*****	*****	*****	*****
6930	15.61	15.61	15.61	15.61	15.61	15.61	15.61
7230	3.963	3.963	3.963	3.963	11.41	11.41	11.41
7530	12.67	11.49	11.49	11.49	11.49	12.84	12.84
Average:	12.11	12.25	12.25	12.60	12.50	12.89	13.26
Standard Deviation:	5.95	5.76	5.76	6.48	5.70	5.65	5.38

Table B49. Skill Score Calculated Using *rawinsonde* Verification at Each Level during Winter for the Atmosphere which was Superrefractive at the Surface

Range: <u>Height (m)</u>	20 km	22 km	24 km	26 km	28 km	32 km
1830	0.0	0.0	0.0	0.0	0.0	0.0
2130	-22.6	-32.5	-32.5	-28.7	0.0	0.0
2430	37.1	0.8	0.8	0.0	0.0	0.0
2730	18.3	26.3	26.3	26.3	26.3	-36.1
3030	25.2	25.2	25.2	25.2	0.0	0.0
3330	-1.5	-1.5	-0.2	0.0	0.0	22.9
3630	10.6	4.8	4.8	4.8	4.4	0.0
3930	*****	*****	*****	*****	*****	*****
4230	8.7	8.7	8.7	8.7	8.7	0.0
4530	*****	*****	*****	*****	*****	*****
4830	22.5	22.5	22.5	0.0	0.0	0.0
5130	-81.3	-81.3	-81.3	-81.3	0.0	0.0
5430	0.0	0.0	0.0	0.0	0.0	0.0
5730	0.0	0.0	0.0	0.0	0.0	-110.2
6030	-8.1	0.0	0.0	0.0	0.0	0.0
6330	*****	*****	*****	*****	*****	*****
6630	*****	*****	*****	*****	*****	*****
6930	0.0	0.0	0.0	0.0	0.0	0.0
7230	65.3	65.3	65.3	65.3	0.0	0.0
7530	1.3	10.5	10.5	10.5	10.5	0.0
Average:	4.7	3.0	3.1	1.9	3.1	-7.7

Table B50. The Number of Matches Made between *rawinsonde* and VAD Data at Each level during **Winter** for the Atmosphere which was **Superrefractive Aloft**

Range: <u>Height (m)</u>	20 km	22 km	24 km	26 km	28 km	30 km	32 km
1830	2	2	2	2	2	2	2
2130	10	10	10	10	0	0	0
2430	1	15	15	15	15	15	15
2730	0	0	0	0	0	7	7
3030	10	10	10	0	0	0	0
3330	2	2	3	2	2	2	0
3630	8	8	8	8	10	9	9
3930	2	2	2	2	2	2	2
4230	9	9	9	9	9	9	9
4530	1	1	1	1	1	1	1
4830	9	9	9	9	9	9	9
5130	2	2	2	2	2	2	2
5430	6	6	6	6	6	6	6
5730	6	6	6	6	6	6	6
6030	8	8	8	8	8	8	8
6330	0	0	0	0	0	0	0
6630	1	1	1	1	1	1	1
6930	3	3	3	3	3	3	3
7230	6	6	6	6	6	6	6
7530	8	8	8	8	8	6	6

Table B51. RMSVD Calculated between *rawinsonde* and VAD Data at Each Level during
Winter for the Atmosphere which was **Superrefractive Aloft**

Range:	20 km	22 km	24 km	26 km	28 km	30 km	32 km
<u>Height (m)</u>							
1830	10.67	10.67	10.67	10.67	10.67	10.67	10.67
2130	11.43	11.43	11.43	11.43	*****	*****	*****
2430	11.65	10.65	10.65	10.65	10.65	10.65	10.65
2730	*****	*****	*****	*****	*****	13.65	13.65
3030	17.82	17.82	17.82	*****	*****	*****	*****
3330	15.4	15.4	15.63	12.95	12.95	12.95	*****
3630	15.91	16.1	16.1	16.1	19.91	19.97	19.97
3930	13.4	13.4	13.4	13.4	13.4	13.4	9.842
4230	11.73	11.73	11.73	11.73	11.73	12.13	12.13
4530	4.946	4.946	4.946	4.946	4.946	4.946	4.946
4830	13.8	13.8	13.8	14.06	14.06	14.06	14.06
5130	15.5	15.5	15.5	15.5	14.16	14.16	14.16
5430	13.75	13.75	13.75	13.75	13.75	13.75	13.75
5730	16.56	16.56	16.56	16.56	16.56	16.56	15.07
6030	16.57	15.93	15.93	15.93	15.93	15.93	15.93
6330	*****	*****	*****	*****	*****	*****	*****
6630	11.59	11.59	11.59	11.59	11.59	11.59	11.59
6930	13.32	13.32	13.32	13.32	13.32	13.32	13.32
7230	22.14	22.14	22.14	22.14	21.46	21.46	21.46
7530	20.58	21.13	21.13	21.13	21.13	17.51	17.51
Average:	14.26	14.21	14.23	13.87	14.14	13.92	13.67
Standard Deviation:	3.92	4.00	4.01	4.01	4.23	3.79	3.99

Table B52. Skill Score Calculated Using *rawinsonde* Verification at Each Level during **Winter** for the Atmosphere which was **Superrefractive Aloft**

Range:	20 km	22 km	24 km	26 km	28 km	32 km
<u>Height (m)</u>						
1830	0.0	0.0	0.0	0.0	0.0	0.0
2130	*****	*****	*****	*****	*****	*****
2430	-9.4	0.0	0.0	0.0	0.0	0.0
2730	*****	*****	*****	*****	*****	0.0
3030	*****	*****	*****	*****	*****	*****
3330	-18.9	-18.9	-20.7	0.0	0.0	*****
3630	20.3	19.4	19.4	19.4	0.3	0.0
3930	0.0	0.0	0.0	0.0	0.0	26.6
4230	3.3	3.3	3.3	3.3	3.3	0.0
4530	0.0	0.0	0.0	0.0	0.0	0.0
4830	1.8	1.8	1.8	0.0	0.0	0.0
5130	-9.5	-9.5	-9.5	-9.5	0.0	0.0
5430	0.0	0.0	0.0	0.0	0.0	0.0
5730	0.0	0.0	0.0	0.0	0.0	9.0
6030	-4.0	0.0	0.0	0.0	0.0	0.0
6330	*****	*****	*****	*****	*****	*****
6630	0.0	0.0	0.0	0.0	0.0	0.0
6930	0.0	0.0	0.0	0.0	0.0	0.0
7230	-3.2	-3.2	-3.2	-3.2	0.0	0.0
7530	-17.5	-20.7	-20.7	-20.7	-20.7	0.0
Average:	-2.3	-1.7	-1.8	-0.7	-1.1	2.2

Table B53. The Number of Matches Made between *rawinsonde* and VAD Data at Each level during **Winter** for the Atmosphere which was **Not Superrefractive**

Range: <u>Height (m)</u>	20 km	22 km	24 km	26 km	28 km	30 km	32 km
1830	9	9	9	9	9	10	9
2130	18	18	18	18	10	10	10
2430	10	14	14	14	14	14	14
2730	11	8	8	8	8	11	8
3030	13	13	13	10	5	5	5
3330	2	2	2	2	2	2	0
3630	7	5	5	5	7	7	7
3930	5	5	5	5	5	5	5
4230	5	5	5	5	5	5	5
4530	0	0	0	0	0	0	0
4830	5	5	5	5	5	5	5
5130	0	0	0	0	1	1	1
5430	1	1	1	1	1	1	1
5730	3	3	3	3	3	3	4
6030	4	4	4	4	4	4	4
6330	1	1	1	1	1	1	1
6630	2	2	2	2	2	2	2
6930	1	1	1	1	1	1	1
7230	4	4	4	4	4	4	4
7530	5	6	6	6	6	5	5

Table B54. RMSVD Calculated between *rawinsonde* and VAD Data at Each Level during Winter for the Atmosphere which was Not Superrefractive

Range:	20 km	22 km	24 km	26 km	28 km	30 km	32 km
<u>Height (m)</u>							
1830	6.934	6.934	6.934	6.934	6.934	6.787	6.934
2130	11.33	11.33	11.33	11.33	5.787	5.787	5.787
2430	5.459	12.02	12.02	12.02	12.02	12.02	12.02
2730	5.841	6.152	6.152	6.152	6.152	7.99	8.669
3030	5.997	5.997	5.997	5.599	5.84	5.84	5.84
3330	23.86	23.86	14.88	14.88	14.88	14.88	*****
3630	8.739	11.22	11.22	11.22	15.46	15.82	15.82
3930	11.14	11.14	11.14	13.32	13.32	13.32	13.32
4230	12.44	12.44	12.44	12.44	12.44	13.76	13.76
4530	*****	*****	*****	*****	*****	*****	*****
4830	17.65	17.65	17.65	18.3	18.3	18.3	18.3
5130	*****	*****	*****	*****	10.53	10.53	10.53
5430	23.4	23.4	23.4	23.4	23.4	20.3	20.3
5730	9.28	9.28	9.28	9.28	9.28	9.28	11.03
6030	12.94	13.41	13.41	13.41	13.41	13.41	13.41
6330	4.491	4.491	4.491	4.491	4.491	4.491	4.491
6630	12.71	12.71	12.71	13	13	13	13
6930	23.6	23.6	23.6	17.13	17.13	17.13	17.13
7230	12.83	12.83	12.83	12.83	13.4	13.4	13.4
7530	14.35	12.57	12.57	12.57	12.57	13.18	13.18
Average:	12.39	12.84	12.34	12.13	12.02	12.06	12.05
Standard Deviation:	6.23	5.89	5.25	4.70	4.86	4.44	4.43

Table B55. Skill Score Calculated Using *rawinsonde* Verification at Each Level during **Winter** for the Atmosphere which was **Not Superrefractive**

Range:	20 km	22 km	24 km	26 km	28 km	32 km
Height (m)						
1830	-2.2	-2.2	-2.2	-2.2	-2.2	-2.2
2130	-95.8	-95.8	-95.8	-95.8	0.0	0.0
2430	54.6	0.0	0.0	0.0	0.0	0.0
2730	26.9	23.0	23.0	23.0	23.0	-8.5
3030	-2.7	-2.7	-2.7	4.1	0.0	0.0
3330	-60.3	-60.3	0.0	0.0	0.0	*****
3630	44.8	29.1	29.1	29.1	2.3	0.0
3930	16.4	16.4	16.4	0.0	0.0	0.0
4230	9.6	9.6	9.6	9.6	9.6	0.0
4530	*****	*****	*****	*****	*****	*****
4830	3.6	3.6	3.6	0.0	0.0	0.0
5130	*****	*****	*****	*****	0.0	0.0
5430	-15.3	-15.3	-15.3	-15.3	-15.3	0.0
5730	0.0	0.0	0.0	0.0	0.0	-18.9
6030	3.5	0.0	0.0	0.0	0.0	0.0
6330	0.0	0.0	0.0	0.0	0.0	0.0
6630	2.2	2.2	2.2	0.0	0.0	0.0
6930	-37.8	-37.8	-37.8	0.0	0.0	0.0
7230	4.3	4.3	4.3	4.3	0.0	0.0
7530	-8.9	4.6	4.6	4.6	4.6	0.0
Average:	-3.2	-6.7	-3.4	-2.1	1.2	-1.6

3) *Spring*

Table B56. The Number of Matches Made between *rawinsonde* and VAD Data at Each level during **Spring** for the Atmosphere which was **Superrefractive at the Surface**

Range: <u>Height (m)</u>	20 km	22 km	24 km	26 km	28 km	30 km	32 km
1830	26	26	26	26	26	26	26
2130	33	33	33	33	22	22	22
2430	21	28	28	28	28	28	28
2730	24	22	22	22	22	30	24
3030	21	21	21	17	13	13	13
3330	3	3	3	3	3	3	0
3630	23	21	21	21	21	19	19
3930	3	3	3	2	2	2	2
4230	14	14	14	14	14	14	14
4530	7	8	8	8	8	8	8
4830	19	19	19	18	18	18	18
5130	2	2	2	2	2	2	2
5430	4	4	4	4	4	3	3
5730	19	19	19	19	19	19	16
6030	16	20	20	20	20	20	20
6330	2	2	2	2	2	2	2
6630	2	2	2	2	2	2	2
6930	0	0	0	0	0	0	0
7230	2	2	2	2	3	3	3
7530	17	15	15	15	15	13	13

Table B57. RMSVD Calculated between *rawinsonde* and VAD Data at Each Level during Spring for the Atmosphere which was **Superrefractive at the Surface**

Range: <u>Height (m)</u>	20 km	22 km	24 km	26 km	28 km	30 km	32 km
1830	7.357	7.357	7.357	7.357	7.357	7.357	7.357
2130	8.023	8.023	8.023	8.023	9.062	9.062	9.062
2430	6.962	9.509	9.509	9.509	9.509	9.509	9.509
2730	8.452	8.327	8.327	8.327	8.327	7.77	9.649
3030	7.913	7.913	7.913	6.32	9.93	9.93	9.93
3330	12.11	12.11	10.75	10.75	10.75	10.75	*****
3630	9.437	10.8	10.8	10.8	11.55	12.28	12.28
3930	12.51	12.51	12.51	7.931	7.931	7.931	7.931
4230	11.67	11.67	11.67	11.67	11.67	14.35	14.35
4530	11.48	18.79	18.79	18.79	18.79	18.79	18.79
4830	13.52	13.52	13.52	13.51	13.51	13.51	13.51
5130	7.387	7.387	7.387	7.387	10.04	10.04	10.04
5430	7.983	7.983	7.983	7.983	7.983	5.66	5.66
5730	11.34	11.34	11.34	11.34	11.34	11.34	11.57
6030	12.18	11.98	11.98	11.98	11.98	11.98	11.98
6330	18.6	18.6	8.106	8.106	8.106	8.106	8.106
6630	15.04	15.04	15.04	16.72	16.72	16.72	16.72
6930	*****	*****	*****	*****	*****	*****	*****
7230	14.79	14.79	14.79	14.79	10.32	10.32	10.32
7530	12.99	13.65	13.65	13.65	13.65	13.82	13.82
Average:	11.04	11.65	11.02	10.79	10.98	11.01	11.14
Standard Deviation:	3.19	3.52	3.16	3.46	3.02	3.33	3.35

Table B58. Skill Score Calculated Using *rawinsonde* Verification at Each Level during Spring for the Atmosphere which was Superrefractive at the Surface

Range <u>Height (m)</u>	20 km	22 km	24 km	26 km	28 km	32 km
1830	0.0	0.0	0.0	0.0	0.0	0.0
2130	11.5	11.5	11.5	11.5	0.0	0.0
2430	26.8	0.0	0.0	0.0	0.0	0.0
2730	-8.8	-7.2	-7.2	-7.2	-7.2	-24.2
3030	20.3	20.3	20.3	36.4	0.0	0.0
3330	-12.7	-12.7	0.0	0.0	0.0	*****
3630	23.2	12.1	12.1	12.1	5.9	0.0
3930	-57.7	-57.7	-57.7	0.0	0.0	0.0
4230	18.7	18.7	18.7	18.7	18.7	0.0
4530	38.9	0.0	0.0	0.0	0.0	0.0
4830	-0.1	-0.1	-0.1	0.0	0.0	0.0
5130	26.4	26.4	26.4	26.4	0.0	0.0
5430	-41.0	-41.0	-41.0	-41.0	-41.0	0.0
5730	0.0	0.0	0.0	0.0	0.0	-2.0
6030	-1.7	0.0	0.0	0.0	0.0	0.0
6330	-129.5	-129.5	0.0	0.0	0.0	0.0
6630	10.0	10.0	10.0	0.0	0.0	0.0
6930	*****	*****	*****	*****	*****	*****
7230	-43.3	-43.3	-43.3	-43.3	0.0	0.0
7530	6.0	1.2	1.2	1.2	1.2	0.0
Average:	-5.9	-10.1	-2.6	0.8	-1.2	-1.5

Table B59. The Number of Matches Made between *rawinsonde* and VAD Data at Each level during **Spring** for the Atmosphere which was **Superrefractive Aloft**

Range: <u>Height (m)</u>	20 km	22 km	24 km	26 km	28 km	30 km	32 km
1830	15	15	15	15	15	15	15
2130	33	35	35	35	14	14	14
2430	15	28	28	28	28	28	28
2730	12	12	12	12	12	12	22
3030	19	21	21	9	2	2	2
3330	5	5	5	5	5	5	2
3630	10	11	11	11	10	10	9
3930	4	5	5	3	3	3	3
4230	4	6	6	6	6	6	6
4530	5	1	1	1	1	1	1
4830	3	3	3	3	3	3	3
5130	2	2	2	2	2	2	2
5430	1	1	1	1	1	1	1
5730	2	2	2	2	2	2	4
6030	3	5	5	5	5	5	5
6330	5	5	7	7	7	7	7
6630	1	1	1	2	2	2	2
6930	3	3	3	3	3	3	3
7230	2	2	2	2	2	2	2
7530	2	2	2	2	2	2	6

Table B60. RMSVD Calculated between *rawinsonde* and VAD Data at Each Level during Spring for the Atmosphere which was Superrefractive Aloft

Range:	20 km	22 km	24 km	26 km	28 km	30 km	32 km
Height (m)							
1830	11.19	11.19	11.19	11.19	11.19	11.19	11.19
2130	13.11	12.99	12.99	12.99	13.07	13.07	13.07
2430	10.08	13.01	13.01	13.01	13.01	13.01	13.01
2730	8.431	8.394	8.394	8.394	8.394	8.394	12.51
3030	10.53	10.9	10.9	7.333	10.22	10.22	10.22
3330	10.73	10.73	12.1	12.55	12.55	12.55	10.39
3630	12.23	13.08	13.08	13.08	15.38	15.38	16.2
3930	11.98	13.78	13.78	14.76	14.76	14.76	17.84
4230	11.97	12.85	12.85	12.85	12.85	12.85	12.85
4530	12.44	19.07	19.07	19.07	19.07	19.07	19.07
4830	15.75	15.75	15.75	15.75	15.75	15.75	15.75
5130	25.45	25.45	25.45	25.45	25.45	25.45	25.45
5430	2.208	2.208	2.208	2.208	2.208	2.208	2.208
5730	3.549	3.549	3.549	3.549	3.549	3.549	5.665
6030	10.01	11.46	11.46	11.46	11.46	11.46	11.46
6330	15.72	15.72	18.02	18.02	18.02	18.02	18.02
6630	6.529	6.529	6.529	7.047	7.047	7.047	7.047
6930	14.73	14.73	14.73	14.73	14.73	14.73	14.73
7230	13.2	13.2	13.2	13.2	13.2	13.2	13.2
7530	11.74	11.74	11.74	11.74	11.74	11.74	11.38
Average:	11.58	12.32	12.50	12.42	12.68	12.68	13.06
Standard Deviation:	4.80	5.06	5.15	5.26	5.19	5.19	5.08

Table B61. Skill Score Calculated Using *rawinsonde* Verification at Each Level during Spring for the Atmosphere which was Superrefractive Aloft

Range:	20 km	22 km	24 km	26 km	28 km	32 km
Height (m)						
1830	0.0	0.0	0.0	0.0	0.0	0.0
2130	-0.3	0.6	0.6	0.6	0.0	0.0
2430	22.5	0.0	0.0	0.0	0.0	0.0
2730	-0.4	0.0	0.0	0.0	0.0	-49.0
3030	-3.0	-6.7	-6.7	28.2	0.0	0.0
3330	14.5	14.5	3.6	0.0	0.0	17.2
3630	20.5	15.0	15.0	15.0	0.0	-5.3
3930	18.8	6.6	6.6	0.0	0.0	-20.9
4230	6.8	0.0	0.0	0.0	0.0	0.0
4530	34.8	0.0	0.0	0.0	0.0	0.0
4830	0.0	0.0	0.0	0.0	0.0	0.0
5130	0.0	0.0	0.0	0.0	0.0	0.0
5430	0.0	0.0	0.0	0.0	0.0	0.0
5730	0.0	0.0	0.0	0.0	0.0	-59.6
6030	12.7	0.0	0.0	0.0	0.0	0.0
6330	12.8	12.8	0.0	0.0	0.0	0.0
6630	7.4	7.4	7.4	0.0	0.0	0.0
6930	0.0	0.0	0.0	0.0	0.0	0.0
7230	0.0	0.0	0.0	0.0	0.0	0.0
7530	0.0	0.0	0.0	0.0	0.0	3.1
Average:	7.3	2.5	1.3	2.2	0.0	-5.7

Table B62. The Number of Matches Made between *rawinsonde* and VAD Data at Each level during **Spring** for the Atmosphere which was **Not Superrefractive**

Range: <u>Height (m)</u>	20 km	22 km	24 km	26 km	28 km	30 km	32 km
1830	9	9	9	9	9	9	9
2130	24	24	24	24	9	9	9
2430	10	28	28	28	28	28	28
2730	9	9	9	9	9	20	18
3030	18	18	18	9	7	7	7
3330	4	4	5	5	5	5	3
3630	11	11	11	11	10	12	12
3930	0	0	0	0	0	0	1
4230	9	9	9	9	9	11	11
4530	0	0	0	0	0	0	0
4830	15	15	15	16	16	16	16
5130	5	5	5	5	5	5	5
5430	9	9	9	9	9	8	8
5730	8	8	8	8	8	8	8
6030	18	17	17	17	17	17	17
6330	5	5	5	5	5	5	5
6630	3	3	3	1	1	1	1
6930	5	5	5	5	5	5	5
7230	14	14	14	14	12	12	12
7530	20	15	15	15	15	14	14

Table B63. RMSVD Calculated between *rawinsonde* and VAD Data at Each Level during Spring for the Atmosphere which was Not Superrefractive

Range: Height (m)	20 km	22 km	24 km	26 km	28 km	30 km	32 km
1830	15.02	15.02	15.02	15.02	15.02	15.02	15.02
2130	15.89	15.89	15.89	15.89	18.11	18.11	18.11
2430	21.41	18.79	18.79	18.79	18.79	18.79	18.79
2730	20.44	21	21	21	21	21.99	22.15
3030	18.13	18.13	18.13	19.45	22.09	22.09	22.09
3330	25.53	25.53	25.04	25.07	25.07	25.07	27.82
3630	16.52	16.93	16.93	16.93	18.78	18.45	18.45
3930	*****	*****	*****	*****	*****	*****	28.72
4230	16.68	16.68	16.68	16.68	16.68	16.23	16.23
4530	*****	*****	*****	*****	*****	*****	*****
4830	13.3	13.3	13.3	13.58	13.58	13.58	13.58
5130	10.13	10.13	10.13	10.13	10.13	10.13	10.13
5430	15.07	15.07	15.07	15.07	15.07	16.04	16.04
5730	16.7	16.7	16.7	16.7	16.7	16.7	17.27
6030	13.55	14.18	14.18	14.18	14.18	14.18	14.18
6330	16.27	16.27	17.91	17.91	17.91	17.91	17.91
6630	8.919	8.919	8.919	9.576	9.576	9.576	9.576
6930	18.53	18.53	18.53	18.19	18.19	18.19	18.19
7230	15.97	15.97	15.97	15.97	14.54	14.54	14.54
7530	14.4	15.92	15.92	15.92	15.92	14.65	14.65
Average:	16.25	16.28	16.34	16.45	16.74	16.74	17.55
Standard Deviation:	3.86	3.70	3.65	3.60	3.86	3.93	4.99

Table B64. Skill Score Calculated Using *rawinsonde* Verification at Each Level during Spring for the Atmosphere which was Not Superrefractive

Range:	20 km	22 km	24 km	26 km	28 km	32 km
Height (m)						
1830	0.0	0.0	0.0	0.0	0.0	0.0
2130	12.3	12.3	12.3	12.3	0.0	0.0
2430	-13.9	0.0	0.0	0.0	0.0	0.0
2730	7.0	4.5	4.5	4.5	4.5	-0.7
3030	17.9	17.9	17.9	12.0	0.0	0.0
3330	-1.8	-1.8	0.1	0.0	0.0	-11.0
3630	10.5	8.2	8.2	8.2	-1.8	0.0
3930	*****	*****	*****	*****	*****	*****
4230	-2.8	-2.8	-2.8	-2.8	-2.8	0.0
4530	*****	*****	*****	*****	*****	*****
4830	2.1	2.1	2.1	0.0	0.0	0.0
5130	0.0	0.0	0.0	0.0	0.0	0.0
5430	6.0	6.0	6.0	6.0	6.0	0.0
5730	0.0	0.0	0.0	0.0	0.0	-3.4
6030	4.4	0.0	0.0	0.0	0.0	0.0
6330	9.2	9.2	0.0	0.0	0.0	0.0
6630	6.9	6.9	6.9	0.0	0.0	0.0
6930	-1.9	-1.9	-1.9	0.0	0.0	0.0
7230	-9.8	-9.8	-9.8	-9.8	0.0	0.0
7530	1.7	-8.7	-8.7	-8.7	-8.7	0.0
Average:	2.7	2.3	1.9	1.2	-0.1	-0.8

4) *Summer*

Table B65. The Number of Matches Made between *rawinsonde* and VAD Data at Each level during **Summer** for the Atmosphere which was **Superrefractive at the Surface**

Range:	20 km	22 km	24 km	26 km	28 km	30 km	32 km
Height (m)							
1830	22	22	22	22	22	22	22
2130	36	36	36	36	18	18	18
2430	23	35	35	35	35	35	35
2730	22	21	21	21	21	36	32
3030	26	26	26	10	9	9	9
3330	9	9	9	11	11	11	6
3630	27	24	24	24	24	27	27
3930	4	4	4	4	4	4	4
4230	20	20	20	20	20	22	22
4530	7	5	5	5	5	5	5
4830	22	22	22	15	15	15	15
5130	0	0	0	0	2	2	2
5430	4	4	4	4	4	3	3
5730	13	13	13	13	13	13	12
6030	11	11	11	11	11	11	11
6330	3	3	3	3	3	3	3
6630	4	4	4	4	4	4	4
6930	2	2	2	2	2	2	2
7230	2	2	2	2	2	2	2
7530	9	9	9	9	9	10	10

Table B66. RMSVD Calculated between *rawinsonde* and VAD Data at Each Level during **Summer** for the Atmosphere which was **Superrefractive at the Surface**

Range:	20 km	22 km	24 km	26 km	28 km	30 km	32 km
<u>Height (m)</u>							
1830	10.33	10.33	10.33	10.33	10.33	10.33	10.33
2130	13.06	13.06	13.06	13.06	9.208	9.208	9.208
2430	15.94	12.39	12.39	12.39	12.39	12.39	12.39
2730	12.63	13.68	13.68	13.68	13.68	13.17	12.23
3030	12.81	12.81	12.81	11.35	13.47	13.47	13.47
3330	8.425	8.425	7.619	8.096	8.096	8.096	8.81
3630	12.64	13.35	13.35	13.35	13.65	13.17	13.17
3930	7.534	7.534	7.534	7.398	7.398	7.398	6.733
4230	13.73	13.73	13.73	13.73	13.73	14.35	14.35
4530	15.4	18.05	18.05	18.05	18.05	18.05	18.05
4830	13.87	13.87	13.87	15.04	15.04	15.04	15.04
5130	*****	*****	*****	*****	11.11	11.11	11.11
5430	24.75	24.75	24.75	24.75	24.75	28.04	28.04
5730	16.02	16.02	16.02	16.02	16.02	16.02	16.44
6030	19.2	19.23	19.23	19.23	19.23	19.23	19.23
6330	23.18	23.18	23.15	23.15	23.15	23.15	23.15
6630	14.86	14.86	14.86	16.54	16.54	16.54	16.54
6930	15.95	15.95	15.95	15.83	15.83	15.83	15.83
7230	9.236	9.236	9.236	9.236	17.45	17.45	17.45
7530	15.82	14.31	14.31	14.31	14.31	15.84	15.84
Average:	14.49	14.46	14.42	14.50	14.67	14.89	14.87
Standard Deviation:	4.44	4.49	4.55	4.59	4.52	4.95	4.99

Table B67. Skill Score Calculated Using *rawinsonde* Verification at Each Level during Summer for the Atmosphere which was Superrefractive at the Surface

Range: <u>Height (m)</u>	20 km	22 km	24 km	26 km	28 km	32 km
1830	0.0	0.0	0.0	0.0	0.0	0.0
2130	-41.8	-41.8	-41.8	-41.8	0.0	0.0
2430	-28.7	0.0	0.0	0.0	0.0	0.0
2730	4.1	-3.9	-3.9	-3.9	-3.9	7.1
3030	4.9	4.9	4.9	15.7	0.0	0.0
3330	-4.1	-4.1	5.9	0.0	0.0	-8.8
3630	4.0	-1.4	-1.4	-1.4	-3.6	0.0
3930	-1.8	-1.8	-1.8	0.0	0.0	9.0
4230	4.3	4.3	4.3	4.3	4.3	0.0
4530	14.7	0.0	0.0	0.0	0.0	0.0
4830	7.8	7.8	7.8	0.0	0.0	0.0
5130	*****	*****	*****	*****	0.0	0.0
5430	11.7	11.7	11.7	11.7	11.7	0.0
5730	0.0	0.0	0.0	0.0	0.0	-2.6
6030	0.2	0.0	0.0	0.0	0.0	0.0
6330	-0.1	-0.1	0.0	0.0	0.0	0.0
6630	10.2	10.2	10.2	0.0	0.0	0.0
6930	-0.8	-0.8	-0.8	0.0	0.0	0.0
7230	47.1	47.1	47.1	47.1	0.0	0.0
7530	0.1	9.7	9.7	9.7	9.7	0.0
Average:	1.7	2.2	2.7	2.2	0.9	0.2

Table B68. The Number of Matches Made between *rawinsonde* and VAD Data at Each level during **Summer** for the Atmosphere which was **Superrefractive Aloft**

Range: <u>Height (m)</u>	20 km	22 km	24 km	26 km	28 km	30 km	32 km
1830	36	36	36	36	36	36	36
2130	42	42	42	42	34	34	34
2430	34	42	42	42	42	42	42
2730	27	27	27	27	27	33	35
3030	19	19	19	16	11	11	11
3330	17	17	18	16	16	16	11
3630	24	14	14	14	14	14	14
3930	6	6	6	6	6	6	6
4230	12	12	12	12	12	11	11
4530	2	1	1	1	1	1	1
4830	15	15	15	12	12	12	12
5130	3	3	3	3	4	4	4
5430	4	4	4	4	4	5	5
5730	8	8	8	8	8	8	10
6030	16	14	14	14	14	14	14
6330	1	1	1	1	1	1	1
6630	5	5	5	5	5	5	5
6930	3	3	3	3	3	3	3
7230	2	2	2	2	3	3	3
7530	13	12	12	12	12	11	11

Table B69. RMSVD Calculated between *rawinsonde* and VAD Data at Each Level during **Summer** for the Atmosphere which was **Superrefractive Aloft**

Range:	20 km	22 km	24 km	26 km	28 km	30 km	32 km
<u>Height (m)</u>							
1830	10.79	10.79	10.79	10.79	10.79	10.79	10.79
2130	13.36	13.36	13.36	13.36	10.3	10.3	10.3
2430	12.25	12.6	12.6	12.6	12.6	12.6	12.6
2730	11.24	12.18	12.18	12.18	12.18	11.88	13.8
3030	13.17	13.17	13.17	13.03	19.56	19.56	19.56
3330	15.39	15.39	15.18	13.09	13.09	13.09	13.86
3630	13.97	15.41	15.41	15.41	15.5	17.04	17.04
3930	15.4	15.4	15.4	16.54	16.54	16.54	16.54
4230	14.01	14.01	14.01	14.01	14.01	14.21	14.21
4530	15.28	20.98	20.98	20.98	20.98	20.98	20.98
4830	16.07	16.07	16.07	16.01	16.01	16.01	16.01
5130	26.15	26.15	26.15	26.15	18.59	18.59	18.59
5430	5.326	5.326	5.326	5.326	5.326	8.773	8.773
5730	12.06	12.06	12.06	12.06	12.06	12.06	13.18
6030	14.76	15.4	15.4	15.4	15.4	15.4	15.4
6330	22.02	22.02	22.02	22.02	22.02	22.02	22.02
6630	11.71	11.71	11.71	10.82	10.82	10.82	10.82
6930	17.84	17.84	17.84	18.2	18.2	18.2	18.2
7230	16.9	16.9	16.9	16.9	17.2	17.2	17.2
7530	13.83	14.66	14.66	14.66	14.66	14.01	14.01
Average:	14.58	15.07	15.06	14.98	14.79	15.00	15.19
Standard Deviation:	4.26	4.44	4.44	4.53	4.07	3.75	3.63

Table B70. Skill Score Calculated Using *rawinsonde* Verification at Each Level during **Summer** for the Atmosphere which was **Superrefractive Aloft**

Range:	20 km	22 km	24 km	26 km	28 km	32 km
Height (m)						
1830	0.0	0.0	0.0	0.0	0.0	0.0
2130	-29.7	-29.7	-29.7	-29.7	0.0	0.0
2430	2.8	0.0	0.0	0.0	0.0	0.0
2730	5.4	-2.5	-2.5	-2.5	-2.5	-16.2
3030	32.7	32.7	32.7	33.4	0.0	0.0
3330	-17.6	-17.6	-16.0	0.0	0.0	-5.9
3630	18.0	9.6	9.6	9.6	9.0	0.0
3930	6.9	6.9	6.9	0.0	0.0	0.0
4230	1.4	1.4	1.4	1.4	1.4	0.0
4530	27.2	0.0	0.0	0.0	0.0	0.0
4830	-0.4	-0.4	-0.4	0.0	0.0	0.0
5130	-40.7	-40.7	-40.7	-40.7	0.0	0.0
5430	39.3	39.3	39.3	39.3	39.3	0.0
5730	0.0	0.0	0.0	0.0	0.0	-9.3
6030	4.2	0.0	0.0	0.0	0.0	0.0
6330	0.0	0.0	0.0	0.0	0.0	0.0
6630	-8.2	-8.2	-8.2	0.0	0.0	0.0
6930	2.0	2.0	2.0	0.0	0.0	0.0
7230	1.7	1.7	1.7	1.7	0.0	0.0
7530	1.3	-4.6	-4.6	-4.6	-4.6	0.0
Average:	2.3	-0.5	-0.4	0.4	2.1	-1.6

Table B71. The Number of Matches Made between *rawinsonde* and VAD Data at Each level during **Summer** for the Atmosphere which was **Not Superrefractive**

Range: <u>Height (m)</u>	20 km	22 km	24 km	26 km	28 km	30 km	32 km
1830	29	29	29	29	29	29	29
2130	47	47	47	47	26	26	26
2430	25	42	42	42	42	42	42
2730	27	25	25	25	25	41	40
3030	31	31	31	18	15	15	15
3330	13	13	13	11	11	11	8
3630	26	26	26	26	27	28	28
3930	7	7	7	5	5	5	5
4230	22	22	22	22	22	20	20
4530	3	2	2	2	2	2	2
4830	21	21	21	19	19	19	19
5130	7	7	7	7	7	7	7
5430	2	2	2	2	2	2	2
5730	9	9	9	9	9	9	7
6030	17	18	18	18	18	18	18
6330	3	3	3	3	3	3	3
6630	3	3	3	3	3	3	3
6930	1	1	1	0	0	0	0
7230	4	4	4	4	5	5	5
7530	8	10	10	10	10	9	9

Table B72. RMSVD Calculated between *rawinsonde* and VAD Data at Each Level during **Summer** for the Atmosphere which was **Not Superrefractive**

Range:	20 km	22 km	24 km	26 km	28 km	30 km	32 km
Height (m)							
1830	8.966	8.966	8.966	8.966	8.966	8.966	8.966
2130	12.24	12.24	12.24	12.24	9.421	9.421	9.421
2430	10.82	11.93	11.93	11.93	11.93	11.93	11.93
2730	10.23	11.8	11.8	11.8	11.8	12.36	12.75
3030	13.24	13.24	13.24	11.51	12.83	12.83	12.83
3330	14.95	14.95	15.53	10.38	10.38	10.38	8.111
3630	13.24	14.23	14.23	14.23	14.14	13.97	13.97
3930	13.85	13.85	13.85	11.26	11.26	11.26	11.98
4230	15.62	15.62	15.62	15.62	15.62	16.75	16.75
4530	12.09	10.18	10.18	10.18	10.18	10.18	10.18
4830	17.71	17.71	17.71	18.17	18.17	18.17	18.17
5130	19.92	19.92	19.92	19.92	20.57	20.57	20.57
5430	10.7	10.7	10.7	10.7	10.7	15.87	15.87
5730	16.01	16.01	16.01	16.01	16.01	16.01	16.15
6030	12.83	11.88	11.88	11.88	11.88	11.88	11.88
6330	13.29	13.29	13.17	13.17	13.17	13.17	13.17
6630	14.64	14.64	14.64	13.41	13.41	13.41	13.41
6930	15	15	15	*****	*****	*****	*****
7230	5.331	5.331	5.331	5.331	10.16	10.16	10.16
7530	7.193	10.7	10.7	10.7	10.7	11.44	11.44
Average:	12.89	13.11	13.13	12.50	12.70	13.09	13.04
Standard Deviation:	3.44	3.22	3.24	3.31	3.07	3.13	3.27

Table B73. Skill Score Calculated Using *rawinsonde* Verification at Each Level during **Summer** for the Atmosphere which was **Not Superrefractive**

Range:	20 km	22 km	24 km	26 km	28 km	32 km
Height (m)						
1830	0.0	0.0	0.0	0.0	0.0	0.0
2130	-29.9	-29.9	-29.9	-29.9	0.0	0.0
2430	9.3	0.0	0.0	0.0	0.0	0.0
2730	17.2	4.5	4.5	4.5	4.5	-3.2
3030	-3.2	-3.2	-3.2	10.3	0.0	0.0
3330	44.0	-44.0	-49.6	0.0	0.0	21.9
3630	5.2	-1.9	-1.9	-1.9	-1.2	0.0
3930	-23.0	-23.0	-23.0	0.0	0.0	-6.4
4230	6.7	6.7	6.7	6.7	6.7	0.0
4530	-18.8	0.0	0.0	0.0	0.0	0.0
4830	2.5	2.5	2.5	0.0	0.0	0.0
5130	3.2	3.2	3.2	3.2	0.0	0.0
5430	32.6	32.6	32.6	32.6	32.6	0.0
5730	0.0	0.0	0.0	0.0	0.0	-0.9
6030	-8.0	0.0	0.0	0.0	0.0	0.0
6330	-0.9	-0.9	0.0	0.0	0.0	0.0
6630	-9.2	-9.2	-9.2	0.0	0.0	0.0
6930	*****	*****	*****	*****	*****	*****
7230	47.5	47.5	47.5	47.5	0.0	0.0
7530	37.1	6.5	6.5	6.5	6.5	0.0
Average:	1.3	-0.4	-0.7	4.2	2.6	0.6

d. Statistics Calculated Between Rawinsonde and Profiler Data

Table B74. Number of Matches and RMSVD Calculated between *rawinsonde* and *profiler* Data for the Atmosphere which was **Superrefractive at the Surface**

HEIGHT (m)	RMSVD				NUMBER OF MATCHES			
	Aut	Win	Spg	Sum	Aut	Win	Spg	Sum
2024	11.93	5.988	6.117	6.442	26	22	29	22
2274	13.91	7.746	7.532	9.904	28	22	29	22
2524	15.23	10.44	7.941	9.783	28	24	30	25
2774	18.36	11.84	7.915	8.571	27	24	29	25
3024	17	14.88	7.036	8.819	26	23	26	20
3274	18.63	10.26	8.847	6.865	9	6	24	20
3524	16.18	16.73	8.957	8.611	17	22	19	14
3774	14.48	16.59	9.545	9.69	27	24	30	25
4024	10.25	19	9.232	11.52	5	5	4	3
4274	14.95	17.05	10.98	10.24	27	24	29	25
4524	16.43	13.29	18.15	6.957	6	4	8	4
4774	15.85	17.75	11.42	11.34	26	24	30	25
5024	17.61	22.13	12.45	12.57	27	23	30	25
5274	17.14	23.6	10.57	7.76	7	10	4	2
5524	18.86	24.27	6.655	11.91	15	18	5	7
5774	20.25	26	13.38	13.12	22	14	30	23
6024	20.2	26.97	13.68	12.89	27	23	30	25
6274	14.99	32.89	20.36	9.022	6	4	5	9
6524	13.47	33.2	22.36	10.09	5	4	4	8
6774	15.12	21.34	11.9	17.3	7	4	7	6
7024	14.3	30.98	15.77	16.92	2	8	3	4
7274	21.44	24.56	16.59	15.6	22	17	5	3
7524	20.62	29.47	14.9	15.71	24	20	28	24
Average:	16.40	19.87	11.84	10.94				
Standard Deviation:	2.84	7.98	4.47	3.17				

Table B75. Number of Matches and RMSVD Calculated between *rawinsonde* and *profiler*
Data for the Atmosphere which was **Superrefractive Aloft**

HEIGHT (m)	RMSVD				NUMBER OF MATCHES			
	Aut	Win	Spg	Sum	Aut	Win	Spg	Sum
2024	8.591	8.539	8.964	7.53	26	29	23	26
2274	12.73	11.3	10.26	9.311	26	29	23	26
2524	12.99	13.32	9.081	8.951	27	28	24	27
2774	12.5	13.98	9.081	10.04	28	29	25	27
3024	12.85	14.49	10.05	11.9	28	26	26	15
3274	12.44	19	8.622	9.279	13	11	16	26
3524	13.53	19.19	10.53	9.033	22	15	9	20
3774	15.51	19.96	13.08	13.08	28	27	25	27
4024	11.76	23.91	15.04	10.39	7	5	6	5
4274	17.26	19.63	13.64	12.57	28	28	25	27
4524	*****	15.65	14.03	9.262	0	5	10	6
4774	18.07	20.79	14.65	13.8	28	28	24	27
5024	19.27	23.29	16.99	14.96	28	29	25	27
5274	20.9	25.31	15.79	18.59	10	4	3	7
5524	20.72	22.21	13.7	11.51	20	24	7	6
5774	22.29	21.85	21.02	13.61	21	11	21	25
6024	24.29	26.11	21.35	13.71	28	28	25	27
6274	19.85	10.34	24.02	12.45	3	1	10	3
6524	23.86	10.25	23.39	13.56	3	1	9	4
6774	22.27	27.15	30.32	18.66	7	5	3	7
7024	23.91	30.66	21.8	15.75	9	15	9	6
7274	27.16	31.93	22.8	12.75	24	23	11	5
7524	26.87	30.98	23.12	16.98	27	29	24	26
Average:	18.16	19.99	16.14	12.51				
Standard Deviation:	5.45	6.93	6.15	3.09				

Table B76. Number of Matches and RMSVD Calculated between *rawinsonde* and *profiler*
 Data for the Atmosphere which was **Not Superrefractive**

HEIGHT (m)	RMSVD				NUMBER OF MATCHES			
	Aut	Win	Spg	Sum	Aut	Win	Spg	Sum
2024	6.796	7.423	11.11	4.511	24	23	29	26
2274	8.285	10.06	12.82	4.968	24	23	29	26
2524	10.49	21.99	12.9	7.284	26	23	30	26
2774	11.65	12.83	13.73	8.778	26	22	30	26
3024	12.61	12.94	13.47	11.59	23	23	30	18
3274	10.02	11.87	15.24	8.285	19	7	9	24
3524	13.49	12.57	15.71	7.086	15	15	15	16
3774	13.84	14.89	17.77	7.391	26	21	30	26
4024	13.89	18.42	15.68	10.41	5	6	7	6
4274	17.43	18.91	17.24	9.369	24	21	29	26
4524	14.79	15.47	16.64	9.112	9	7	5	5
4774	17.47	19.99	17.52	10.71	24	22	29	26
5024	20.01	21.03	19.17	11.73	26	22	30	26
5274	23.7	18.56	17.79	13.74	2	8	10	7
5524	27.09	21.93	19.21	10.76	9	20	24	3
5774	19.22	20.26	24.81	12.98	24	10	15	26
6024	21.15	23.68	19.09	13.07	25	23	29	25
6274	26.44	17.82	21.45	11.44	4	7	3	5
6524	31.7	18.07	24.52	11.8	2	6	3	5
6774	20.09	21.32	24.72	8.129	5	4	3	4
7024	29.17	28.59	20.49	9.459	4	8	16	4
7274	26.79	22.76	26.26	14.84	14	12	21	3
7524	28.78	28.02	25.73	15.48	18	20	27	24
Average:	18.47	18.23	18.39	10.13				
Standard Deviation:	7.33	5.39	4.48	2.90				

References

American Meteorological Society, 1989: Glossary of Meteorology. Boston.

Babin, S.M., 1995: A Case Study of Subrefractive Conditions at Wallops Island, Virginia. *J. Appl. Meteor.*, 34, 1028-1038.

-----, 1996: Surface duct height distributions for Wallops Island, Virginia, 1985-1994. *J. Appl. Meteor.*, 35, 86-93.

Barth, M.F., R.B. Chadwick, and D.W. van de Kamp, 1994: Data processing algorithms used by NOAA's Wind Profiler Demonstration Network. *Ann. Geophys.*, 12, 512-528.

Battan, L.J., 1973: *Radar Observation of the Atmosphere*. The University of Chicago Press, Chicago, 324 pp.

Bean, B.R. and E.J. Dutton, 1966: *Radio Meteorology*. Natl. Bur. Stand. Monogr. 42, U.S. GPO, 435 pp.

Bluestein, H.B., 1992: *Synoptic-Dynamic Meteorology in Midlatitudes, Volume 1: Principles of Kinematics and Dynamics*. Oxford University Press, New York, 431 pp.

Bolton, D., 1980: *The computation of equivalent potential temperature*, Mon. Wea. Rev., 108, 1046-1053.

Caya, D., and I. Zawadzki, 1992: VAD analysis of nonlinear wind fields. *J. Atmos. Oceanic Technol.*, 9, 575-587.

Crum, T.D., and R.L. Albert, 1993: The WSR-88D and the Operational Support Facility. *Bull. Amer. Meteor. Soc.*, 74, 1669-1687.

Davis, J.L., R.R. Lee, and J.L. Ingram, 1995: Comparing rawinsonde and WSR-88D wind profiles. *Preprints, 27th Conf. on Radar Meteor.*, Vail, CO, Amer. Meteor. Soc., 409-411.

Doggett, M.K., 1997: *An Atmospheric Sensitivity and Validation Study of the Variable Terrain Radio Parabolic Equation Model (VTRPE)*. M.S. Thesis, Department of Engineering Physics, Air Force Institute of Technology, Wright-Patterson Air Force Base, Ohio, 79 pp.

Douglas, M.W., and D.J. Stensrud, 1996: Upgrading the North American upper-air observing network: what are the possibilities? *Bull. Amer. Meteor. Soc.*, 77, 907-924.

Doviak, R.J., and D.S. Zrnic, 1993: *Doppler Radar and Weather Observations*, 2nd Ed., Academic Press, Inc., San Diego, CA, 562 pp.

Farris, D.R., 1997: *Optimization of the Velocity Azimuth Display (VAD) Algorithm's Adaptable Parameters in the WSR-88D System*. M.S. Thesis, Department of Engineering Physics, Air Force Institute of Technology, Wright-Patterson Air Force Base, Ohio, 218 pp.

Federal Meteorological Handbook No. 11 (Interim Version One), 1990: Doppler radar meteorological observations. Part B, Doppler radar theory and meteorology. FCM-H1 1B-1990, Office of the Federal Coordinator for Meteorological Services and Supporting Research, Rockville, Maryland, 228 pp.

----, 1991a: Doppler radar meteorological observations. Part A, System concepts, responsibilities, and procedures. FCM-H1 1A-1991, Office of the Federal Coordinator for Meteorological Services and Supporting Research, Rockville, Maryland, 58 pp.

----, 1991b: Doppler radar meteorological observations. Part C, WSR-88D products and algorithms. FCM-H11C-1991, Office of the Federal Coordinator for Meteorological services and Supporting Research, Rockville, Maryland, 210 pp.

----, 1992: Doppler radar meteorological observations. Part D, WSR-88D unit description and operational applications. FCM-H11D-1992, Office of the Federal Coordinator for Meteorological services and Supporting Research, Rockville, Maryland, 208 pp.

Fleagle, R.G., and J.A. Businger, 1980: *An Introduction to Atmospheric Physics*. Academic Press, London, 432 pp.

Golden, J.H., R. Serafin, V. Lally, and J. Facundo, 1986: Atmospheric Sounding Systems. *Mesoscale Meteorology and Forecasting*. P.S. Ray, Ed., Amer. Meteor. Soc., 50-70.

Jain, M., M. Eilts, and K. Hondl, 1993: Observed differences of the horizontal wind derived from Doppler radar and a balloon-borne atmospheric sounding system. *Preprints, 8th Symp. on Meteor. Observations and Instrumentation*, Anaheim, CA, Amer. Meteor. Soc., 189-193.

Klazura, G.E., and D.A. Imy, 1993: A description of the initial set of analysis products available from the NEXRAD WSR-88D System. *Bull. Amer. Meteor. Soc.*, 74, 1293-1311.

Larkin, R.P., 1991: Sensitivity of NEXRAD algorithms to echoes from birds and insects. *25th Int. Conf. on Radar Meteor.*, Paris, Amer. Meteor. Soc., 203-205.

Lawrence, T.R., B.F. Weber, M.J. Post, R.M. Hardesty, R.A. Richter, N.L. Abshire, and F.F. Hall, 1986: *A Comparison of Doppler LIDAR, Rawinsonde, and 915-MHz UHF Wind Profiler Measurements of Tropospheric Winds*. NOAA/ERL WPL-130, Boulder, CO, 84 pp.

Lee, R.R., and J.L. Ingram, 1995: "Comparing KMLB-KAMX-KSC Rawinsonde and WSR-88D Wind Profiles." Draft, WSR-88D Operational Support Facility, Norman, OK, 5 pp.

-----, J.L. Ingram, and G.E. Klazura, 1994: A comparison of data from the WSR VAD Wind Profile product and rawinsondes at twelve sites - preliminary results. *Postprints, 1st WSR-88D Users' Conf.*, Norman, OK, OSF/JSPO, 55-61.

Martner, B.E., D.B. Wuertz, B.B. Stankov, R.G. Strauch, E.R. Westwater, K.S. Gage, W.L. Ecklund, C.L. Martin, and W.F. Dabberdt, 1993: An evaluation of wind profiler, RASS, and microwave radiometer performance. *Bull. Amer. Meteor. Soc.*, 74, 599-611.

McLaughlin, S.A., 1993: Potential Errors in Doppler Radar Wind Measurements Caused by Migrating Point Targets as Seen by the ARL FM-CW Radar. *27th Int. Conf. Radar Meteor.*, Norman, OK, Amer. Meteor. Soc., 643-645.

Naval Ocean Systems Center. Climatology of Marine Atmospheric Refractive Effects: A Compendium of the IREPS Historical Summaries. NOSC TD 573, DTIC AD-A 155 241. San Diego: NOSC, 20 December 1982.

Nastrom, G.D., and T.E. VanZandt, 1996: Biases due to gravity waves in wind profiler measurements of winds. *J. Appl. Meteor.*, 35, 243-257.

Nelson, S.E., 1994: *Intercomparison of Velocities Observed from Operational Wind-Finding Systems*. M.S. Thesis, School of Meteorology, University of Oklahoma, Norman, Oklahoma, 99 pp.

O'Bannon, T., 1994: Anomalous WSR-88D wind profiles - migrating birds? *Postprints, 1st WSR-88D Users' Conf.*, Norman, OK, OSF/JSPO, 83-94.

Ralph, F.M., P.J. Neiman, D.W. van de Kamp, and D.C. Law, 1995: Using spectral moment data from NOAA's 404 MHz radar wind profilers to observe precipitation. *Bull. Amer. Meteor. Soc.*, 76, 1717-1738.

Schwartz, B.E., 1989: Rawinsonde data: operational and archival concerns. *12th Conf. on Wea. Forecasting and Analysis*, 52-57.

Steadham, R., and R.R. Lee, 1995: Perceptions of the WSR-88D performance. *Preprints, 27th Conf. on Radar Meteor.*, Vail, CO, Amer. Meteor. Soc., 173-175.

Stensrud, D.J., M.H. Jain, K.W. Howard, and R.A. Maddox, 1990: Operational systems for observing the lower atmosphere: importance of data sampling and archival procedures. *J. Atmos. Oceanic Technol.*, 7, 930-937.

van de Kamp, D.W., 1988: *Profiler Training Manual #1 - Principles of Wind Profiler Operation*. NOAA/ERL, 49pp.

WATADS 9.0 (WSR-88D Algorithm Testing and Display System) Algorithm Reference Guide. Applications Branch, WSR-88D Operational Support Facility (OSF), Norman, OK, April, 1997.

Weber, B.L., D.B. Wuertz, D.C. Law, A.S. Frisch, and J.M. Brown, 1992: Effects of small-scale vertical motion on radar measurements of wind and temperature profiles. *J. Atmos. Oceanic Technol.*, 9, 193-209.

----, D.B. Wuertz, R.G. Strauch, D.A. Merritt, K.P. Moran, D.C. Law, van de Kamp, R.B. Chadwick, M.H. Ackley, M.F. Barth, N.L. Abshire, P.A. Miller, and T.W. Schlatter, 1990: Preliminary evaluation of the first NOAA Demonstration Network wind profiler. *J. Atmos. Oceanic Technol.*, 7, 909-918.

Wilczak, J.M., R.G. Strauch, F.M. Ralph, B.L. Weber, D.A. Merritt, J.R. Jordan, D.E. Wolfe, L.K. Lewis, D.B. Wuertz, J.E. Gaynor, S.A. McLaughlin, R.R. Rogers, A.C. Riddle, and T.S. Dye, 1995: Contamination of wind profiler data by migrating birds: characteristics of corrupted data and potential solutions. *J. Atmos. Oceanic Technol.*, 12, 449-467.

Wilks, D.S., 1995: *Statistical Methods in the Atmospheric Sciences*. Academic Press, San Diego, CA, 467 pp.

Vita

Captain David L. Craft was born on 2 July 1971 in Englewood, Colorado. In 1989 he graduated from Thomas Jefferson High School and began undergraduate studies at Texas A&M University with a four-year ROTC scholarship. In 1993 he graduated with a Bachelor of Science degree in Meteorology and received his commission into the Air Force.

After graduation, he forecasted weather operationally for 2 1/2 years as a Wing Weather Officer at McGuire AFB, New Jersey. During that time, he successfully completed the WSR-88D Operations Course offered by the National Weather Service in Norman, Oklahoma. In August 1996, he enrolled in the Graduate Meteorology program at the Air Force Institute of Technology.

Permanent Address: 1902 Colquitt, Apt 23C
Houston, TX 77098

REPORT DOCUMENTATION PAGE

Form Approved
OMB No. 0704-0188

Public reporting burden for this collection of information is estimated to average 1 hour per response, including the time for reviewing instructions, searching existing data sources, gathering and maintaining the data needed, and completing and reviewing the collection of information. Send comments regarding this burden estimate or any other aspect of this collection of information, including suggestions for reducing this burden, to Washington Headquarters Services, Directorate for Information Operations and Reports, 1215 Jefferson Davis Highway, Suite 1204, Arlington, VA 22202-4302, and to the Office of Management and Budget, Paperwork Reduction Project (0704-0188), Washington, DC 20503.

1. AGENCY USE ONLY (Leave blank)	2. REPORT DATE	3. REPORT TYPE AND DATES COVERED	
	March 1998	Final	
4. TITLE AND SUBTITLE		5. FUNDING NUMBERS	
Azimuth & Range Optimization of the Velocity Azimuth Display (VAD) Algorithm in the WSR-88D		none	
6. AUTHOR(S)		7. PERFORMING ORGANIZATION NAME(S) AND ADDRESS(ES)	
David L. Craft, Capt, USAF		AFIT/ENP 2950 P. St. Wright-Patterson AFB, OH 45433	
Attn: Lt Col Cecilia Askue e-mail: caskue@afit.af.mil phone: (com) 937-255-3636 x4645 (dsn) 785-3636 x4645		8. PERFORMING ORGANIZATION REPORT NUMBER	
9. SPONSORING/MONITORING AGENCY NAME(S) AND ADDRESS(ES)		10. SPONSORING/MONITORING AGENCY REPORT NUMBER	
WSR-88D Operational Support Facility 1200 Westheimer Dr. Norman, OK 73069 Attn: Lt Col Andy White email: awhite@osf.noaa.gov phone: (com) 405-366-6500			
11. SUPPLEMENTARY NOTES			
12a. DISTRIBUTION AVAILABILITY STATEMENT		12b. DISTRIBUTION CODE	
distribution unlimited			
13. ABSTRACT (Maximum 200 words)			
<p>The Velocity Azimuth Display (VAD) algorithm occasionally produces inaccurate wind estimates for the VAD Wind Profile (VWP) product of the Weather Surveillance Radar - 1988 Doppler (WSR-88D) System. Weather forecasters have observed differences between the radar's wind profiles and wind profiles produced by rawinsondes and vertical wind profilers, when radiation and subsidence inversions in the atmosphere caused the radar beam to superrefract.</p> <p>This thesis sought to improve the operational use of the VWP product for the WSR-88D near Denver, CO, by finding the optimal VAD algorithm Azimuth and Range parameter settings to overcome data contamination by hills located at the default range used by the algorithm. The WSR-88D Algorithm Testing and Display System (WATADS) processed 24 weeks of archived (level II) VAD wind data, which was verified by rawinsonde and vertical wind profiler data.</p> <p>Azimuth optimization was unsuccessful. However, reducing the range not only provided an average improvement in the accuracy of winds obtained under superrefractive conditions, but also in the accuracy of those winds obtained when the atmosphere was not superrefractive. In the overall average, the range which produced the most improvement over default range (30 km) accuracy was 28 km. The 26-km range also performed well.</p>			
14. SUBJECT TERMS		15. NUMBER OF PAGES	
WSR-88D, Operational Support Facility, OSF, Velocity Azimuth Display, VAD, Velocity Wind Profile, VWP, Superrefraction, Ducting		144	
16. PRICE CODE			
17. SECURITY CLASSIFICATION OF REPORT	18. SECURITY CLASSIFICATION OF THIS PAGE	19. SECURITY CLASSIFICATION OF ABSTRACT	20. LIMITATION OF ABSTRACT
unclassified	unclassified	unclassified	UL